2020-07-08

It's About Time: Monitoring The Circadian Clock From a Cre-Dependent Reporter

Ciearra B. Smith
University of Massachusetts Medical School

IT'S ABOUT TIME: MONITORING THE CIRCADIAN CLOCK FROM A CRE-DEPENDENT REPORTER

A Dissertation Presented

By

CIEARRA BRITNEY SMITH

Submitted to the Faculty of the

University of Massachusetts Graduate School of Biomedical Sciences, Worcester

in partial fulfillment of the requirements for the degree of

DOCTOR OF PHILOSOPHY

July 8, 2020

CIRCADIAN RHYTHMS

IT'S ABOUT TIME: MONITORING THE CIRCADIAN CLOCK FROM A CRE-DEPENDENT REPORTER

A Dissertation Presented

By

CIEARRA BRITNEY SMITH

This work was undertaken in the Graduate School of Biomedical Sciences

The Neuroscience Program

Under the mentorship of

David R. Weaver, Ph.D., Thesis Advisor

Patrick Emery, Ph.D., Member of Committee

John Landers, Ph.D., Member of Committee

Brian Lewis, Ph.D., Member of Committee

Frank Scheer, Ph.D., External Member of Committee

Michael Francis, Ph.D., Chair of Committee

Mary Ellen Lane, Ph.D.,

Dean of the Graduate School of Biomedical Sciences

July 8, 2020

DEDICATION

This thesis work is dedicated to two of my rocks in human form, my momma Allicia Smith-Brown and my boyfriend Joshua Stacker. I would like to dedicate this work to you two as you have provided constant encouragement, love (sometimes tough), support, and prayers throughout my entire journey in graduate school. You two always have the right things to say to get me back focused. Your loving words and advice never went unnoticed and I couldn't have achieved this great milestone without you two.

ACKNOWLEDGEMENTS

Jeremiah 29:11 "For I know the plans I have for you", declares the Lord, "plans to prosper you and not harm you, plans to give you hope and a future."

First and foremost I would like to thank my God who continues to order my steps and reveal His purpose for my life. The Lord has brought me through some of the lowest points in my life and continues to show me favor. The faith I have in God has helped me overcome all of the obstacles graduate school has put in my way. I am a living testament of how good God is and how He can turn nothing into something.

Next, I would like to acknowledge my family, first starting with my parents, Allicia Smith-Brown and Gary Smith. Mom, thank you for being my superwoman all of my life. Your motto "failure is not an option" has pushed me to be the successful woman and scientist I am today. Thank you for our daily phone calls, your hugs, prayers, tough love, and believing in me even when I doubted myself. Thank you for reminding me that during my darkest hours, I should turn to God. Dad, thank you for your motivation and encouraging words every time I needed a "pick me up." Thank you for instilling the importance of education in me. Importantly, thank you mom and dad for cultivating a love for science at such a young age that inspired me to become a scientist. To my bonus dad, Tim Brown,

thank you for all of your prayers and encouraging spiritual text messages; those messages reminded me that I am truly an Angel living in God's purpose. To my brother Justin Smith and sister-in-love Jazmyn Smith, thank you for all of the support over the years. Justin, thank you for your random phone calls of encouragement; even if they were few and far between those phone calls made all the difference. Thank you for encouraging me to not give up, but most importantly, thank you Justin and Jazmyn for my nephew Caleb! To my grandma Elsa Smith and nana Carrie Stroud, thank you for all of your prayers and encouraging words. Grandma, thank you for setting the example of what determination, sacrifice, and focus can lead to. The determination you had in pursuing your nursing degree has motivated me not to quit. Nana, thank you for our conversations and lessons you taught me about faith and talking to God during my time of need. To my grandad, Joseph Smith, thank you for the jokes and reassurance that I can accomplish anything I set my mind to; your smile and jokes are truly missed. I wish you were here to see this amazing accomplishment, but I know you are super proud and looking down on me with the biggest smile. To my aunt and uncles, Gina Stroud, Wayne Smith, and Peter Smith, thank you for being my cheerleaders throughout the years. To my fur baby Shadow, thank you for all of the cuddles and late night company! To my extended families, the Stacker and Hawkins families, thank you for the prayers and kind words I needed to succeed in graduate school.

To my best friend and boyfriend Joshua Stacker, thank you for all that you do. Thank you for your love, laughs, sacrifices, keeping me company in lab, motivating me, listening to me vent, helping me with my “checks” etc., and the list can literally go on forever. You made a lot of sacrifices in order for me to accomplish my ambitious goal of attaining a Ph.D. and I never took that for granted. I can truly say that I would not have been able to achieve this momentous goal without you by my side.

I would like to acknowledge my best friend since kindergarten, Michelle Gibson and my college friend Kenneth Powell. Michelle, thank you for your phone calls and the laughs. Thank you for always thinking about me even though our schedules can get busy. Kenny P., thank you for checking up on me and supporting me throughout graduate school, especially for listening to me when I was freaking out about qualifying. Thank you to my college mentors Dr. Catherine White and Dr. Checo Rorie for pushing me to pursue a Ph.D. and constantly supporting me.

It takes a village to raise a child; this is also true to raise a scientist. My growth as a scientist is partly attributed to my amazing UMASS Medical School friends whom now I consider family. First, I would like to thank my two besties and twinny twin twins Dr. Asia Matthew-Onabanjo and Dr. Ashley Matthew. I am incredibly blessed to have met you two in graduate school. We have gotten so close over the years and you two continue to amaze me! Thank you for

supporting me during my darkest moments and celebrating my accomplishments. Thank you for helping me with my “checks” in lab and always willing to listen when I needed an ear. You two will be amazing physicians and I can’t wait to see you guys sprinkle your black girl magic wherever you go. Next, I would like to thank my classmate Rita Fagan who will be defending her thesis a week before me. Rita, you are one of the smartest graduate students I know. I am so proud of you and all of the obstacles you overcame. Thank you for your scientific advice and being a sounding board. I know you will do great defending your thesis! I would like to thank my friends Fran Clark and Oghomwen Igiesuorobo for holding me down throughout the years. Fran, thank you for our coffee dates and always being there when I needed you. Oghomwen, thank you for your positive energy and believing in me. Fran and Oghomwen, you two are fantastic scientists and will accomplish so many great things in the future. I would like to thank Babafemi Onabanjo, Paul Charles, Jessie Long, and Ganga Bey for becoming my UMASS family and supporting me on this journey.

I would like to thank my Neuroscience Scholars Program (NSP) family for accepting me into the program and providing a support system that was necessary for my success in graduate school. I would also like to acknowledge the Initiative for Maximizing Student Development (IMSD) program and the Diversity Interest Group (DIG) for providing support and safe spaces for underrepresentative graduate students.

I definitely have to acknowledge the members of the Gardner/Tapper lab, as well as the Weaver lab. Thank you to all of the members of the Tapper and Gardner labs for training and advising me during my time in the lab. I learned a lot from you all and the training I received in the lab gave me the confidence to complete my Ph.D. Thank you Dr. Alison Casserly for allowing me to help you with your thesis project and in doing so obtaining a co-authorship. Also, thank you for the laughs and advice I needed to stay focus. Alison, you will be a great physician. To the Weaver lab, specifically Dr. Vincent van der Vinne, thank you for contributing to my thesis work and providing input on my dissertation. Thank you Jamie Black and Christopher Lambert for maintaining the mouse colonies and genotyping, respectively.

Lastly, but certainly not least, I would like to acknowledge my mentors Dr. Paul Gardner and Dr. David Weaver. Words cannot express how grateful I am for you two. Paul, thank you for taking a young, naïve scientist under your wing and training me to become a confident and independent scientist. Thank you for testing my knowledge and challenging me to step outside my comfort zone. Thank you for the laughs and conversations I needed to set me straight. Your training made it possible for me to switch fields with confidence. Dave, thank you for seeing something in me that I didn’t see in myself. Thank you for believing in me and giving me a second chance to complete my Ph.D. Thank you for always being on my side and teaching me the field of circadian rhythms. Both of you

were integral in my growth as a scientist and I am blessed to call you two my mentors.

ABSTRACT

Circadian rhythms are the outward manifestation of an internal timing system that measures time in 24-hr increments. The mammalian circadian system is hierarchical, with a pacemaker in the suprachiasmatic nucleus (SCN) synchronizing cell-autonomous oscillators in peripheral tissues. Much of what we know about rhythmicity in peripheral tissues comes from studies monitoring bioluminescence rhythms in PERIOD2::LUCIFERASE knock-in mice. A limitation with this model is that rhythmicity cannot be monitored in specific cells due to widespread reporter expression.

To address this shortcoming, we generated a mouse that expresses *luciferase* from the *Dbp* locus only after Cre-mediated recombination. I validated this conditional mouse to provide a tool for monitoring circadian rhythms in a tissue/cell-specific manner. Crossing the conditional reporter mice with mice expressing Cre recombinase in various cell types allowed detection of rhythmic bioluminescence in the expected tissues, *in vivo* and *ex vivo*, as well as in slice cultures containing the SCN. The phase of bioluminescence rhythms from explants of mouse peripheral tissues indicated that $Dbp^{Luc/+}$ bioluminescence rhythms have an earlier phase than PER2::LUC/+ rhythms. Importantly, we confirmed that editing of the *Dbp* locus did not alter the period of circadian locomotor activity rhythms and did not alter liver *Dbp* RNA rhythms. Finally, the reporter mouse allows for monitoring rhythms in specific tissues in ambulatory

mice. Thus, this mouse line is useful for studying circadian rhythms in a tissue/cell-type specific manner, which can be used to better monitor phase relationships between tissues at baseline and after environmental perturbations that disrupt circadian rhythms.

TABLE OF CONTENTS

LIST OF TABLES

LIST OF FIGURES

LIST OF THIRD PARTY COPYRIGHT MATERIAL

Figure 1.2, 1.3, and Table 1.1: Adapted from Reppert SM, Weaver DR. Coordination of circadian timing in mammals. Nature. 2002;418(6901):935-41. doi: 10.1038/nature00965. PubMed PMID: 12198538. Copyright 2002, with permission from Springer Nature Publishing Group (License Number: 4796111452211).

LIST OF ABBREVIATIONS

Ach	Acetylcholine
Alb	Albumin
AVP	Arginine vasopressin
bHLH	Basic helix-loop-helix
BMAL1	Brain and Muscle ARNT-Like 1
Cas9	CRISPR associated protein 9
CK1δ	Casein kinase 1 delta
CK1ε	Casein kinase 1 epsilon
CLOCK	Circadian locomotor output cycles kaput
CPA	Conditioned Place Aversion
CRISPR	Clustered regularly interspaced short palindromic repeats
CRY	Cryptochrome
CycLuc1	Cyclic alkylaminoluciferin
CYP2A5	Coumarin 7-hydroxylase
DBP	Albumin D-element binding protein

DD	Constant Darkness
DIG	Digoxigenin
DWT	Discrete wavelet transform
EGFP	Enhanced Green Fluorescence Protein
EPM	Elevated plus maze
FBS	Fetal Bovine Serum
GFP	Green Fluorescence Protein
GWAS	Genome-wide association study
I.p	Intraperitoneal
IPN	Interpeduncular Nucleus
IVIS	*In vivo* imaging system
KI	Knock-in
KO	Knockout
Ksp1.3	Cadherin 16
LCM	Laser-capture microdissection
LD	Light/dark

MBT	Marble burying test
MEM	Minimum Essential Medium
mHb	Medial Habenula
N2A	Neuro2A
nAChR	Nicotinic Acetylcholine Receptor
NMS	Neuromedin S
NPAS2	Neuronal PAS domain protein 2
OFT	Open field test
PA	Polyadenylation
PCR	Polymerase Chain Reaction
PER	Period
PER2::LUC	PERIOD2::LUCIFERASE
PMT	Photomultiplier tube
Prrx-1	Paired related homeobox 1
REV-ERB	Nuclear receptor subfamily 1, group D, member 1
RHT	Retinohypothalamic tract

ROI	Region of Interest
ROR	Retinoic acid receptor-related orphan receptor
RT-qPCR	Reverse Transcription-quantitative polymerase chain reaction
SCN	Suprachiasmatic Nucleus
shRNA	Short hairpin RNA
SNP	Single Nucleotide Polymorphism
SPP	Skeleton photoperiod
SPVZ	Lateral subparaventricular zone
T2A	2A self-cleaving peptide
Vgat	Vesicular GABA transporter
VIP	Vasoactive Intestinal polypeptide
VPAC2	Vasoactive intestinal peptide receptor 2
WT	Wild-type
ZT	Zeitgeber Time

PREFACE

This dissertation contains a culmination of my work during graduate school. I first present my thesis research in which I validated a conditional mouse reporter to monitor circadian rhythms in specific tissue- and cell-types and present various experiments in which the conditional reporter mouse can be utilized. Additionally, I present work from my previous laboratory in which I investigated the role of α3-containing nicotinic acetylcholine receptors (nAChRs) in behaviors involved in the susceptibility to nicotine addiction, as well as nicotine addiction itself.

CHAPTER I

Introduction

1.1 Overview

The term circadian stems from the Latin word "*circa diem*," meaning about a day (1). Circadian clocks provide an internal timing system that is synchronized to the solar day and drive the rhythms of downstream physiological and behavioral outputs. Circadian rhythms have three hallmarks: 1) Rhythms are endogenously generated and persist in constant conditions with a period of approximately 24 hours, 2) Circadian clocks entrain to external stimuli called Zeitgebers or "time givers", and 3) Rhythms are temperature compensated, meaning the period is independent of the ambient temperature. Period, phase, and amplitude are used to define rhythms, where period and phase are described as the time it takes for a rhythm cycle to complete and a point in the cycle relative to external time, respectively and amplitude is defined as the level of oscillation between the peak and the trough (1-3) (Fig. 1.1). Circadian rhythms are an adaptation in organisms that provides optimal timing for various physiological, metabolic, and behavioral processes (1). Indeed, circadian rhythms are advantageous to organisms by synchronizing behavioral and physiological processes to the environmental light/dark cycle, as well as coordinating internal metabolic processes (4). Circadian rhythms are widespread, ranging from bacteria and fungi to mammals.

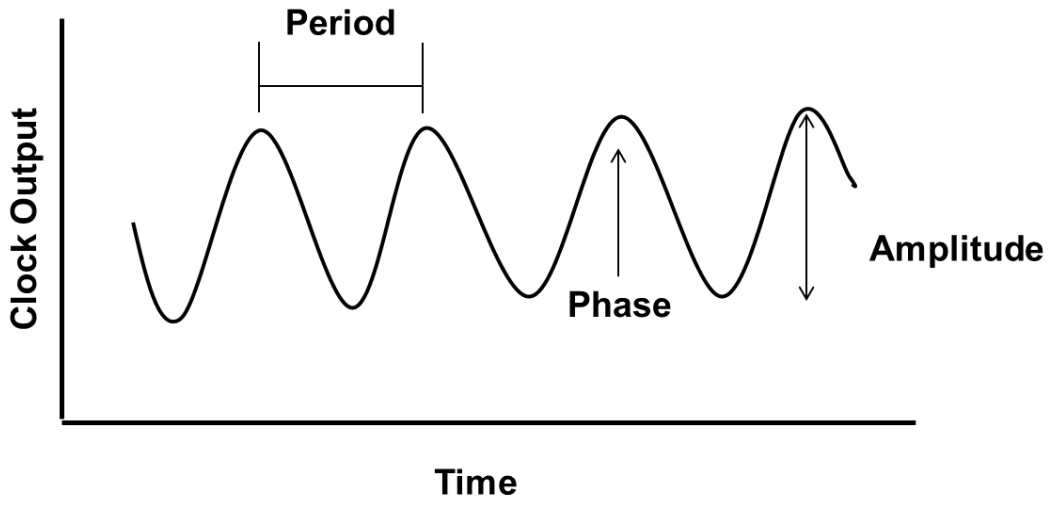

Figure 1.1 Illustration that represents rhythm oscillations

Clock output is measured as a function of time, in which clock output could mean physiological, metabolic, or gene rhythms. Period, phase, and amplitude are shown to describe the characteristics of circadian rhythms.

1.2 History of Circadian Rhythms

The earliest recorded observation of endogenous rhythms was made in plants by the French astronomer Jean-Jacques d'Ortous de Mairan in 1729, where he reported that the daily leaf movements of the heliotrope plant persisted in constant darkness, highlighting one of the hallmarks of circadian rhythms (3). Future studies sought to further characterize these plant rhythms. The first characterization of circadian rhythm periodicity was from Augustin Pyramus de Candolle in 1832, where he observed the *Mimosa pudica* plant rhythm as having an endogenous period of 22-23 hours (5). This finding was confirmed by Wilhelm Pfeffer, a German botanist who showed that there were endogenous rhythms in leaf movement and also saw that leaf movement had a period of less than 24 hours in constant conditions validating that rhythms, at least in plants, are in fact endogenous due to the period being different from the Earth's day/night cycle (3). Interestingly, in the early 1930s, Erwin Bünning discovered that circadian rhythms in plants also have a genetic component in which the period length is inheritable (6).

Early studies of circadian rhythms in plants opened the door for circadian rhythm investigation in other organisms such as *Neurospora crassa*, *Drosophila melanogaster*, and rodents. *Neurospora crassa* was identified as having circadian rhythms by Colin Pittendrigh in 1959, when he showed that the fungus has alternating zones of different growth types, termed "zonation," and that this rhythm in zonation is not only capable of responding to external rhythmic stimuli,

but can also persist in constant darkness and constant temperature (7). In the early 1970s, a turning point in the circadian rhythm field emerged. The research by Ronald Konopka and Seymour Benzer uncovered some of the underpinnings of the circadian system by isolating the first circadian clock mutants by chemical mutagenesis in *Drosophila melanogaster* (8). They found that the mutagenized flies had different circadian phenotypes, such as arrythmicity, a shorter period, or a longer period. These phenotypes mapped to a single locus, *period* (*per*) (8) (*per* described in detail in section 1.3.1). The *per* gene was subsequently cloned by Michael Rosbash and colleagues (9), and independently by Michael Young (10). *Drosophila melanogaster* became a useful genetic tool for uncovering clock mechanisms (8, 11-13).

Richter and colleagues suggested that there was a hypothalamic ‘clock’ (14). Indeed, lesioning studies by Friedrich Stephan and Irving Zucker uncovered the anatomy of the circadian circuit in mammals. Lesioning the suprachiasmatic nucleus (SCN) located in the anterior hypothalamus in rats eliminated the rhythms of drinking and locomotor activity (15). Moore and Eichler also showed that the effects of SCN lesioning was not exclusive to drinking and locomotor rhythms, but also hormone rhythms (16). These data suggest that the SCN is essential for rhythmicity. Research in rodents expanded the knowledge of the genetic basis of circadian rhythms (17-22) and the brain structure involved (15, 16). A defining moment in the field occurred in the late 1980s in which Martin Ralph and Michael Menakar, serendipitously, found a mutation in golden

hamsters that resulted in a dramatically shorter period in circadian locomotor rhythms, with hamsters heterozygous for the mutation exhibiting a period of 22 hours and hamsters homozygous for the mutation showing a period of approximately 20 hours (18). Furthermore, mutant hamsters either had abnormal entrainment or were unable to entrain to the standard 12 hour light: 12 hour dark cycle (18). Ralph and Menakar also contributed to our understanding of the SCN in circadian rhythms by transplanting healthy fetal SCN to a recipient hamster that had a damaged SCN; this restored rhythms in the recipient, with a period of the donor, demonstrating a pacemaker role for the SCN (23, 24). The studies described above enhanced our understanding of circadian rhythm biology, by introducing genetic components as well as an anatomical center for modulating rhythmic outputs.

1.3 Molecular Mechanisms of Circadian Rhythms

1.3.1 Transcriptional-Translational Feedback Loop

Drosophila melanogaster clock genes have homologues in mammals, and mutations in these clock genes result in various circadian phenotypes (Table 1.1) (12, 13). The molecular mechanism of circadian oscillations is controlled by a negative transcriptional-translational feedback loop. In mammals, two basic helix-loop-helix (bHLH)-Period-Arnt-Single-minded heterodimers (25), circadian locomotor output cycles kaput (CLOCK), and Brain and Muscle ARNT-Like 1 (BMAL1) activate negative regulators *Per1*, *Per2*, and *Per3* as well as *cryptochrome 1* and *2* (*Cry*)

genes by binding to their Ebox enhancers (Fig. 1.2) (26, 27). After transcription and translation, PER and CRY proteins return to the nucleus to inhibit the activity of CLOCK and BMAL1, thus negatively regulating their own transcription (Fig. 1.2); this cycle lasts approximately 24 hours. *Bmal1* expression is antiphase to *Per* and *Cry* expression. CLOCK:BMAL1 transcriptionally activates expression of the nuclear orphan receptor *Rev-Erbα* which in turn represses *Bmal1* expression by binding to Rev-Erb/ROR response elements (RORE) in its promoter (28). Notably, during BMAL1 activation of *Per* and *Cry* genes, BMAL1 is also activating *Rev-Erbα* transcription which results in low levels of *Bmal1* mRNA and high levels of *Per* and *Cry*. While PER:CRY complexes inhibit their own transcription through deactivation of the CLOCK:BMAL1 heterodimer, they also inhibit *Rev-Erbα* transcription. RAR-related orphan receptor alpha (RORα) activates *Bmal1* expression in the SCN by binding to ROREs within the *Bmal1* promoter (29). These data show that there are two aspects of the transcriptional-translational loop that are controlled by various protein complexes (13).

Table 1.1 Components of the mouse clock mechanisms

Proteins		Mutations*	
Family	Member	Gene(s)	Behavioural phenotype†
bHLH-PAS	CLOCK‡	*Clock*§	Long period, then arrhythmic
	BMAL1 (MOP3)	*Bmal1 (Mop3)*	Arrhythmic
PER-PAS	PER1	*Per1* or *Per1* + *Per3*	Short period, then arrhythmic
	PER2	*Per2* or *Per2* + *Per3*	Short period, then arrhythmic
	PER3	*Per3*	Short period
		Per1 + *Per2*	Arrhythmic
Flavoproteins	CRY1	*Cry1*	Short period
	CRY2	*Cry2*	Long period
		Cry1 + *Cry2*	Arrhythmic
Casein kinase	CKIε	*CKIε*‖	Short period
Orphan nuclear receptor	REV-ERBα	*Rev-Erbα*	Short period

*Unless otherwise noted, the mutations listed are deletion mutations induced by targeted mutagenesis.
†The most severe phenotypes of homozygous mutant animals studied under constant conditions are listed.
‡A CLOCK-like role has been described for MOP4 (also known as NPAS2)—a bHLH-PAS transcription factor closely related to CLOCK—in the cerebral cortex[82] and in the vasculature[41].
§Ethylnitrosourea-induced semidominant autosomal mutation. The mutation is a nucleotide transversion in a splice donor site causing exon skipping and deletion of part of the transactivation domain[34].
‖Spontaneous semidominant autosomal mutation described in the Syrian hamster (the *tau* mutation). The mutant enzyme is deficient in its ability to phosphorylate PER[35].

The table displays various mutated clock mechanism components and their behavioral phenotypes in constant darkness. These mutations are deletion mutations done via targeted mutagenesis. Image acquired from Reppert and Weaver, 2002 with permission (13).

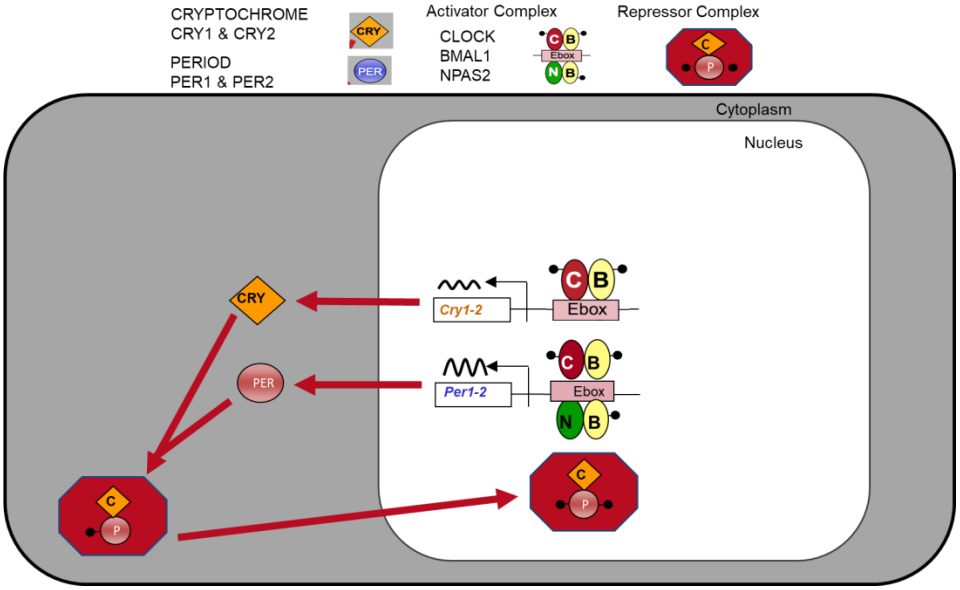

Figure 1.2 Schematic of the mammalian transcriptional-translational negative feedback loop

The activator complex which includes BMAL1 and CLOCK or NPAS2 binds to *Per* and *Cry* genes to promote their transcription. *Per* and *Cry* are translated and form a repressor complex, that after phosphorylation (indicated by the small black dot), translocate back into the nucleus to deactivate the activator complex, thus inhibiting their own transcription. Adapted from Reppert and Weaver, 2002 with permission (13).

Interestingly, mice with *Bmal1* knocked out have immediate arrhythmicity in their locomotor activity when placed in constant darkness (17). Unlike *Bmal1*, the lack of *Per1* or *Per2* genes results in a shorter period and delayed arrhythmicity (22). However, knockout of both *Per1* and *Per2* causes immediate arrhythmicity in locomotor activity when placed in constant darkness (22). Compensation is proposed as an explanation as to why only knocking out one *Per* does not result in immediate arrhythmicity, however it is important to mention that this compensation is not complete as there are period differences in mice that have only one *Per* knocked out. *Per3* is not essential for circadian rhythmicity as *Per3* knockout mice have continued rhythms and only display a short period (22, 30). Functional redundancy was raised to explain the lack of robust phenotype in *Per3* knockout mice; this concept was also raised when assessing circadian rhythmicity in *Cry1* and *Cry2* null mutants (21, 22). Indeed, if *Per3* is playing an important role in the molecular circadian clock, then mice with null mutations in *Per1* and *Per3* or *Per2* and *Per3* should have a more severe circadian phenotype than mice with individual *Per1* or *Per2* null mutations. Bae et al. showed that double mutant mice (*mPer1/mPer3 and mPer2/mPer3*) had similar locomotor activity rhythms compared to mutant mice with one *Per1* or *Per2* null mutation, which included a short period and delayed arrhythmicity (22), suggesting that *Per3* is not necessary for modulating the circadian molecular clock.

Another molecular component of the circadian clock is the Neuronal PAS domain protein 2 (NPAS2) co-activator. NPAS2 plays a key role in transcriptional

activation of *Per* and *Cry* by dimerizing with BMAL1. Mice with CLOCK null mutations retain their rhythmicity and have shortened periods and mice with NPAS2 null mutations have rhythms as well and a slightly shortened period (31). Only after knocking out both CLOCK and NPAS2 the mice became arrhythmic (31). This is due to the overlapping roles of CLOCK and NPAS2 in regulating the circadian clock. Data also shows CLOCK and NPAS2 may have different binding affinities to various E-boxes as single knockout of either CLOCK or NPAS2 have different gene expression profiles (31).

On a molecular level, DeBruyne et al. hypothesized that the lack of *Clock* will increase *Npas2* mRNA expression in the SCN, however this was not the case (19). They were unable to detect *Npas2* mRNA expression in the SCN of WT and CLOCK null mice; this could be due to the less sensitive *in situ* hybridization approach they used to detect *Npas2* mRNA. DeBruyne et al. later showed that there was an increase in *Npas2* mRNA expression in the SCN of CLOCK null mice by RT-qPCR compared to WT (31). These data suggest that there is compensation between CLOCK and NPAS2.

1.3.2 Post-translational Regulation of the Circadian Clock

In addition to transcriptional regulation control of the molecular clock timing, post-translational mechanisms also contribute to adjusting the clock so that it cycles with a period of approximately 24 hours. Phosphorylation of clock proteins by casein kinases are known to regulate the speed of the clock (32, 33).

Phosphorylation of clock proteins by casein kinases is involved in the CLOCK:BMAL1-dependent transcriptional activity, as well as, nuclear translocation of the negative arm of the cycle (PER:CRY) (34, 35). In particular, BMAL1 is a substrate of the casein kinase epsilon (CKIε) protein which is known to regulate CLOCK:BMAL1 heterodimer transcriptional activity (36). *In vitro* studies showed that by co-expressing a dominant-negative mutant of CK1ε (K38A) with *Per1-luciferase* reporter, this decreased luciferase expression by 40%; this was not seen with co-expression of the active CK1ε and *Per1-luciferase* reporter (36). To complement this experiment, expression of the dominant-negative CK1ε mutant *in vitro*, also decreased the levels of phosphorylated BMAL1 (36). This data suggests that CLOCK:BMAL1 heterodimer-dependent transcriptional activity is modulated by the phosphorylation of BMAL1 by CK1ε. Interestingly, during negative loop transcription, BMAL1 and CLOCK nuclear levels are low suggesting that the phosphorylation of BMAL1 by CK1ε modulates the transcriptional activity of the positive heterodimer complex (13, 37).

The levels of PER proteins are the rate limiting step for initiating the negative feedback loop (37). Western Blot analyses of liver tissue revealed that double mutant *Per1* and *Per2* mice had less nuclear CRY compared to wild-type mice, suggesting that PER is involved in the nuclear translocation of CRY (37). PER acts as a scaffold for CK1ε and casein kinase 1 delta (CK1δ), as well as CRY, to form a multimeric complex that is required for initiating the negative

feedback loop. Within this complex, CRY proteins specifically stabilize casein kinase-dependent phosphorylated PER2 and aid in nuclear translocation of the complex (37). PER2 not only acts as a scaffold for multimeric complex formation, but also aids in phosphorylation of the CRY proteins by the casein kinases (13, 36), most likely by bringing the CRY proteins and casein kinases together. The casein kinases' role in maintaining the period of the circadian clock was demonstrated in mutant casein kinase mice (*Vgat-Cre*$^{+}$*; CK1*$\delta^{fl/fl}$ $\varepsilon^{fl/+}$) in which the period of locomotor activity became longer (38). Interestingly, CK1ε and CK1δ seem to be playing different roles in modulating the molecular clock. For example, CK1ε is not as important for setting the speed of the clock compared to CK1δ as deletion of Ck1ε in GABAergic neurons showed no period difference in locomotor activity compared to *Vgat-Cre*$^{+}$ control (38). These data suggest that these two kinases, although highly conserved, act on different aspects of the molecular clock.

Other post-translational modifications include acetylation and SUMOylation of various clock proteins. For example, CLOCK has histone acetyltransferase activity that is necessary for rhythmic expression of core clock genes such as BMAL1 and other circadian output genes (39). The acetylation of BMAL1 by CLOCK is necessary for clock function, as well as required to inactivate BMAL1 transcriptional activity (39). PER2 is also acetylated which increases its stability. In addition, BMAL1 is modified by a small ubiquitin-like modifier (SUMO) that leads to its ubiquitylation, subnuclear foci, and increased transcriptional activity

(39). These post-translational modifications are important for the sustainability of the molecular clock and rhythm output.

1.4 Circadian Hierarchy

1.4.1 The Central Clock

The majority of SCN neurons are GABAergic, with minimum glutamatergic neurons and various peptide-releasing neurons (40). The SCN contains a ventral core and dorsal shell, with specific neuronal types in each region. The core receives input from the retina and communicates with the shell. The distinct populations of neurons within the core include the vasoactive intestinal polypeptide (VIP) neurons, calretinin, neurotensin, and gastrin releasing peptide expressed neurons (41, 42). The shell contains arginine vasopressin (AVP) neurons, angiotensin II, and met-enkephalin expressing neurons (41, 42). Neurons in the core and shell have different patterns of projections. Core neurons densely project to the peri-suprachiasmatic area, lateral subparaventricular zone hypothalamus (SPVZ), and ventral tuberal area. Shell neurons densely project to the medial preoptic area, medial SPVZ, and the dorsomedial nucleus hypothalamus (43).

Intriguingly, animals lacking VIP or the VIP receptor (VPAC(2)) have disrupted behavioral rhythms (44), and the addition of a VPAC2 agonist to *VIP*$^{-/-}$ SCN neurons restored rhythms and synchrony (45), suggesting that VIP transmission is involved in synchronizing rhythms in the SCN (46). Similar to

other SCN neurons (47), AVP neurons also have pacemaker qualities as they are involved in setting the speed of the clock. PER proteins are phosphorylated by casein kinases and deletion of theses kinases results in lengthened period in several tissues (32). Interestingly, deletion of the *CK1δ* gene, specifically in AVP neurons, lengthened the free-running period of circadian behavior (48). The opposite phenotype, shortened free-running period, was seen after overexpressing CK1δ in AVP neurons, suggesting a role of AVP neurons in modulating period (48). The above studies reveal the neuronal types underlying the SCN's master pacemaker activity.

1.4.2 Entrainment of the Central Clock

Robert Moore and colleagues identified a direct connection from the eye to the hypothalamus, termed the retinohypothalamic (RHT) tract (49, 50). Moore identified the RHT by following the projection tract from the retina to the bilateral SCN after injecting labelled amino acids into the eye of rats and viewing the anatomy via autoradiography (49). This direct connection suggested a function of the SCN in receiving inputs from external stimuli. Indeed, upon light exposure, the RHT sends signals to the SCN which results in SCN oscillator entrainment (13). Light is the strongest Zeitgeber for SCN entrainment, with the behavioral output being locomotor activity. Entrainment is the synchronization of the internal rhythms to external time cues, such as the light/dark cycle. C57BL/6J mice can

entrain to a 12 hour light: 12 hour dark cycle, with locomotor activity arising in the dark phase and inactivity occurring in the light phase.

In vitro studies showed that after dissociation and culturing of SCN neurons from rats, the neurons were able to fire rhythmically for 7 weeks and had a period of about 24 hours (51). In contrast, control hippocampal cultured neurons were unable to show circadian firing rhythms (51), suggesting specificity of circadian rhythmic firing in SCN neurons. This *in vitro* study highlighted one of the characteristics of SCN neurons; they are able to fire cell autonomously as the cultured SCN neurons had varying periods and phases of firing rhythms (51). SCN neurons can also synchronize their phases as shown in SCN tissue slice culture where communication between neurons in the tissue contributes to the robust output signal in *Cry1*$^{-/-}$ SCN slices (52). The SCN can oscillate without the presence of a Zeitgeber, this endogenous coupling allows for rhythms to continue even in constant conditions.

1.4.3 Peripheral Clocks

The SCN is at the top of the circadian hierarchy. The SCN entrains subordinate brain regions as well as peripheral oscillators (Fig. 1.4). Evidence from circadian gene expression and luciferase reporter analyses in the SCN and peripheral organs showed that the phase of the SCN was earlier than the phase in peripheral tissues (53-55). Although peripheral tissues are entrained by the SCN, they too can oscillate cell autonomously without signals from the central

pacemaker. This was supported by the evidence that peripheral tissues contain similar circadian molecular machinery to that of the SCN (56-58). Additionally, cell culture studies supported the idea of peripheral oscillators (59, 60). A serum shock to rat fibroblast cells induced circadian gene expression (61). Rhythmic expression of several clock-relevant genes was also observed in rat H35 hepatoma cells (61). Yamazaki et al. took this investigation of endogenous peripheral oscillators a step further by showing that peripheral tissues in fact do not need signals from the master pacemaker in order to produce rhythms. Peripheral tissues dissected from a bioluminescent rat reporter under the control of a rhythmic promoter revealed that peripheral tissues can produce rhythms *in vitro*, although damped over time (62). Interestingly, reinstatement of rhythms occurred after introducing fresh medium. The damping of organ-level rhythms over time suggests that the SCN plays a role in rhythm sustainability, possibly by strengthening the cell coupling within a tissue. Indeed, Guo et al. showed that the SCN is required for downstream synchronization of cells within a given tissue (63). Notably, damping of *in vivo* rhythms is unlikely due to signal from the SCN (62, 64, 65).

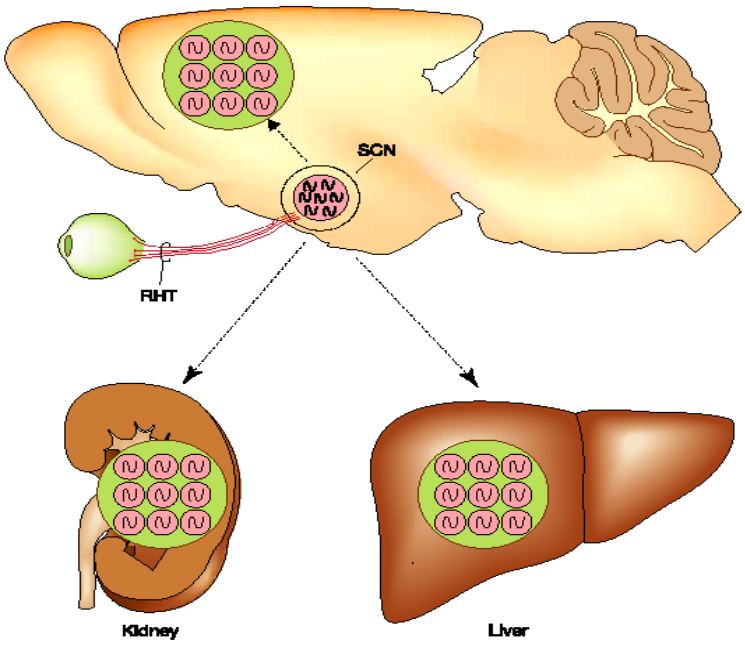

Figure 1.3 Schematic of the mammalian circadian hierarchy

The brain and peripheral organs contain circadian oscillators. Light synchronizes SCN oscillations via input through the retinohypothalamic tract (RHT) to synchronize the SCN to the 24-h day/night cycle. The SCN in turn entrains subordinate oscillators in the brain, as well as peripheral oscillators such as the kidney and liver. Image acquired from Reppert and Weaver, 2002 with permission (13).

In contrast, a study from Yoo and colleagues suggested endogenous cell coupling within a peripheral tissue, as rhythms in PER2::LUCIFERASE (PER2::LUC) liver and lung tissue explants persisted for 20 days, which was not seen previously by Yamazaki et al. (53). Although rhythms persisted for a long period of time, the phases were different within and among animals, suggesting a role for the SCN in synchronizing peripheral cells (53). One must take into account that Yamazaki and Yoo's studies were done with two different transgenic rodent lines, *Per1-luciferase* in rats and PER2::LUC in mice, respectively, which can be attributed to the prolongation or damping of *in vitro* rhythms seen. The studies described above showed that the SCN is not required for peripheral rhythms, but instead acts as a synchronizer for peripheral oscillators.

1.4.4 Entrainment of Peripheral Clocks

Peripheral clock entrainment can occur through SCN humoral factors (66-69). Parabiosis experiments of SCN-lesioned and SCN-intact mice suggested non-neural inputs are sufficient to maintain circadian rhythms in the liver and kidney, but not in the heart, spleen, or skeletal muscle (70); this is interesting as it indicates different responsiveness of various tissues to different signals. Humoral signals have phase-shifting properties. Glucocorticoid hormones are suggested as being one of these phase-resetting blood-borne elements. This was demonstrated in studies showing dexamethasone, a glucocorticoid receptor agonist, causing a phase shift in peripheral tissues, but not in the SCN (66).

Additionally, melatonin is important for rhythmic signaling in the Pars tuberalis as it is involved in the long-term regulation of *Per1* rhythms (71). Research from Sassone-Corsi and colleagues further showed evidence of SCN communication to peripheral tissues by transplanting mouse embryonic fibroblast (MEFs) cells from *Per1* null mice back into a host mouse with intact SCN. The period from the MEFs was that of the host mouse, suggesting that there are factors from the SCN that can modulate period and that there is a hierarchical dominance of the SCN on peripheral tissues (72). Additionally, they performed a control experiment in which they implanted *Per1*$^{-/-}$ MEFs into *Per1*$^{-/-}$ hosts and showed that *Per2* mRNA expression oscillations in *Per1*$^{-/-}$ MEFs had a period and phase that of the *Per1*$^{-/-}$ host (72).

Temperature can also entrain peripheral oscillators (73-75). Real-time bioluminescence recording of PER2::LUC peripheral tissue explants revealed phase resetting and increased amplitude after 38.5ºC temperature pulses (75). Interestingly, the SCN was not reset after temperature pulses, suggesting that the SCN is resistant to temperature-induced phase resetting and that this mechanism of resetting is specific to peripheral organs; this could be due to the strong cell-coupling within the SCN as disrupting SCN cellular communication results in sensitivity to temperature fluctuation (75). Notably, the mechanism in which peripheral organs are reset by warmer temperatures includes the heat shock pathway. Exposing peripheral tissues to warmer temperatures and

simultaneously blocking the Heat shock factor 1 protein with an inhibitor, repressed phase-resetting (75).

Mechanisms of peripheral oscillator entrainment can be independent from the SCN. The dominant Zeitgeber for peripheral organ entrainment is feeding time (76). A seminal study by the Schibler group showed that gene expression rhythms in the liver were reset after a 7 hour advance of feeding time, while the phase of gene expression rhythms in the SCN was unaffected (77). Interestingly, advancing the light/dark cycle under restricted feeding does not reset the liver clock, suggesting that restricted feeding has a more principal role in entraining the liver clock compared to the light/dark cycle (77). Furthermore, liver resetting of animals under restricted feeding occurred even in SCN-lesioned animals, suggesting that the SCN is not required for liver resetting during a restricted feeding diet (77).

1.5 Circadian Rhythms and Disease

1.5.1 Circadian Disruption

Circadian disruption is the disturbance of biological time (78). There are two primary aspects of circadian disruption, misalignment and desynchronization. Circadian misalignment refers to the abnormal phase angle between two or more different rhythms, such as the endogenous SCN rhythms displaying an odd phase angle with the external environment, such as the case of shift work or jet lag (78). Unlike misalignment, internal desynchrony refers to the difference in

period, rather than phase angle, between two or more rhythms. For example, internal desynchrony occurs when the period of the central pacemaker or rhythms are atypically aligned with peripheral tissues (78). Circadian disruption also encompasses external desynchrony which is when there is a period difference between the SCN and peripheral organs with light/dark and fasting/feeding cycles, respectively (78). This disruption can occur at different organizational levels, ranging from molecular rhythms in individual cells and between and within tissues, to behavioral rhythms (79). Examples of how circadian disruption can occur and the adverse health consequences that can result from it will be explained in further detail in section 1.5.2.

1.5.2 Adverse Health Consequences of Circadian Disruption

Human studies of circadian disruption due to clock gene mutations

Human gene association studies showed that single nucleotide polymorphisms (SNPs) within clock genes are associated with metabolic syndrome, cardiovascular disease, and cancer (80-84)**.** Metabolic syndrome includes obesity, dyslipidemia, hyperglycemia, and hypertension (85). A haplotype study from Scott et al. showed that individuals from families with metabolic syndrome have a common haplotype, CAT at position rs4864548 within the *Clock* gene (81). rs4864548 was also highly correlated to disease severity in nonalcoholic fatty liver disease patients and fibrosis score in nonalcoholic steatohepatitis patients (82), as well as a 1.8-fold risk of obesity

compared to controls (83). Complementary studies investigated the association of SNPs in other clock genes, including *Npas2* and *Per2*, with metabolic syndrome in which haplotypes in *Npas2* and *Per2* were associated with hypertension and high fasting blood glucose, respectively (84). Additionally, SNPs in *Per1*, *Per2* and *Cry2* were highly associated with increased risk for breast cancer (80). Altered expression of core clock genes in tumor samples from patients who have these SNPs may be a functional explanation as to why these SNPs are correlated to breast cancer risk (80). The studies described above suggest that there are genetic factors that contribute to risk of disease. It would be interesting to investigate the functional role of these SNPs on tissue-specific circadian rhythms, *in vivo*.

Human studies of circadian disruption caused by environmental factors

Environmental factors also influence circadian rhythms that can result in deleterious health outcomes. Shift workers, people who have atypical work schedules, are more likely to be overweight (86, 87), have increased risk of insulin resistance (88), diabetes (89-91), dyslipidemia (92-94), and breast cancer (95, 96). By shifting activity schedules, sleep and feeding timing become disrupted, which results in endocrine alterations (97). For example, the reduction of lipid metabolism in night shift workers could be due to the low expression of metabolic enzymes required for lipid breakdown during the time when food ingestion now falls, thus resulting in a higher risk of obesity. Shift workers have

rhythm misalignment as they have to entrain their internal rhythms to their work schedules and this entrainment can occur over the span of days or not even at all. This can become problematic especially for night shift workers as certain hormone rhythms lack full re-entrainment to a night schedule (97). Indeed, a study from Weibel et al. showed that cortisol levels were quiescent during the night shift workers' active phase as compared to the high levels of cortisol during the daytime workers' active phase. Additionally, there was an increase in thyrotropin levels in nighttime workers during their active phase compared to daytime workers in which thyrotropin levels were low (97). These data suggest that hormonal rhythms were unable to entrain to the night shift schedule in night shift workers. Although there are studies showing the lack of re-entrainment of circadian rhythms to a night shift schedule, there is still some controversy as other studies argue that night workers are able to entrain to their change in schedule (98, 99), albeit after a certain period of time. Regardless, our current society which demands operations to be functional 24/7 warrants more investigation on the adverse health outcomes of shift workers.

Similar to shift work, chronic jet lag can result in health issues as the internal body rhythms are misaligned with the time zone, thus requiring the internal timing system to shift according to the external environment (100-102). The internal circadian rhythms have to reset to the external time zone and this process can take more than 1 week, resulting in the feeling of jet lag. Interestingly, the severity of jet lag can depend on direction of travel (103). For

example, jet lag is more severe if traveling from West to East, compared to travelling from East to West as it is harder for the endogenous clock to advance its phase than to delay it (103).

To investigate circadian disruption and its effects on behavioral, endocrine, metabolic, and autonomic output rhythms, Scheer et al. performed an experiment in which period length of environmental cycles was lengthened to 28 hours, so subjects ate and slept at all phases of their near-24 h circadian cycle (104). When subjects were misaligned (e.g., eating and sleeping approximately 12 hours out of phase of their normal sleep/wake cycle, hormone rhythms were altered, mean arterial pressure and glucose were increased, and sleep efficiency was reduced, as well as several subjects were considered pre-diabetic (104). Additional evidence by Morris et al. showed that short-term circadian misalignment in healthy adults resulted in increased 24-h blood pressure and inflammatory markers (105). Altered endocrine function and sleep quality, due to circadian disruption, can deplete physical and mental health. Thus, studying circadian disruption and how it can result in adverse health outcomes is necessary.

Briefly, treatment for jet lag, shift work, and sleep disorders (i.e phase-advance sleep or delayed-sleep wake phase), requires phase resetting mechanisms. Light treatment can lead to either a phase advance or a phase delay, depending on the time of day the light is administered. For example, if light is administered early or late within the sleep episode, this can cause a phase

delay or phase advance, respectively (103). Similarly, consuming melatonin pills can either cause a phase advance or a phase delay if taken in the afternoon or in the morning, respectively (103).

Rodent studies of circadian disruption due to clock gene mutations

Rodents are great models for investigating circadian disruption. Similar to humans, genetic perturbations in clock genes or environmental disruption can result in disease phenotypes (106-108). Many of the studies investigating the consequences of clock gene manipulation were done using whole body knockouts of clock genes. For example, young *Bmal1*-knockout (KO) mice have increased weight compared to wild-type littermates (109) and adults have metabolic disturbances that include impaired glucose metabolism and insulin hypersensitivity (109, 110). To address whether the metabolic disturbance in *Bmal1*-KO mice was due to absence of BMAL1 specifically in liver, *Bmal1* was knocked out of liver hepatocytes using Cre-lox technology and an *Albumin-cre* driver (*Alb-Cre*) (109). There were metabolic defects, but behavioral rhythms were still intact, suggesting that *Bmal1* has a specific role in the liver (109). This reinforces the concept of physiological functions operating both under the control of the central pacemaker, as well as, endogenously within peripheral organs.

Like *Bmal1*, *Clock*, *Per*, and *Rev-Erbα* were also manipulated to study the consequences of circadian disruption. Mice with a dominant-negative mutation in *Clock* (CLOCK-Δ19), not only have altered periods lengths of locomotor activity (56, 111-113), they are hyperphagic and show reduced energy expenditure

(114). *Clock* mutants also develop metabolic syndrome (114, 115). Additionally, *Per* gene mutations show varied metabolic outcomes. Although both *Per2*^{Brdm1} and *Per2*^{ldc} lead to a loss of function of *Per2* (22, 116), they display different metabolic outcomes; *Per2*^{Brdm1} mice have metabolic syndrome and *Per2*^{ldc} mice do not (114). Moreover, triple knockout of *Per1*, *Per2*, and *Per3* results in obesity in males when fed a high fat diet compared to wild-type controls (117). Lastly, loss of *Rev-Erbα/β* has been shown to deregulate glucose and lipid metabolism (118). Although there are numerous studies demonstrating the effects of clock gene mutation on disease, a study from our lab showed that disrupting the clock via mutating the casein kinases in GABAergic neurons did not result in adverse metabolic outcomes (38). In this study, mice null of CK1δ and with one copy of CK1ε in GABAergic neurons had longer periods in the central pacemaker, but not in peripheral tissues. The authors were able to separate the rhythms of the central pacemaker from peripheral oscillators as a form of circadian disruption. The lack of adverse metabolic outcomes in the CK1 mutant mice is interesting as one would expect to observe this phenotype as a result of disruption of the molecular clock. This result suggests that there are additional mechanisms that could be contributing to circadian disruption (38). In addition to metabolic syndrome, clock gene manipulation has been shown to increase tumor incidence and progression in rodents (106, 119). These studies demonstrate that genetic manipulation of clock genes in rodents can result in multiple adverse health outcomes, however there are scenarios where this is not the case. A speculation

as to why there are differences in health outcomes between these mutants is that the genes mutated are involved in difference processes, thus depending on the mutation this can result in different outcomes.

Rodent studies of circadian disruption caused by altering environmental lighting

Investigators have used multiple approaches for altering the environment to investigate circadian disruption. Some of the ways the endogenous circadian system can be misaligned in rodents are by lengthening or shortening of the T-cycle (T=period) (120) or by shifting the light/dark cycle (121, 122). For example, West et al. tested for disruption in mice that had altered T-cycles. Although mice were able to entrain to a T=22.5 and T=27 hour light/dark cycles, there was misalignment between the endogenous rhythms and the external environment; mice that entrained to the shorter period had a phase delay and mice that entrained to a longer period had a phase advance in locomotor activity and body temperature rhythms relative to the onset of night (120). The amplitude of the SCN and corticosterone rhythms in mice with the 22.5 hour T-cycle were reduced, but the peripheral tissues produced robust rhythms with the phase consistent with the locomotor activity and physiological rhythms (120). Interestingly, although the peripheral organs seem to be aligned with each other, mice with the 22.5 hour T-cycle showed cardiac dysfunction that include slowed heart rate and lengthened cardiac conduction parameters. Additionally, amplitude and phase of various physiological output genes were altered from mice

entrained to the T=22.5 cycle relative to mice entrained to the T=24 cycle (120). Moreover, slowed heart rate was seen in mice switched from the 24 hour light/dark cycle to constant light and in 24 hour T-cycle mice that had a 2 hour light pulse early in the active phase (120). These findings suggest that misalignment of endogenous rhythms to the external environment, due to aberrant light cycle exposure, can lead to cardiac dysfunction.

Several methods have been used to assess re-entrainment or resetting of the SCN, behavior and peripheral tissues in rodent models (62, 122-124). Studies to investigate resetting are performed by measuring gene expression from a population of animals (121, 125, 126), or by collecting explants from reporter mice and monitoring rhythmic reporter expression *in vitro* (53, 62, 127). A small number of studies also assessed oscillator re-entrainment directly by monitoring reporter rhythms from animals *in vivo* (128-131).

Phase-resetting studies provide information on the time it takes for the circadian system to reset after a phase shift, as well as determine the impact of the shift on endogenous rhythms by placing the rodent in constant darkness after a phase shift (124). Yamaguchi et al. showed that mice were able to reset their locomotor activity faster, after an 8 hour delay in the light/dark cycle, compared to when the phase was advanced 8 hours (122). This study, along with others (62, 132, 133), provided the evidence that behavioral rhythms reset slower when the light/dark cycle is advanced rather than delayed. Mice in the process of resetting their endogenous phase to the new environmental phase are considered “jet

lagged", and chronic jet lag specifically in aged mice, can result in increased mortality rate (134).

Phase resetting can be seen in locomotor behavior, but is also apparent via assessing gene expression and, in reporter lines, bioluminescence rhythms. For example, studies measuring clock gene rhythms from dissected tissues after a phase shift show similar results in phase resetting as in locomotor activity (i.e. clock gene rhythms shift slower when phase is advanced compared to a phase delay) (121).

As far as monitoring phase resetting via bioluminescence, tissues can be dissected from phase-shifted reporter rodent lines and exposed to luciferin *in vitro* to measure their bioluminescence rhythms in real-time, unlike looking at gene rhythms where it is only a snapshot of the rhythm (126). One of the issues with monitoring bioluminescence rhythms *in vitro* is that dissection may reset the clock, especially following phase shifts (123, 135). Thus, monitoring *in vivo* bioluminescence rhythms is critical for our understanding of resetting after a phase shift. Mei et al. showed that tissue phase resetting can be monitored in freely moving mice (129). By injecting a fluorescent reporter, specifically in the VIP neurons of the SCN in mice that had a phase shift, phase resetting of the VIP neurons could be monitored over time (129). Although this technique of monitoring phase resetting in specific cells of freely moving mice was a tremendous step forward in understanding circadian disruption *in vivo*, this approach is very invasive as it requires surgery for viral delivery. Another study,

from the Schibler lab, showed resetting of the liver in freely moving mice after tail vein injection of Adv-Bmal1-Luc virus and an intraperitoneally (i.p) injection of Luciferin (130). This model was able to successfully monitor bioluminescence rhythms in the liver of freely moving mice, however using the tail vein method only infects liver hepatocytes, and so monitoring phase resetting in other tissues is not be feasible with this method (130). Therefore, a mouse model that can monitor specific tissues and cell types *in vivo*, in a less invasive and more feasible manner, is necessary.

1.5.3 The use of Reporter Genes for Studying Circadian Rhythms

The ability to longitudinally monitor circadian rhythms has made it possible to observe how dynamic the circadian system is (136). Monitoring circadian rhythms using a gene reporter dates back to the early 1990s in which bioluminescence rhythms were observed in plants and cyanobacteria. Steve Kay and his group created transgenic plants that had a *luciferase* gene fused to a rhythmic gene (137). They were able to detect bioluminescence rhythms in intact plants. Moreover, Kondo et al. expressed a *luciferase* reporter gene in cyanobacteria to monitor circadian rhythms, and by doing this, discovered that cyanobacteria have similar circadian rhythms to eukaryotes (138). Brandes et al. studied the transcriptional regulation of *per* in *Drosophila melanogaster* by monitoring bioluminescence originating from a *luciferase* gene fused to *per* (139).

Bioluminescence allowed recognition of widespread, functionally independent and entrainable circadian clocks (140).

Investigators utilized clock genes *Per1* and *Per2* as reporters to monitor circadian rhythms in mammalian cell culture and mammals. Due to the widespread expression of *Per1* and *Per2*, these clock genes were good candidates to use as reporters. Monitoring circadian rhythms via bioluminescence output has provided insight on how these molecular clock genes function. For example, monitoring transgenic mice that express *luciferase* under the promoter of *Per1* showed not only bioluminescence rhythms within the SCN but also uncovered a possible post-transcriptional regulation mechanism of endogenous *Per1*, after administering a 6 hour light pulse in the early subjective day (141). The reporter approach was also demonstrated by Yamaguchi et al. where by infusing luciferin in a lateral ventricle and inserting an optical fiber that is attached to a photon counter, above the SCN of a *Per1-luciferase* mouse, they were able to monitor SCN biolumicescence rhythms in the intact brain (142). Gene reporters can also shed light on the phase response to environmental factors. Yamazaki et al. generated transgenic rats that express *luciferase* under the control of the *Per1* promoter. After advancement or delay of the light/dark cycle, the SCN resets at a faster rate than peripheral tissues when observed in tissue culture (62). Central and peripheral oscillators shifting at different rates leads to internal desynchrony and misalignment. Although this was a novel

finding, the fact that dissection can reset the circadian clock should still be taken into consideration.

Per2's promoter fused to *luciferase* also allowed assessment of bioluminescence rhythms in mouse fibroblast cells, which suggest that rhythms in peripheral cells are cell-autonomous (136). Although clock gene promoters are sufficient to produce bioluminescence rhythms, the most widely used reporter model is the PERIOD2::LUCIFERASE (PER2::LUC) mouse that expresses PER2 and LUCIFERASE as a fusion protein. The advantage of PER2::LUC is that it can produce persistent rhythms in peripheral organs as compared to the *Per1-luciferase* tissues where their rhythms damp relatively faster (53, 62). The persistent rhythms seen in PER2::LUC tissues and the damped rhythms seen in *Per1-Luciferase* tissues suggest the absence of regions in the full protein that is promoting rhythm sustainability, or enhancer regions that promote persistent rhythms are absent, respectively (53). PER2::LUC rhythms can also be monitored *in vivo* using the *in vivo* imaging system (IVIS) (38, 143). Shibata's group used IVIS imaging to assess resetting of peripheral tissues after various interventions including restricted feeding, warm baths, different diets, and drugs (74, 131, 143, 144). IVIS imaging is a common technique that we use in the laboratory (38). Other bioluminescence reporters include *Cry1-luciferase* and *Bmal1-luciferase* which also can produce bioluminescence rhythms (136).

In addition to bioluminescence reporters, investigators used fluorescent reporters to monitor circadian rhythms (59, 129, 145-149). Douglas McMahon's

group used the *Per1-EGFP* reporter to monitor rhythms in cells of the mouse SCN and found that expression of *EGFP*, driven by the *Per1* promoter, was suffcient to view gene expression dynamics within clock neurons (145). The advantage of using fluorescent reporters is that it is easier to view subcellular protein localization as fluorescent reporters are quite bright (146, 150). For example, by utilizing the fluorescence reporter PER2::VENUS, Smyllie et al. showed that PER2's mobility and nuclear localization are regulated by casein kinases (146). Additionally, there are many reporter colors to choose from, thus viewing co-localization of two different proteins is more feasible than bioluminescence reporters (150). One of the disadvantages of using fluorescent proteins is that the GFP half life is longer than the half life of luciferase (151), which can be problematic when measuring rhythms. Additionally, fluorescent proteins can produce high background which can confound the study (152). Nevertheless, the circadian field has not only used *Per1-EGFP* transgenic mice to monitor rhythms, but also *Per2-GFP* exressing human fibroblast cells to investigate the role of clock genes in autophagy regulation (153). Transgenic animal reporters are not the only source for monitoring bioluminescence rhythms; viral-mediated delivery of luciferase or fluorescence-encoded reporters has proved to be an efficient approach for viewing rhythms *in vivo*, especially for viewing cell-type specific rhythms in the SCN (129). The disadvantage with using a viral-mediated approach is that surgery is necessary, whether for delivering the virus in the brain or optical fiber implantation (129). This approach is much more

technically difficult and time consuming as compared to using transgenic animals.

1.6 *Albumin D-element binding protein (Dbp)*

Genes such as *Bmal1*, *Npas2*, *Clock*, *Per*, and *Cry* are a part of the core molecular clock and disruption of all members within these gene families may result in altered circadian rhythmicity (Table 1.1). In contrast, rhythmic genes such as *Dbp* do not play such a significant role in maintaining the molecular clock, although it does oscillate and regulate downstream functions, thus ensuring certain physiological processes are occurring at the correct times. *Dbp* is a PAR basic leucine bZIP transcription factor that binds to gene promoters to regulate transcription. *Dbp* is widely expressed, with high levels in the liver. Some of the genes that *Dbp* modulate are involved in regulating metabolism and the oncotic pressure in blood, such as, the 15 alpha-hydroxylase (*CYP2A4*) and coumarin 7-hydroxylase (*CYP2A5*) enzymes (154), and *albumin* (155), respectively. *In vitro* studies by Yamajuku et al. showed that *Dbp* is critical for determining the period length of the clock (156). Indeed, knockout of *Dbp* in mice resulted in a shorter period, however their locomotor activity rhythms were still intact (157). These findings suggest that DBP is not required for circadian rhythms, but is important for determining the period of the clock and modulating circadian gene output.

1.7 Scope of Thesis

Over the years the field of circadian rhythms has expanded our knowledge of the mechanisms that control circadian rhythms and how disruption of these rhythms can negatively affect human health. Although transgenic animal models that report widespread bioluminescence rhythms have been essential for identifying the organ-level impact of circadian disruption, the current models cannot resolve tissue- or cell-specific period or phase differences, *in vivo*. This is a major shortcoming when trying to discern resetting rates between the central pacemaker and specific peripheral organs within the whole animal. To circumvent this, we have developed a conditional mouse model that enables monitoring of circadian bioluminescence rhythms in a tissue- and cell-type specific manner, *in vivo* and in SCN slice culture. The mouse line was generated by CRISPR-Cas9 editing, through which a reporter construct was knocked into the fourth exon of the *Dbp* locus. The reporter construct contains a floxed destabilized *GFP* upstream from a *luciferase* reporter gene, so that after Cre-mediated recombination, the destabilized *GFP* is deleted and *Dbp* and *luciferase* RNA sequences are expressed as a single transcript. Without Cre-recombination, *Dbp* and *GFP* RNA sequences are expressed as a single transcript. The construct also contains a T2A linker that allows for separation of DBP from the reporter protein (GFP or LUCIFERASE). The *Dbp* locus was chosen for manipulation as it is widely and rhythmically expressed in virtually all tissues, it is not necessary for circadian rhythms, and it has high amplitude in

peripheral tissues such as the liver (157-159). This conditional mouse model will be the first of its kind for measuring bioluminescence rhythms in specific tissue- and cell-types, *in vivo*, which will provide a new approach for studying circadian disruption.

CHAPTERS II and III

Generation and validation of a conditional reporter mouse line for studying circadian rhythms

Ciearra B. Smith[1,2], Vincent van der Vinne[1], Adam C. Stowie[3], Mary E. Harrington[4], Tanya Leise[5], Christopher M. Lambert[1], Alec J. Davidson[3], Robert Dallmann[6], and David R. Weaver[1,2]

[1]Department of Neurobiology, [2]Graduate Program in Neuroscience, UMass Medical School, Worcester, MA, USA, [3]Neuroscience Institute, Morehouse School of Medicine, Atlanta, GA, USA, [4]Neuroscience Program, Smith College, Northampton, MA, USA, [5]Department of Mathematics and Statistics, Amherst College, Amherst, MA, USA, [6]MRC Doctoral Training Program in Interdisciplinary Biomedical Research and Warwick Medical School, University of Warwick, UK

Author Contributions

D.R.W and R.D were involved in the conception of the project. D.R.W generated the non-conditional and conditional reporter mice. C.B.S performed northern blot experiments and analyses. D.R.W performed locomotor behavioral assays and analyses. C.B.S and D.R.W performed *in vitro* and *ex vivo* bioluminescence experiments and analyses. V.V conducted *in vivo* bioluminescence rhythm experiments and analyses, as well as helped with the *in vitro* analyses. M.H and T.L performed ambulatory experiments and V.V helped with analyses. A.D and A.S performed SCN cell-type specific bioluminescence rhythm experiments and T.L did the analyses. C.B.S wrote Chapters II and III, with editing from D.R.W.

CHAPTER II

Materials and Methods

Animals and Housing Conditions

All procedures and experiments were reviewed and approved by the Institutional Animal Care and Use Committee (IACUC) of the University of Massachusetts Medical School, Smith College, and Morehouse School of Medicine. Since some of the animal experiments were performed at other institutions, statements indicating approval of the IACUCs Unless otherwise noted, animals were maintained in a 12h light: 12h dark (LD) lighting cycle with access to food (Prolab Isopro RMH3000; LabDiet) and water available *ad libitum*. Zeitgeber Time (ZT) refers to time relative to the lighting cycle. ZT 0-12 is the light phase and ZT 12-24 is the dark phase.

Cre recombinase-expressing lines were obtained from the Jackson Labs and were crossed to mice bearing the conditional (Dbp^{KI}) reporter allele to generate mice expressing luciferase in specific cells or tissues. The following Cre lines were used:

Albumin-Cre (B6.Cg-*Speer6-ps1*$^{Tg(Alb\text{-}Cre)21Mgn}$/J ; JAX 003574), **AVP-IRES2-Cre** (B6.Cg-*Avp*$^{tm1.1(Cre)Hze}$/J; JAX 0023530), and **NMS-Cre** (Tg(Nms-iCre)^{20Ywa}, JAX 027205). These lines direct Cre recombinase expression to hepatocytes, neurons expressing arginine vasopressin, and neurons expressing neuromedin S, respectively. Whole-body deletion of the floxed GFP was achieved by crossing

the conditional reporter allele to a female *Prrx-1Cre* mouse (B6.Cg-Tg(Prrx1-Cre)^{1Cjt}/J; JAX 005584). This caused germline deletion of the floxed GFP, resulting in widespread expression of luciferase from the *Dbp* locus.

Founder PER2::LUC mice with an in-frame fusion of firefly luciferase to PER2, and an SV40 polyadenylation signal (60, 160) were generously provided by Dr. Joseph Takahashi, University of Texas Southwestern Medical School, Dallas. This line was maintained by backcrossing to C57BL/6J mice (JAX 000664).

CRISPR/Cas9 targeting the *Dbp* locus

The mutant allele was generated by CRISPR/Cas9 mediated engineering of the *Dbp* locus. The targeting construct consisted of a 5′ homology arm terminating just 5′ of the *Dbp* stop codon followed by in-frame sequences encoding a T2A linker, LoxP, GFP with the bovine growth hormone polyadenylation signal, LoxP, and Luc2 followed by the 3′-UTR of Dbp (3′ homology arm). C57BL/6J blastocyst were microinjected with the donor construct, short guide RNAs (MmDBPki_gR49f 5′ GCCCAGCATGGGACACTGTGAGG 3′ and MmDBPki_gR69f 5′ AGGCCACCTCCACCCTGCCAGGG 3′), Cas9 mRNA and (in the successful injection set) with Cas9 protein and an inhibitor of non-homologous end-joining (SCR7). A total of 51 mice were generated. Two putative founders were identified using a primer pair internal to the construct (primer pair C, see Table 2.1).

Primer pairs consisting of a primer in flanking DNA, external to the construct, and a primer within the construct were used to confirm that one of these animals had the desired targeting event (primer pairs F and H spanned the 5′ and 3′ ends, respectively). Genomic DNA from this mouse was then amplified using a primer pair flanking the entire construct; sequencing the product confirmed the construct was inserted properly, *in vivo*. The founder carrying the targeted (knock-in or Dbp^{KI}) allele and its offspring were backcrossed to C57BL/6J mice (JAX 000664) for three generations before any intercrossing to reduce off-target mutations. All Cre-expressing lines were on the C57BL/6J background.

To generate mice with germline deletion of GFP (and thus leading to expression of luciferase) throughout the body, a male $Dbp^{KI/+}$ was bred to a *Prrx1-Cre* female (JAX 005584), which we had on hand and which produces germline deletion of floxed alleles at high frequency. Several mice bearing the newly generated Dbp^{Luc} allele were identified and backcrossed to C57BL/6J, selecting against the *Prrx-Cre* allele.

Genotyping

Genotyping was performed by PCR amplification of DNA extracted from ear punches. Amplification products were separated by agarose gel electrophoresis. Genotyping protocols for Cre recombinase and PER2::LucSV have been published previously (38, 40). A primer set (“4A”) capable of detecting all possible *Dbp* allele combinations was used for colony genotyping; each of the

three possible alleles (Dbp^{+} , Dbp^{KI}, Dbp^{Luc}) produces an amplicon of different size with this primer set. Primer sets are listed in Table 2.2.

Generation of Digoxigenin (DIG) DNA Probes and Northern Blot Assay

DIG-labeled DNA probes were generated by PCR in reactions containing 28 μM of DIG-labeled UTP following the manufacturer's protocol (59). Primer sets for PCR amplification are listed in Table 2.3.

WT, $Dbp^{KI/+}$, $Dbp^{KI/KI}$, $Dbp^{Luc/+}$, and $Dbp^{Luc/Luc}$ mice were euthanized by Euthasol injection and liver tissue was collected at 4-h intervals (ZT 2, 6, 10, 14, 18, 22). RNA was isolated from the liver tissue by Trizol extraction (Ambion). RNA was quantitated by Nanodrop. Five micrograms per lane was separated by electrophoresis on a 1.2% formaldehyde gel. RNA was transferred to a nylon membrane (59) and cross-linked by UV exposure. Blots were prehybridized, probed and detected following the manufacturer's protocol (59), bagged and exposed to X-ray film.

Assessing Locomotor Activity Rhythms

Male and female mice of five genotypes (WT, $Dbp^{KI/+}$, $Dbp^{KI/KI}$, $Dbp^{Luc/+}$, and $Dbp^{Luc/Luc}$) were transferred to the experimental room and single-housed with a running wheel. Animals had access to food and water *ad libitum*. Running-wheel activity was monitored using Clock collection software (Actimetrics). Mice were entrained to a 12-h light/12-h dark cycle for 18 days, then were placed into

constant darkness for 15 days. The free-running period for each animal was determined on days 4-15 in DD by periodogram analysis using ClockLab analysis software.

Ex Vivo Imaging of Widespread Bioluminescence Signal

PER2::LUC/+ and *Dbp*$^{Luc/+}$ mice were anesthetized with isoflurane and injected with D-luciferin (i.p., 100 μl at 7.7 mM, Gold Biotechnology) at peak phase of expression, ZT 18 and ZT 11, respectively. Mice were euthanized, and tissues were dissected and imaged using the IVIS-100 imaging system (Xenogen Imaging Technologies) of the University of Massachusetts Medical School Small Animal Imaging Core Facility.

Bioluminescence Recordings from Tissue Explants

Tissue explants were prepared late in the afternoon from PER2::LUC/+ and *Dbp*$^{Luc/+}$ mice housed on a 12-h light/12-h dark lighting cycle. Mice were deeply anesthetized with Euthasol and decapitated. Tissues were dissected and immediately placed in ice-cold 1X HBSS (Gibco). Pituitary gland was subdivided into 4 sections (~2mm^3) with a scalpel and each piece was cultured separately. Lung explants were placed three per dish. Up to three replicate dishes were studied per tissue per animal. Explants were placed on sterile 35-mm Millicell culture plate inserts (Millipore) in a sealed petri dish containing air-buffered bioluminescence medium (161) plus luciferin (100 μM) (Gold Biotechnology) and

incubated at 32ºC. Bioluminescence was measured from each dish for 1 minute every 15 minutes using a Hamamatsu LM-2400 luminometer.

Bioluminescence records were analyzed to determine period and phase. The first 12-h were discarded to exclude acute responses to explant preparation. Photon counts were smoothed to a 3-h running average and baseline subtracted using a 24-h running average. Circadian period was determined from the average of the period between each peak, trough, upward crossing and downward crossing between 24 and 88 hr of recording for each record. Phase was calculated as the clock time of the first peak in the background-subtracted data. Tissues from mice of the two genotypes were studied together in each run.

IVIS Imaging of *In Vivo* Bioluminescence Rhythms and Tissue Signal

IVIS bioluminescence imaging was performed as previously described (38). *Alb-Cre*$^{+}$*; Dbp*$^{KI/+}$, *Dbp*$^{Luc/+}$, and PER2::LUC/+ mice were anesthetized with 2% isoflurane (Zoetis Inc.) and skin covering the liver, kidneys and submandibular glands was shaved. Mice were injected with D-luciferin (i.p., 100 μl at 7.7 mM, Gold Biotechnology) and Dorsal (9 minute post-injection) and Ventral (10.5 post-injection) images were captured from each animal using the IVIS-100 imaging system (Xenogen Imaging Technologies) of the University of Massachusetts Medical School Small Animal Imaging Core Facility. To assess bioluminescence rhythms, anesthesia, luciferin injection and imaging was repeated at 4-8 hour intervals over approximately 30 hours. Experiments to

localize the source of bioluminescence utilized a single injection of luciferin at the time of the expected peak bioluminescence, followed by euthanasia and dissection.

IVIS images were analyzed using Caliper Life Sciences' Living Image software (version 4.4). Region of Interest (ROI) for each mouse was determined and analyzed as previously described (38).

Ambulatory Bioluminescence Rhythms in Liver Reporter Mice

Bioluminescence was measured in freely moving *Alb-Cre*$^{+}$ *; Dbp*$^{KI/+}$ reporter mice using the "Lumicycle *In Vivo*" system (Actimetrics). Each unit contained two PMTs (Hamamatsu H8259-01), and programmable LED lights. A programmable shutter blocked the PMTs during periods of light exposure and to measure 'dark counts'. Each 1-minute dark-count value was subtracted from the counts recorded during the subsequent 14 minutes to obtain the background-corrected count values, to compensate for the effect of temperature fluctuations on PMT signal. Locomotor activity was recorded using passive infrared motion sensors and Clocklab software (RRID:SCR_014309). Animals were checked daily at varied times using an infrared viewer (Carson OPMOD DNV 1.0), or goggles (Pulsar Edge Night Vision Goggles PL75095).

Mice previously housed in 12L:12D were entrained to a skeleton photoperiod (SPP) consisting of four 1-hour light pulses. We used a lighting cycle in which there was illumination during 4 1-hour blocks of the light phase in the

preceding lighting cycle. A skeleton photoperiod was used, as periods of darkness are needed to record bioluminescence. Pulses occurred from ZT 0-1, 2-3, 9-10, and 11-12, so the first and last hours of light in SPP coincided with light onset and offset, respectively in the full photocycle. (e.g., 1L:1D:1L:6D:1L:1D:1L:12D). On the seventh day of SPP entrainment, mice were given analgesics (0.05 mg/kg Buprenorphine and 2.0 mg/kg Meloxicam), anesthetized with 3% isoflurane, shaved from hips to shoulders, and a primed mini-osmotic pump (Alzet Model 1002, 0.25µl per hour, 14 day) containing D-Luciferin (100 mM dissolved in PBS) was implanted subcutaneously. Mice were returned to their cages with a warming disc and were provided soft food during the first 24 hours of recovery. Animals were placed into the LumiCycle *In Vivo* unit 2.5 days after surgery.

To perform long-term and minimally invasive recording of bioluminescence rhythms, delivering the substrate in the drinking water would be ideal. Bioluminescence rhythms recorded from animals administered luciferin in the drinking water could reflect a combination of the temporal pattern of water (and substrate) intake and rhythmicity of luciferase. To determine whether rhythmic substrate intake influences the pattern of bioluminescence, we compared the time of peak bioluminescence between animals receiving continuous administration of substrate (by subcutaneous osmotic mini-pump) with trials in which the same mice receiving luciferin in the drinking water (2 mM) and implantation of a PBS-filled osmotic pump, with the method of administration

being counterbalanced. The circadian phase of peak bioluminescence was determined relative to the peak of locomotor activity by wavelet analysis on the first day in constant darkness.

Additional studies were conducted to assess re-entrainment of the bioluminescence rhythms after a shift of the light-dark cycle. Animals previously entrained to a full 12L:12D lighting cycle were transferred to the skeleton photoperiod described above for several days before study. Skeleton photoperiod lighting conditions were either maintained at the initial phase or advanced by 6 hr. Phase of bioluminescence and locomotor activity rhythms were determined for each day, for each animal, and are expressed as mean and +/- SEM for the group on each day.

Ambulatory bioluminescence data were analyzed using RStudio. A discrete wavelet transform (DWT) was applied to each time series to detrend and to calculate the time of peaks using the wmtsa R package (https://cran.r-project.org/web/packages/wmtsa/index.html), as described (162, 163). The S12 filter was applied on 15-min median binned data; medians were used to reduce the effect of large outliers. Data before the first trough and after the last trough were discarded to avoid edge effects. The peak phase of both the locomotor activity rhythms and bioluminescence rhythms were normalized to day 2 and the average relative peak phase was calculated for each day. Statistical analysis of resetting between locomotor activity rhythms and bioluminescence rhythms were done using a General Linear Model.

Bioluminescence Imaging of SCN explants

Coronal sections containing SCN from *NMS-Cre; DBP*$^{KI/+}$, *AVP-IRES-CRE; DBP*$^{KI/+}$, and *DBP*$^{Luc/+}$ mice were dissected, cultured, and imaged as reported in Evans et al., 2011 (164). Briefly, sections containing SCN (150 μm) were collected from adult mice, cultured on a membrane (Millicell CM; Millipore) in 1.2 mL of air-buffered media containing 100 μM luciferin (Gold Biotechnology), and imaged for 5 days using a Stanford Photonics XR/MEGA-10Z cooled intensified charge-coupled device camera.

Rhythmic parameters of luciferase expression were calculated for each slice and for cell-like regions of interest (ROIs) within each slice using computational analyses in MATLAB (R2018a, MathWorks) as described previously (165). Briefly, to locate and extract data from cell-like ROIs, we employed an iterative process identifying clusters of at least 20 bright pixels after background and local noise subtraction (through application of a 2D wavelet transform using Wavelab 850, (https://statweb.stanford.edu/~wavelab/)) of a slice image summed across 24 h of bioluminescence. To extract time series for the ROI's, each image in the sequence was smoothed via convolution with a Gaussian kernel applied to 12x12-pixel regions and reduced from 512x640 resolution to 256x320. A discrete wavelet transform (DWT) was applied to each time series to remove the trend and to extract the circadian and noise components using the *wmtsa* toolbox for MATLAB (https://atmos.uw.edu/~wmtsa/). The criteria for circadian rhythmicity in the ROI

time series were a peak autocorrelation coefficient of at least 0.2, a circadian component peak-to-peak time between 18 and 30 h, an amplitude above baseline noise (standard deviation of noise component), and a cross-correlation coefficient of at least 0.4 with an aligned sine wave over a 48h window. Peaks of the DWT circadian component were used to estimate peak time of each ROI. Rhythmicity index (RI) is the peak in the autocorrelation of the DWT-detrended time series, corresponding to a lag between 16 hours and 36 hours. RI was calculated as previously described (166).

Table 2.1 Confirming the targeted *Dbp* locus

Primer pair C (Internal to the construct; forward in GFP, reverse in Luc2)	
Forward	5′–CAAGGTGAACTTCAAGATCCGC–3′
Reverse	5′–CCCATGCTGTTCAGCAGCTCG–3′
Primer pair F (Forward in intron 3 outside construct, reverse in T2A sequence)	
Forward	5′–GGAAGCATCTTTTCCAGCTGG–3′
Reverse	5′–TTCCTCTGCCCTCTCCACTGC–3′
Primer Pair H (Forward in Luciferase, reverse in 3- UTR outside construct)	
Forward	5′–GATTCTCATTAAGGCCAAGAAGG–3′
Reverse	5′–CATGGCGAGTTGGTGGAACCAGC–3′

Primer Pair 'confirm' (External to and spanning the entire construct) (Forward in intron 3, reverse in 3′-UTR; both outside the construct)	
Forward	5′–GATGTGTCCTAACAAGCTGGAGC–3′
Reverse	5′–AAGCCACAAGCCTGAACGAGC–3′

Table 2.2 Genotyping primer sets

***Dbp* Primer set 4A: (Common forward primer in exon 4, allele-specific reverse primers)**	
Forward	5′–TGCTGTGCTTTCACGCTACCAGG–3′
Reverse in GFP	5′–AGTCGTGCTGCTTCATGTGGTCG–3′
Reverse in Luc2	5′–TCGTTGTAGATGTCGTTAGCTGG–3′
Reverse in 3′-UTR	5′–TTCAGGATTGTGTTGATGGAGGC–3′
Primer set Clock/Cre {Clock J (internal control) plus Cre-370}	
Cre forward	5′–ACCTGAAGATGTTCGCGATTATCT–3′

Cre reverse	5′–ACCGTCAGTACGTGAGATATCTT–3′
Clock Forward	5′–GCAAGAAGAACTAAGGAAAATTCAAGAGCAA TTCAGATGGTCTGGTCAAGGGCTACAGTT–3′
Clock Reverse	5′–TAGTGCCCTAGATGGCCCTGTTGG–3′
Per2::LUCIFERASE(167)	
Per2 Common Forward	5′–CTGCGAGAGTGAGGAGAAAGGC–3′
Per2 WT Reverse	5′–GGATTTCCTCCTAAACCTCCC–3′
Luc-specific Reverse	5′–GTAGATGAGATGTGACGAACG–3′

Table 2.3 Primer sets for DIG-labeled probe generation

Actin	
Forward	5′–TCAGAAGGACTCCTATGTGGG–3′
Reverse	5′–GATCCACACAGAGTACTTGCG–3′
Dbp	
Forward	5′–AATGACCTTTGAACCTGATCCC–3′
Reverse	5′–TCACAGTGTCCCATGCTGGG–3′
GFP	
Forward	5′–CTGAAGTTCATCTGCACCACCG–3′
Reverse	5′–GTGCTCAGGTAGTGGTTGTCGG–3′
Luc2 (Luciferase)	
Forward	5′–GCTTCGAGGAGGAGCTATTCTTGC–3′
Reverse	5′–CAGCAGGATGCTCTCCAGTTCGG–3′

CHAPTER III

Results

Generation of conditional and non-conditional *Dbp* reporter mice

CRISPR/Cas9 genome editing was used to introduce a bifunctional reporter into the mouse *Dbp* locus (Fig 3.1). *Dbp* was chosen as it is widespread and rhythmically expressed, as well as, knockout of this gene does not result in arrythmicity (157). The reporter was engineered at the stop codon of *Dbp*, and consists of a T2A sequence (to allow expression of separate proteins from a single transcript (168)), *GFP* sequence flanked by loxP sites, and a downstream *luciferase* gene. In the absence of Cre-mediated recombination, DBP and GFP are expressed as separate proteins. After Cre-mediated recombination, the floxed GFP is removed, and *luciferase* is expressed from the *Dbp* locus, as well as *Dbp* itself. Sequencing of genomic DNA and the results below confirm successful generation of the reporter allele and the Cre-dependence of luciferase reporter activity.

Dbp transcript and circadian locomotor activity rhythms are not altered in reporter mice

For a reporter line to be useful in analysis of circadian rhythmicity, the genomic manipulation must not by itself alter circadian rhythms. To verify this for our newly generated reporter line, we assessed the integrity and rhythmicity of the *Dbp* transcript and determined the free-running period of locomotor activity

rhythms in constant darkness. WT, *Dbp*$^{KI/+}$, *Dbp*$^{KI/KI}$, *Dbp*$^{Luc/+}$, and *Dbp*$^{Luc/Luc}$ mouse lines were used for these analyses. *Dbp*$^{KI/+}$ and *Dbp*$^{KI/KI}$ are reporter lines that express a *GFP*-containing transcript either on one allele or both, and the *Dbp*$^{Luc/+}$ and *Dbp*$^{Luc/Luc}$ express a *Luciferase*-containing transcript.

RNA was isolated from livers collected at 4-h intervals over 24-h from male WT and reporter mice. Northern blots were prepared and probed for *Dbp* and *Actin* (loading control). Blots were generated and probed for *GFP* and *luciferase* to confirm the identity of the bands (data not shown).

As expected, transcript sizes were different for the various alleles, with *GFP*-containing transcripts and *luciferase*-containing transcripts migrated more slowly than WT transcripts (Fig. 3.2a). Peak levels of *Dbp* expression occurred at ZT 10 in all genotypes, as expected based on previous studies (157, 158) (Fig. 3.2b, 3.2c, 3.2d). Comparison of the band intensity between WT and reporter-containing transcripts within heterozygous animals indicates that the signal intensity for the two bands was comparable; strongly suggesting that transcript regulation was not dramatically altered by the reporter sequences (Fig. 3.2e).

To ensure that free-running rhythms were not disrupted, WT and reporter mice were entrained to a 12-h light/12-h dark cycle and then placed into constant darkness (DD). The free-running period lengths in DD did not differ significantly between WT and reporter mice of either sex (Fig. 3.3), suggesting that incorporation of the reporter sequences into the *Dbp* locus did not alter circadian locomotor activity rhythms.

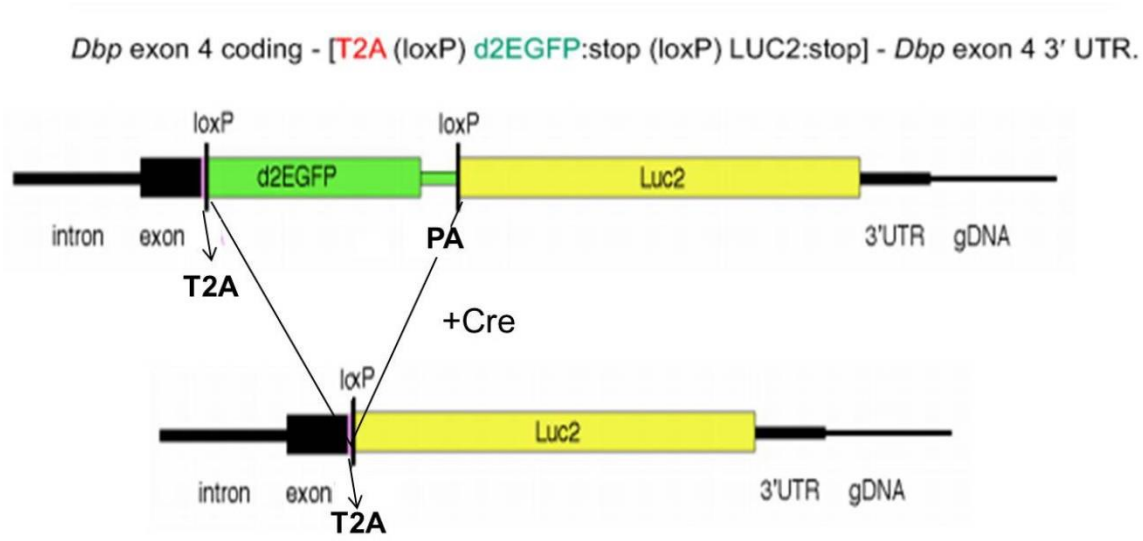

Figure 3.1 The luciferase reporter construct

The luciferase reporter construct contains a destabilized *GFP* with an artificial polyadenylation site (PA), flanked by loxP sites. Downstream of *GFP* is a *luciferase* reporter gene. Without Cre-mediated recombination *Dbp* and *GFP* are expressed as a single transcript. With Cre recombination *Dbp* and *luciferase* are expressed as a single transcript. The T2A linker allows for separation of DBP from the reporter proteins (GFP or LUCIFERASE).

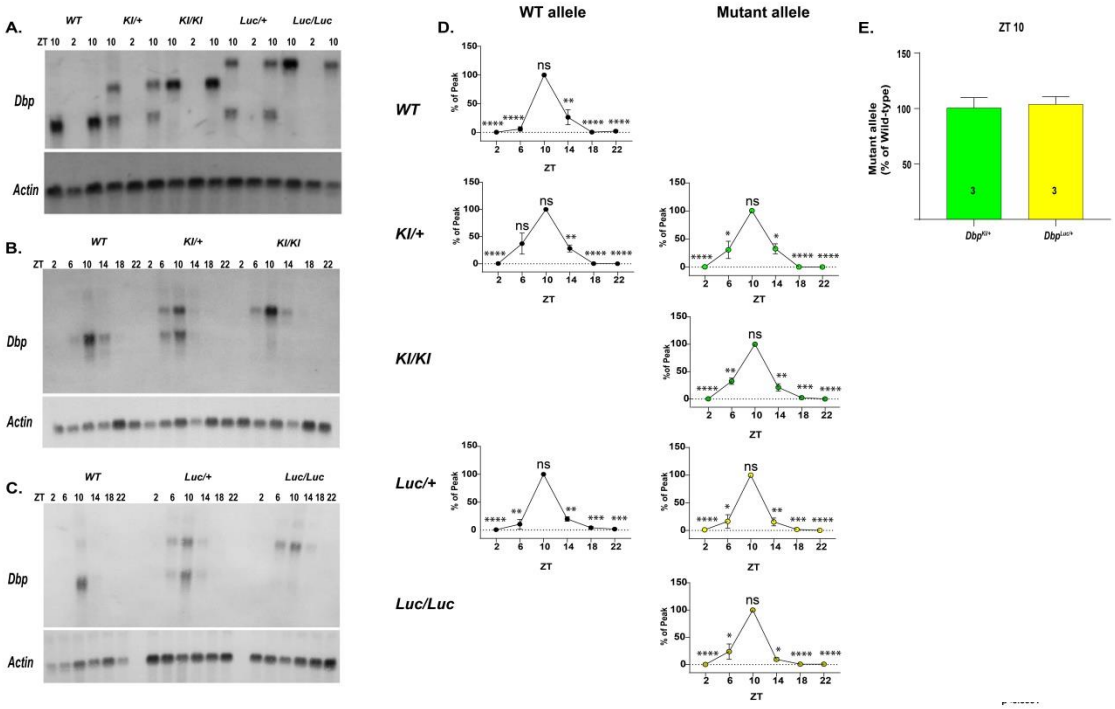

Figure 3.2 *Dbp* rhythms are not altered in reporter mice

A. Representative Northern Blot of *Dbp* mRNA collected from WT and reporter mouse liver at ZT 2 and 10. For each genotype, there are two samples at ZT 10 and one sample at ZT 2. **B.** and **C**. Representative Northern Blots of *Dbp* mRNA collected from WT and reporter mouse liver at each ZT shown. **D.** Quantification of *Dbp* mRNA levels relative to *Actin* mRNA levels. Results are expressed as percent of the peak within each of 6 blots. **E.** Quantification of the *Dbp* reporter allele intensity as a percentage of the WT allele in individual $Dbp^{Kl/+}$ and $Dbp^{Luc/+}$ reporter mice. Results are expressed as percentage of the WT allele from 3 ZT 10 samples per genotype. One-sample t-tests (vs 100%) were used for statistical analyses. ns, $p > 0.05$, *$p<0.05$, **$p<0.01$, ***$p<0.001$, ****$p<0.0001$.

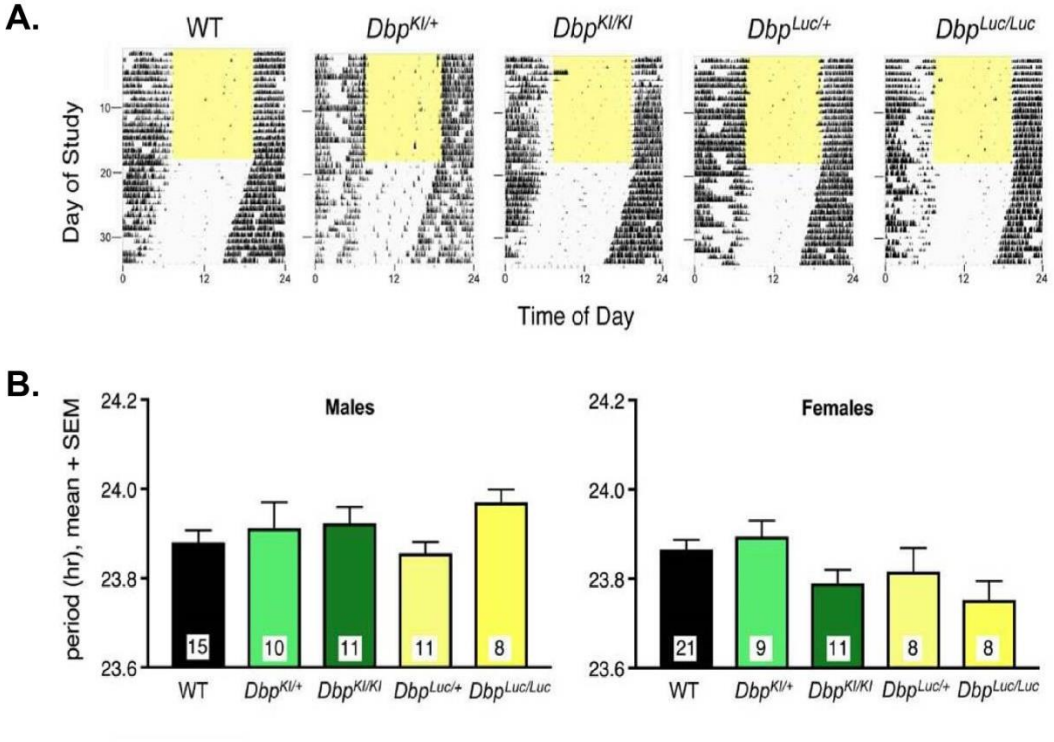

Figure 3.3 Reporter mice do not have altered period

A. Representative single-plotted actograms of WT and reporter mice entrained to a 12-h light/12-h dark cycle. After entrainment, mice were placed in constant darkness to measure their free-running period. Period of light exposure are indicated by yellow shading. **B.** Quantification of the period of male and female WT and reporter mice. Data are expressed as the mean + SEM. Sample size is located inside each bar. One-way ANOVA's with Dunnett's test were used for statistical analysis. $p>0.05$ for each sex.

Dbp$^{Luc/+}$ reporter mice have widespread bioluminescence signal

To rapidly assess the anatomical extent of luciferase expression in *Dbp*$^{Luc/+}$ reporter mice, we performed *ex vivo* IVIS imaging. PER2::LUC/+ mice were included as a positive control. Mice were injected with luciferin (i.p) at the anticipated time of peak expression (ZT 11-12 for *Dbp*$^{Luc/+}$, ZT16-18 for PER2::LUC/+ mice). Ten minutes after substrate injection, mice were euthanized, dissected and tissues were spread out to localize bioluminescence signal. Widespread bioluminescence signal was apparent in both *Dbp*$^{Luc/+}$ and PER2::LUC/+ reporter mice (Fig. 3.4). The data are displayed as two replicate images. These data show the capability of the *Dbp*$^{Luc/+}$ reporter line to produce robust bioluminescence signal, *ex vivo*.

Dbp$^{Luc/+}$ reporter mice have rhythmic bioluminescence in pituitary and lung tissue explants

Reporter mice such as the PER2::LUC/+ have been used to monitor tissue rhythms *in vitro* (53). In a number of mouse tissues, *Dbp* gene expression peaks earlier than *Per2* (158, 169, 170). To determine if this phase difference was preserved between the reporter lines, we compared the phases of PER2::LUC/+ and *Dbp*$^{Luc/+}$ tissue explants *in vitro* (Fig. 3.5). Pituitary and lung were dissected from PER2::LUC/+ and *Dbp*$^{Luc/+}$ mice and bioluminescence rhythms were measured at 15-min intervals for 4 days. As expected, bioluminescence rhythms were observed in both pituitary and lung explants. Importantly, bioluminescence

rhythms in *Dbp*$^{Luc/+}$ explants peaked earlier (~ZT 12) than in PER2::LUC/+ tissue explants (~ZT 18). These data indicate that the *Dbp*$^{Luc/+}$ reporter line not only has *in vitro* bioluminescence rhythms, but also has the expected relative phase. Unexpectedly, the period of PER2::LUC/+ explants was significantly longer than the period of *Dbp*$^{Luc/+}$ in both tissues (Fig 3.5c). One speculation is that because PER2::LUC is a fusion protein, this can disrupt interactions between PER2 and post-translational modifiers that play important roles in modulating period.

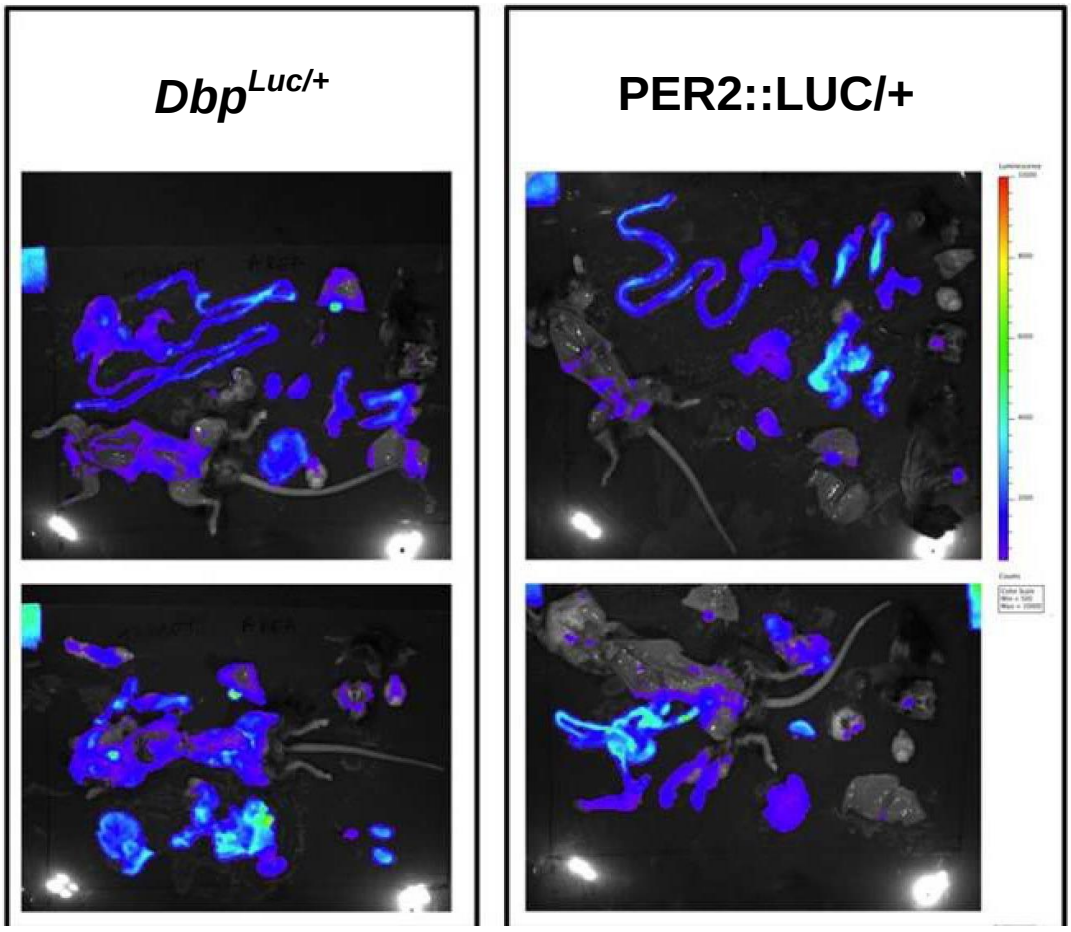

Figure 3.4 Widespread bioluminescence signal in *Dbp*$^{Luc/+}$ and PER2::LUC/+ reporter mice

Ex vivo IVIS imaging of *Dbp*$^{Luc/+}$ and PER2::LUC/+ reporter mice at peak times ZT 11 and ZT 18, respectively. Mice were injected intraperitoneally with luciferin, euthanized, and organs were spread out for IVIS imaging. Bioluminescence signal was widespread in both genotypes. Images represent two different mice for each genotype. The white objects in the lower corners of the images are light artifacts. *Dbp*$^{Luc/+}$ image is a representative of 10 mice. PER2::LUC/+ image is a representative of 6 mice.

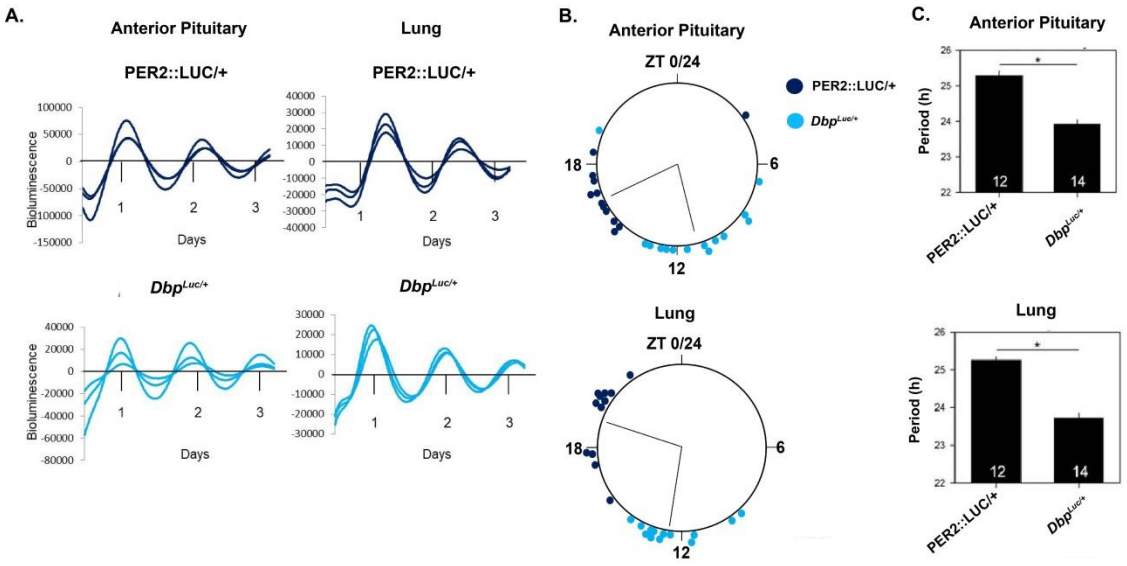

Figure 3.5 *Dbp*$^{Luc/+}$ bioluminescence rhythms from tissue explants have an earlier phase than PER2::LUC/+ rhythms *in vitro*

A. Representative graphs showing bioluminescence rhythms in anterior pituitary and lung of the PER2::LUC/+ and *Dbp*$^{Luc/+}$ mice (done in triplicate). **B.** Circular graphs, expressed in ZT, of *in vitro* bioluminescence rhythms. Dark blue circles are PER2::LUC/+ tissue explants and light blue circles are *Dbp*$^{Luc/+}$ tissue explants. n=12-14. To compare phase between genotypes, Watson-Williams tests were used; $p<0.001$ for each tissue. **C.** Quantification of period in PER2::LUC/+ and *Dbp*$^{Luc/+}$ pituitary and lung tissue explants. Sample sizes are located within each bar. To compare period between genotypes, a General linear model was used; *$p<0.05$ for each tissue.

Dbp$^{Luc/+}$ reporter mice have widespread bioluminescence rhythms

Next, we investigated whether bioluminescence rhythms are apparent *in vivo* in *Dbp*$^{Luc/+}$ mice, with PER2::LUC/+ mice included as a positive control. At 4-6 hour intervals spanning ~30 hours, mice were injected with luciferin, anesthetized and imaged at various ZTs. Mice were returned to their home cage in 12L:12D between images. Both *Dbp*$^{Luc/+}$ and PER2::LUC/+ mice displayed robust bioluminescence rhythms (Fig. 3.6a,b,d), and from both reporters, the areas expressing highest levels of bioluminescence in these images were the liver, intestines, submandibular gland and kidneys. Note, however, that small tissues and those in areas not shaved would not be readily detected, with either reporter. As seen in tissue explants, the phase of *Dbp*$^{Luc/+}$ was earlier than PER2::LUC/+ mice, with *Dbp*$^{Luc/+}$ peaking at ZT 11 and PER2::LUC/+ peaking at ZT 17 (Fig. 3.7). The peak time of PER2::LUC/+ is also similar to what is seen in the literature (171, 172).

Alb-Cre^{+} *; Dbp*$^{KI/+}$ reporter mice have liver-specific bioluminescence rhythms

A tissue-specific reporter will aid in monitoring rhythms of smaller tissues that would otherwise be drowned out by the signal from larger surrounding tissues. We hypothesized that crossing the *Dbp*$^{KI/+}$ mouse to a mouse expressing Cre solely in the liver (*Alb-Cre*$^{+}$ *; Dbp*$^{KI/+}$), would lead to liver-specific luciferase

expression. After injecting luciferin intraperitoneally into *Alb-Cre*$^{+}$ *; Dbp*$^{KI/+}$ ("liver reporter") mice and capturing images at different ZTs, we observed bioluminescence rhythms only in the liver (Fig. 3.6c,d). The peak phase of the liver reporter bioluminescence rhythm is ZT 11, similar to the peak phase from several organs recorded from *Dbp*$^{Luc/+}$ mice and earlier than tissues from PER2::LUC/+ mice (Fig. 3.7). The peak phase of *Alb-Cre*$^{+}$ *; Dbp*$^{KI/+}$ liver bioluminescence also complements what we see at the mRNA level. Notably, *ex vivo* IVIS imaging confirmed that bioluminescence signal is indeed originating exclusively from the liver (Fig. 3.8). There was no apparent bioluminescence signal in Cre-negative mice (data not shown). These data show the utility of the *Dbp* reporter mice in monitoring circadian rhythms in a tissue-specific manner, *in vivo*.

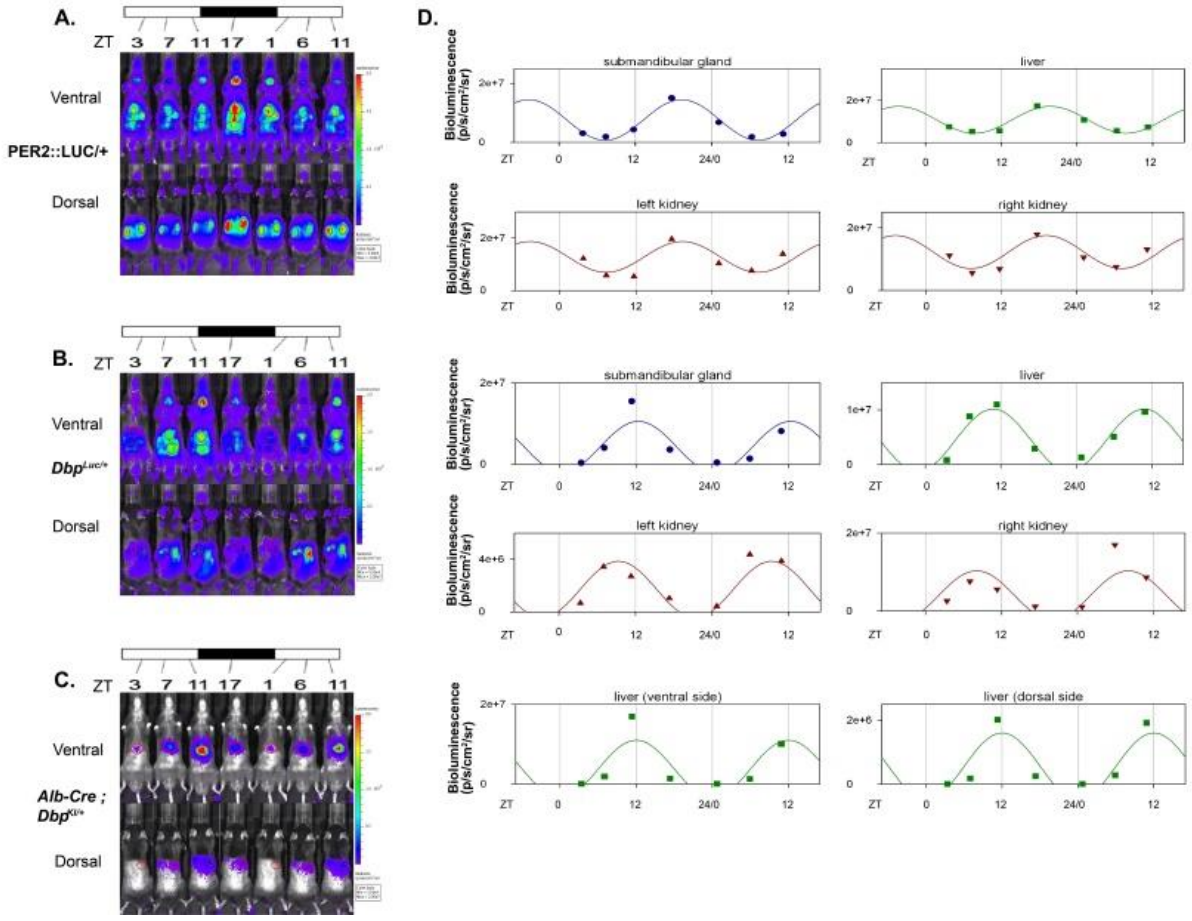

Figure 3.6 Representative *in vivo* bioluminescence rhythms

A-C. IVIS images captured at 4-6 hr intervals from a representative mouse of each genotype. **A.** PER2::LUC/+, **B.** *Dbp*$^{Luc/+}$, **C.** *Alb-Cre*$^{+}$ *; Dbp*$^{KI/+}$. Ventral views (at 9 min after luciferin injection) and dorsal views (at 10.5 min after injection) are shown for each mouse. **D.** Plots of bioluminescence signal vs. time for the animals in Panels A-C. Curve-fitting to determine peak phase performed as described in Methods. Bioluminescence rhythms are apparent from Submandibular gland, Liver, and Kidneys of PER2::LUC/+ and *Dbp*$^{Luc/+}$ reporter mice, and from liver of *Alb-Cre*$^{+}$ *; Dbp*$^{KI/+}$ mice.

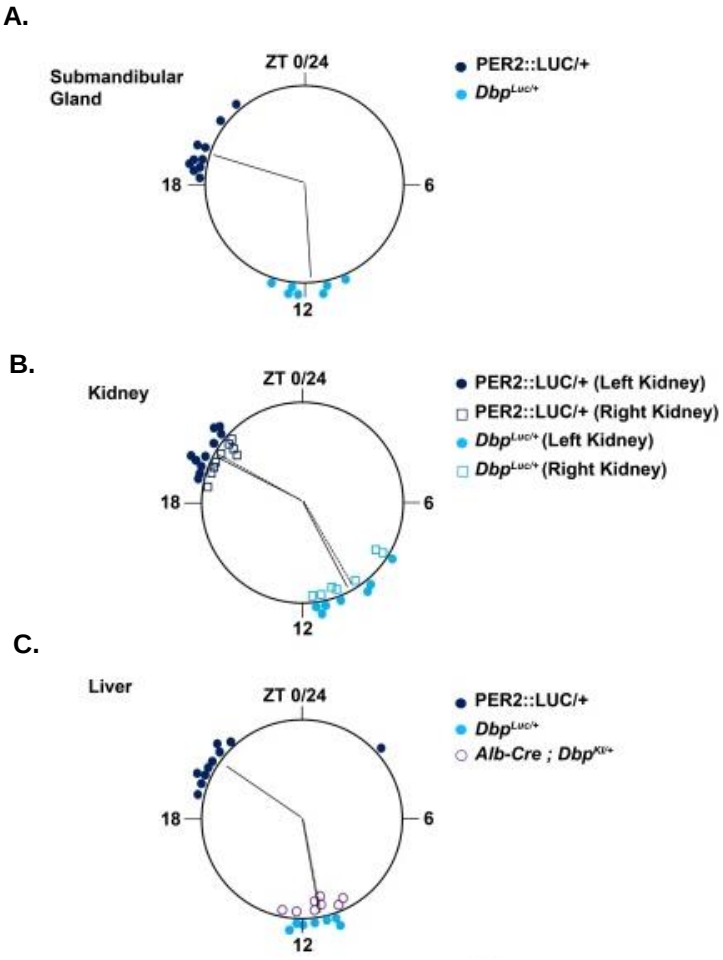

Figure 3.7 Summary of peak bioluminescence

A-C. Circular graphs displaying ZTs of peak bioluminescence from PER2::LUC/+, *Dbp*$^{Luc/+}$, and *Alb-Cre*$^{+}$ *; Dbp*$^{KI/+}$ tissues. **A.** Submandibular gland, **B.** Kidneys, and **C.** Liver. n=7-10. To compare phase between genotypes for each tissue, Watson-Williams tests were used. For all comparisons PER2::LUC/+ differed from *Dbp*$^{Luc/+}$ and *Alb-Cre*$^{+}$ *; Dbp*$^{KI/+}$ significantly (p=0.002). There was no significant phase difference between *Dbp*$^{Luc/+}$ and *Alb-Cre*$^{+}$ *; Dbp*$^{KI/+}$ tissues.

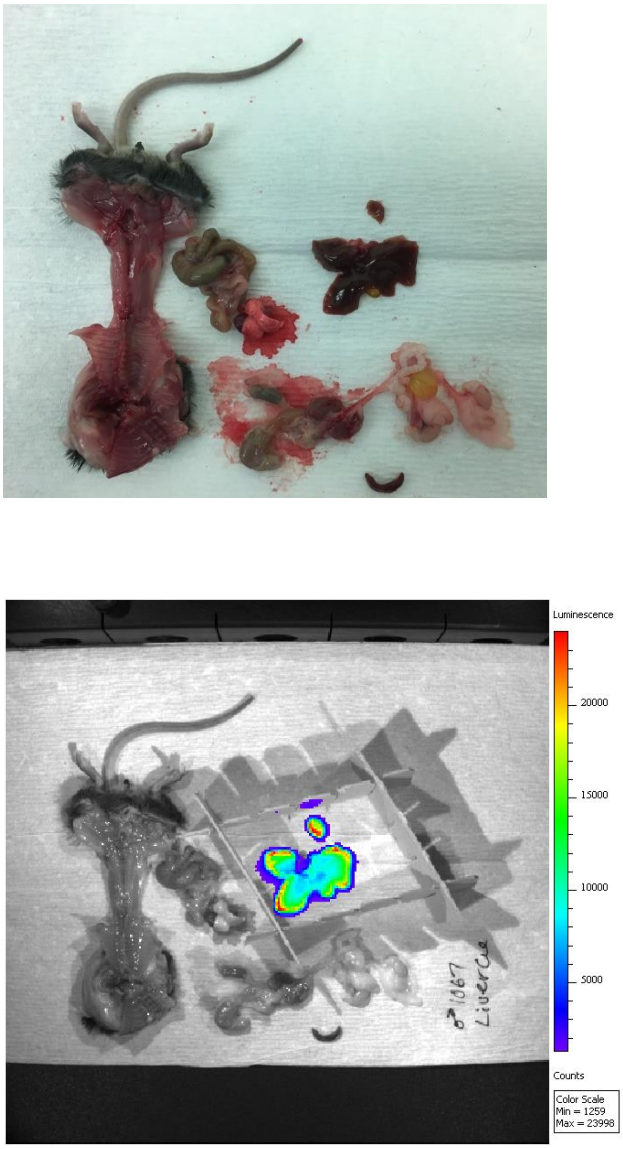

Figure 3.8 Liver-specific bioluminescence signal of *Alb-Cre ; Dbp$^{KI/+}$* liver reporter mouse at peak expression time

Ex vivo bright field (top) and IVIS (bottom) images of *Alb-Cre ; Dbp$^{KI/+}$* liver reporter mouse. At ZT 11, the liver reporter mouse was injected with luciferin (i.p), euthanized, and organs were spread out for imaging. The bioluminescence signal is coming exclusively from the liver. Image is a representative of 10 mice.

Monitoring *in vivo* tissue bioluminescence rhythms from awake, behaving mice

Addressing issues of internal desynchrony and phase misalignment of oscillators will require monitoring the dynamics of tissue resetting over time after a phase-shifting stimulus. The use of IVIS imaging for repeated assessments of organ-level regions of interest over multiple days is feasible but requires multiple, potentially disruptive anesthesia sessions per circadian cycle and intensive effort over several cycles. IVIS imaging has generally been relegated to assessing phase of reporter gene oscillations on relatively few occasions after a shifting stimulus (143, 173). An attractive alternative is to perform long-term, non-invasive bioluminescence recordings, as pioneered by Saini et al. (130). Our development of a Cre-dependent luciferase reporter allows monitoring bioluminescence rhythms from specific tissues over long periods. Here, we show the usefulness of this reporter line for monitoring rhythms in hepatic gene expression, using *Alb-Cre ; Dbp*$^{KI/+}$ "liver reporter" mice.

We first determined that administration of luciferin (2 mM) in the drinking water did not significantly influence the phase of recorded bioluminescence rhythms, relative to rhythms recorded from when the same mice received luciferin from an implanted mini-osmotic pump (Alzet Model 1002, 0.25 µl per hour, containing 100 mM luciferin). There was no difference in peak phase based on whether luciferin was delivered in the drinking water or by mini-osmotic pumps (ZT 8.75 +/- 0.54 and ZT 8.76 +/- 0.5, respectively; t-test, $p>0.05$). Thus, the presumed behavioral rhythm of substrate intake, secondary to the rhythm of

water intake, does not influence the phase of the bioluminescence rhythm from liver reporter mice; subsequent studies used luciferin administered in the drinking water.

We next assessed the rate at which hepatic bioluminescence rhythms re-entrained after a 6-hr phase advance of the skeleton photoperiod lighting cycle. Control mice remaining in the original (non-shifted) lighting regimen had a stable phase of hepatic bioluminescence, with peak bioluminescence levels occurring at the end of the circadian day (Fig 3.9). In contrast, phase-shifted mice displayed a gradual phase-advance in both locomotor activity rhythms and hepatic bioluminescence rhythms. Notably, on day 9 there is a significant difference in phase resetting between locomotor activity rhythms and bioluminescence rhythms. Locomotor activity rhythms re-entrain fully by day 10 and hepatic bioluminescence rhythms lag behind: the liver rhythms only shift substantially toward the target phase on day 7 after the shift (Fig. 3.9). This provides clear evidence for internal misalignment of SCN-driven behavioral rhythms and rhythms in one peripheral oscillator, the liver. To our knowledge, these data are the most clear ever produced in showing the time course of internal misalignment and recovery after a phase shift, due to the unprecedented ability to monitor rhythmicity from a peripheral oscillator over days, while simultaneously recording an SCN-driven behavioral rhythm. Future studies to compare the response of additional tissues will help to decipher the response of the hierarchical, multi-oscillatory circadian system to disruptive stimuli.

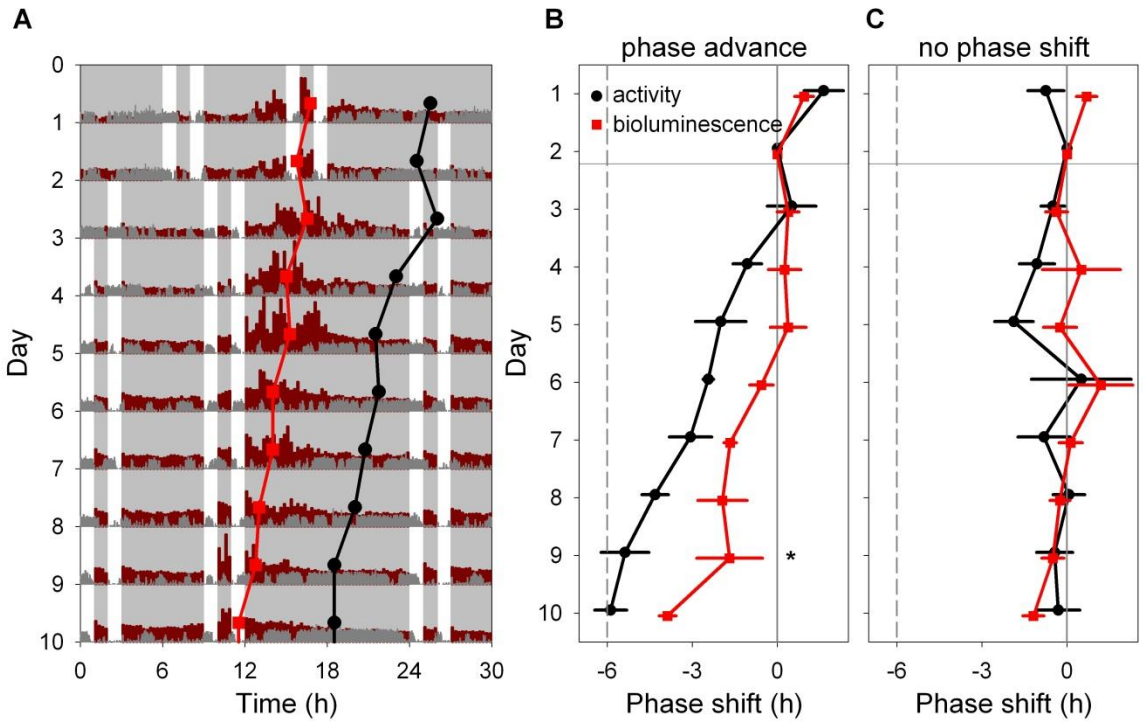

Figure 3.9 *Alb-Cre ; Dbp$^{KI/+}$* mouse liver resets more slowly than locomotor activity after a 6-h light/dark phase advance

A. Representative double-plotted actogram showing locomotor activity and bioluminescence of an *Alb-Cre ; Dbp$^{KI/+}$* liver reporter mouse before and after a 6-h advance of the skeleton photoperiod. Mice previously exposed to a 12L:12D lighting cycle were transferred to a skeleton photoperiod (four 1-h periods of light per 24-h day, as indicated in white), and then the skeleton photoperiod was advanced by 6 h. **B.** Peak phase of locomotor activity rhythms gradually reset after a 6-h phase advance in the skeleton photoperiod and liver bioluminescence rhythms shift but do not reset completely. **C.** Peak phase of locomotor activity and bioluminescence rhythms from mice that were not shifted. Peak phases were determined by wavelet analysis. n=4. Values are mean +/- SEM. The resetting of locomotor activity rhythms and bioluminescence rhythms were compared using a General Linear Model. *p<0.05.

Cell-type specific bioluminescence rhythms in reporter mouse SCN explants

The SCN is a heterogeneous nucleus containing neurons that secrete different neurotransmitters, neuropeptides, cytokines, and growth factors (174). Two neuronal types present in the SCN are neurons expressing Neuromedin S (NMS) and neurons expressing Arginine Vasopressin (AVP). To determine if we can monitor bioluminescence rhythms within specific subpopulations of SCN neurons, we generated *NMS-iCre* ; $Dbp^{KI/+}$ mice and *AVP-IRES2-Cre ;* $Dbp^{KI/+}$ mice. *In vitro* slice culture shows global LUCIFERASE expression in the SCN of $Dbp^{Luc/+}$ reporter mice (Fig. 3.10a,b). For the conditional mice, LUCIFERASE expression was apparent in a subset of cells within the SCN (Fig. 3.10a,b). The anatomical pattern of bioluminescence signal in the SCN differed based on the Cre line used, consistent with the expected distribution for each neuronal subtype (174, 175). Peak time of bioluminescence was assessed in individual neurons. NMS neurons peaked later than both AVP neurons and the SCN as a whole (Fig. 3.10c). Additionally, NMS cells had a higher rhythmicity index than AVP neurons and the SCN as a whole (Fig. 3.10d). These data show the utility of this conditional mouse model for monitoring bioluminescence rhythms in a cell-type specific manner. Furthermore, they reveal unanticipated phase and amplitude differences among neuropeptide-containing SCN subpopulations. Future studies monitoring neuronal subpopulations following phase-shifting stimuli (applied *in*

vivo or *in vitro*) will help unravel the complicated cellular responses that underlie phase resetting of the central circadian pacemaker.

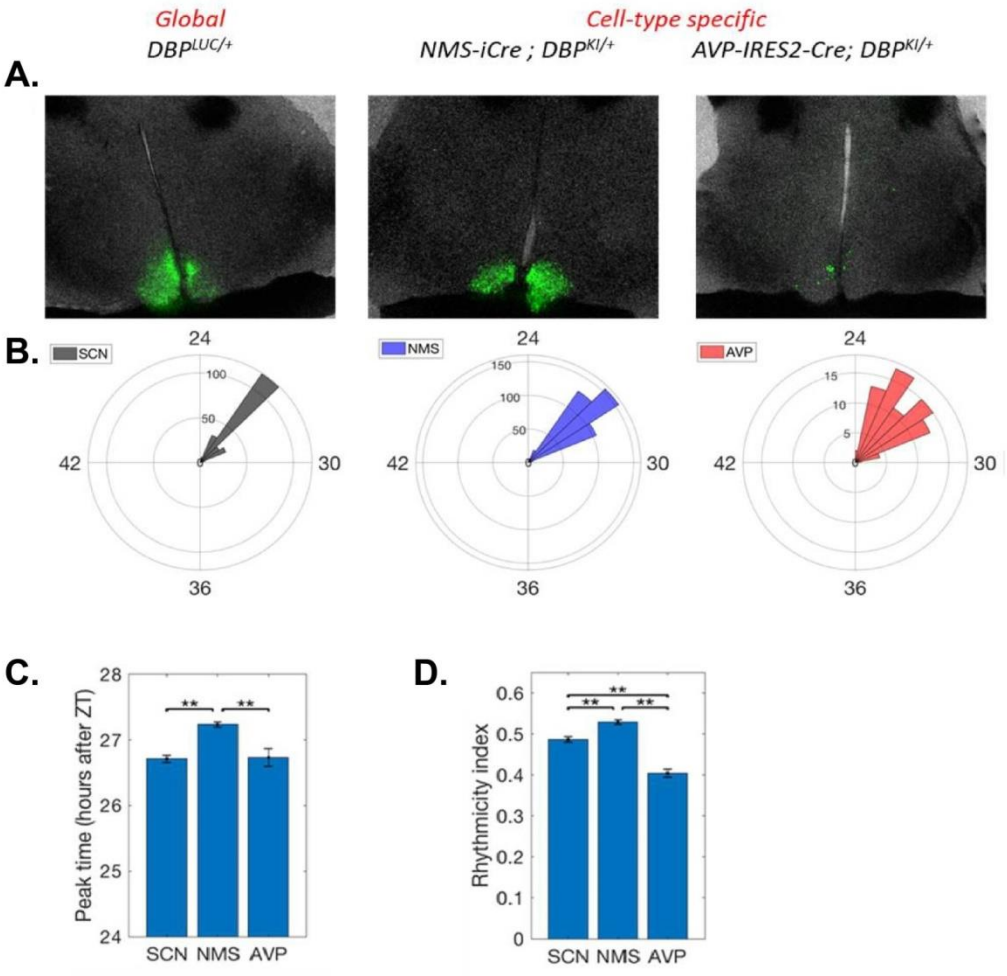

Figure 3.10 Cell-type-specific imaging of LUCIFERASE expression in SCN slices

A. 24h summed bioluminescence overlaid onto bright field images in *DBP*$^{Luc/+}$ (global expression, left), and in specific subsets of SCN neurons (NMS+ cells, center; AVP+ cells, right). **B.** Circular phase frequency histograms indicating the number of neurons recorded and when each peaked relative to the light-dark cycle the mice were housed in prior to sacrifice. Numbers >24 are used to indicate that these are *in vitro* measures plotted relative to previous *in vivo* lighting conditions. **C.** Mean peak times by genotype. **D.** Mean rhythmicity index by cell type. n = 4,9,8 slices for *DBP*$^{Luc/+}$, *NMS-iCre; DBP*$^{KI/+}$, and *AVP-IRES2-Cre; DBP*$^{KI/+}$, respectively. ANOVA with multiple comparisons was used for statistical analysis. **p<0.01.

CHAPTER IV

Discussion and Future Directions

4.1 Summary of findings

The circadian timing system is hierarchical and consists of endogenous oscillators that produce circadian rhythms at the molecular, cellular, tissue, systemic, and behavioral levels (176, 177). Both the SCN and peripheral tissues, including the kidneys and liver, have the capacity to endogenously generate self-sustained oscillations. The SCN, containing the central pacemaker, can entrain subordinate brain and peripheral oscillators by controlling systemic rhythms in behavior and physiology. Through direct communication of light stimuli via the RHT, the SCN rhythms can be entrained (13). If the SCN is exposed to light at biologically inappropriate times, this can reset the SCN and in turn peripheral tissues become desynchronized. Misalignment or desynchrony of these rhythms are termed circadian disruption. Circadian disruption has shown to increase the risk of various diseases, such as metabolic syndrome, cardiovascular disease, cancer, and mental health issues (85, 105, 108, 178-180). Thus, it is critical that we understand circadian disruption in hopes of developing therapies that can modulate resetting rates and prevent downstream adverse health outcomes.

Circadian rhythms' research has utilized bioluminescence and fluorescence reporter mice to monitor circadian rhythms in a host of model

systems. The most widely used reporter mouse for monitoring circadian rhythms is the PER2::LUC reporter mouse (53). PER2::LUC is a fusion protein in which *luciferase* is expressed under the *Per2* promoter. *In vitro* bioluminescence assays demonstrate rhythms in PER2::LUC tissue explants, including the SCN and liver (53). Additionally, the PER2::LUC mouse has been used to demonstrate bioluminescence rhythms *in vivo* in the liver, kidneys and submandibular gland (131). Although the PER2::LUC mouse produces a robust, and rhythmic, bioluminescence signal, the presence of the PER2::LUC reporter throughout the body does however limit its utility when assessing rhythmicity in specific tissues. For most tissues of the body, dissection is required to enable assessment of rhythmicity of the tissue of interest. Since tissue dissection followed by *ex vivo* rhythm assessment can cause resetting of the local clock, this method is not ideal when studying the effects of circadian disruption on tissue rhythmicity. In addition, *ex vivo* culturing of tissues doesn't enable the assessment of rhythmicity within the context of the hierarchical clock system. A better way of studying the effects of circadian disruption on individual tissue rhythms is by monitoring rhythms in a tissue-specific manner, *in vivo*. Various approaches have previously been used to monitor rhythms *in vivo*, such as a fluorescence reporter virus injection into the brain (149); however this approach is technically difficult and invasive. To circumvent this, we generated a conditional reporter mouse that enables us to express a novel rhythmic luciferase reporter in specific cells and tissues, and assess their rhythmicity *in vitro* and *in vivo*, respectively.

For my thesis work, I describe the generation and characterization of a conditional reporter mouse, as well as provide evidence for one of the ways the field can use this mouse as a tool for studying circadian disruption. The reporter contains a floxed *GFP* upstream of a *luciferase* gene, which was knocked into the *Dbp* locus via CRISPR/Cas9. Without Cre recombinase, DBP and GFP are expressed as two separate proteins due to a T2A linker between *Dbp* and *GFP*. With Cre recombinase, *GFP* is deleted and DBP and LUCIFERASE are expressed as two separate proteins. The goal was to generate a conditional reporter mouse so that individual tissues or cells can be measured *in vivo*, which can provide information on individual tissue- or cell-type resetting mechanisms after a phase shift.

To be a good reporter mouse, the locus that is used for a knock-in should not have disrupted expression, thus we assessed whether expression from the *Dbp* locus of reporter mice was disrupted. Liver tissue from male WT, $Dbp^{KI/+}$, $Dbp^{KI/KI}$, $Dbp^{Luc/+}$, and $Dbp^{Luc/Luc}$ mice were collected at 4-h intervals (ZT 2, 6, 10, 14, 18, 22). RNA was isolated and a series of Northern Blot assays were performed to detect *Dbp* and *Actin* mRNA at each of the six ZTs. The mice with reporter construct had unaltered *Dbp* rhythms, suggesting that knock-in of the construct did not alter the *Dbp* locus. We also verified that the circadian locomotor activity was not disturbed by placing WT and the reporter mice in separate cages with running wheels and measuring their free-running period. There was no statistical difference in period between WT and reporter mice, in

both males and females. Now that we have determined the reporter mice do not have altered *Dbp* and locomotor activity rhythms, next we tested if the reporter mice have widespread bioluminescence signal. *Ex vivo* IVIS imaging confirmed that the $Dbp^{Luc/+}$ mouse has widespread bioluminescence signal. We confirmed that $Dbp^{Luc/+}$ lung and pituitary tissue explants had rhythmic bioluminescence, with the expected phase. We also showed that there was a period difference between PER2::LUC/+ and $Dbp^{Luc/+}$ tissues which was unexpected. These data highlight a shortcoming of the PER2::LUC/+ mouse model, as one would expect that the period would be closer to 24 hours.

We next examined $Dbp^{Luc/+}$ mice for rhythmic bioluminescence, *in vivo*, by IVIS imaging. *In vivo* IVIS imaging showed widespread bioluminescence rhythms of both $Dbp^{Luc/+}$ and PER2::LUC/+ mice, with $Dbp^{Luc/+}$ peaking earlier than PER2::LUC/+, which complemented what we saw *in vitro*. Importantly, by crossing the conditional reporter mouse with a liver Cre mouse (*Alb-Cre ;* $Dbp^{Kl/+}$), bioluminescence rhythms were apparent solely in the liver. Bioluminescence signal from the liver was confirmed by *ex vivo* IVIS imaging. This is the first evidence showing tissue-specific luciferase expression, *in vivo*, using a non-invasive cre-lox approach.

The ability to monitor circadian disruption will help us understand how this disruption can lead to downstream adverse health outcomes. One way of inducing circadian disruption is by advancing or delaying the light/dark cycle. Liver reporter mice with luciferin in their drinking water were entrained to a 4-h

skeleton photoperiod. After a 6-h advance in the light/dark cycle, the mice experienced internal desynchrony: locomotor activity rhythms reset faster than liver bioluminescence rhythms.

Peripheral tissues reset slower than the central pacemaker (62), this is due to the hierarchy of the circadian system described in section 1.4. By shifting the photoperiod, the SCN first responds to the shifted stimuli, and then the SCN sends signals to peripheral organs to then shift. One could argue that this resetting lag in the liver could be due to the change in fasting/feeding cycles as feeding time is a strong Zeitgeber of peripheral organs (126). However, it is more likely that the rest/activity and fasting/feeding cycles are coupled, and thus the resetting lag in liver could be attributed to both, as shown in van der Vinne et al. where the timing of food intake and activity maintained their phase relationship after a shift in the light/dark cycle (133).

These data highlight the novelty of this conditional reporter mouse in monitoring phase resetting in a tissue-specific manner, in freely moving mice. This approach is certainly ideal for monitoring long-term bioluminescence rhythms as monitoring *in vivo* bioluminescence rhythms using IVIS imaging can be laborious. Lastly, we showed that the conditional reporter can produce cell-type (NMS and AVP) specific rhythms in the SCN, and that these cell types have different phases.

The data described in my thesis demonstrate that the *Dbp* reporter mouse can be a tool for monitoring bioluminescence rhythms in a tissue-specific manner

in vivo and in specific cells in tissue slice culture. Monitoring specific tissue resetting *in vivo* can also be done using our conditional reporter mouse. Notably, this tool will open doors to new investigations and understanding of circadian disruption, and how it affects individual tissues or cells leading to negative health outcomes.

4.2 Limitations of the model

One of the limitations with the reporter mouse model is that the destabilized GFP signal is not robust (data not shown). The reason for this could be due to GFP being destabilized thus resulting in low GFP protein levels. To circumvent this, one could generate a reporter mouse model that has a different fluorescent protein expressed, other than GFP. The benefit with using fluorescent reporters is that there are many to choose from, thus providing a greater number of options for reporting.

For IVIS experiments, a limitation is that mice have to be anesthetized for imaging which can potentially affect the clock by altering the rest/activity rhythms (181). Additionally, depending on when the anesthesia is administered (i.e., during the active or rest phase), anesthesia can shift the rest/activity phase (181). Anesthesia can also shift molecular clock gene rhythms such as *Per2* (181). Although we used isoflurane to anesthetize the mice, we did not see any altered phase of bioluminescence signal from the genotypes imaged. The *in vivo* bioluminescence signal from each genotype peaked at the appropriate ZTs,

suggesting that anesthesia did not affect the *Per2* or *Dbp* rhythms. One explanation for this is that previous studies investigating the outcomes of anesthesia on the clock, specifically done with isoflurane, had exposure duration on the order of hours which is chronic exposure. In contrast, the IVIS experiments we conducted did not have chronic exposure of isoflurane, but more of an acute exposure. Our data suggests that anesthesia did not alter PER2::LUC/+ or $Dbp^{Luc/+}$ rhythms, however these were under normal conditions. When investigating the effects of environmental or genetic perturbations on the clock, anesthesia maybe a concern as the clock is already compromised. Therefore, monitoring bioluminescence rhythms while the mouse is awake would be a better approach.

Optimizing the Bioluminescence Signal

To obtain good bioluminescence signal *in vivo*, the hair of the mouse has to be shaved, both dorsal and ventral sides, depending on which tissue is being imaged. For the IVIS approach, this technique is sufficient as the amount of time to image the mouse is relatively short compared to approaches that monitor bioluminescence for longer durations. For experiments monitoring ambulatory reporter mice, the hair eventually grows back which can be an issue as the dark coat can block the light that is emitting from the reporter mouse. Thus, the coat would have to be consistently shaved. This can be problematic as there should be as little disturbances as possible during the experiment, as well as consistently shaving causes an increase in skin pigmentation. An alternative to

shaving mice is using albino reporter mice as they have white coats, thus less of the light is blocked by pigment in the skin and the hair. Preliminary studies using *in vivo* IVIS imaging of the *Ksp1.3-Cre* ; $Dbp^{KI/+}$ “kidney reporter” mouse showed that the albino kidney reporter had greater bioluminescence signal than the C57BL/6J kidney reporter (Fig. 4.1). Notably, signal is only coming from the kidneys. Both the black and albino mice were not shaved as we wanted to see if the color of the fur coat mattered in regards to signal intensity. These data suggest that lighter fur allows less light to be blocked compared to the darker fur, thus shaving the animal is not necessary.

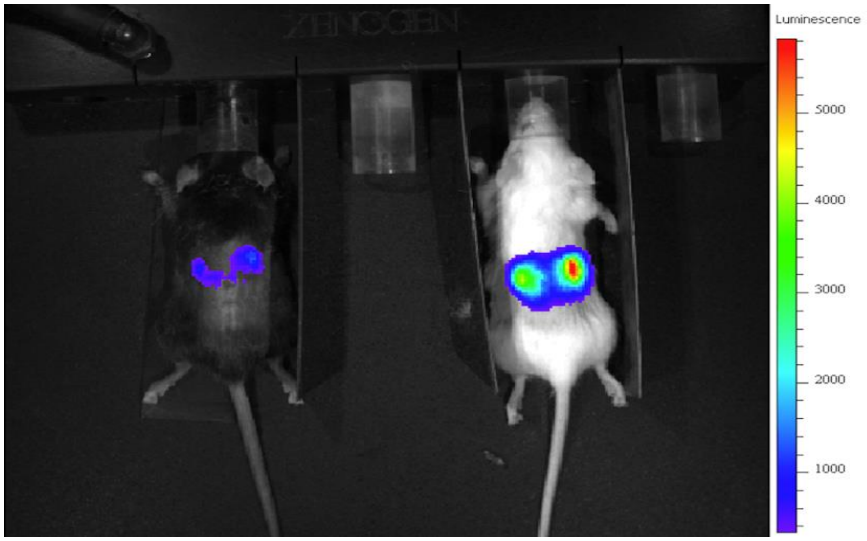

Figure 4.1 Dorsal view of an *in vivo* IVIS image of *Ksp1.3-Cre* ; *Dbp*$^{KI/+}$ "kidney reporter" mice

D-luciferin was injected intraperitoneally in kidney reporter mice on a C57BL/6J and albino background. Bioluminescence signal was captured at peak phase (ZT 12). n=2

One of the drawbacks of the *Dbp*$^{KI/+}$ conditional mouse model is that signal from certain parts of the animal is weak, such as the brain in *Vgat-Cre ;* *Dbp*$^{KI/+}$ mice where *luciferase* is expressed only in GABAergic neurons. A longer integration time was needed to see a signal (data not shown).

To look at bioluminescence signal from peripheral reporter mice, we injected the D-luciferin substrate intraperitoneally. D-luciferin is an efficient substrate for luciferase activity in peripheral tissues; however it is difficult for this substrate to penetrate the brain (182). Thus, different luciferin substrates such as cyclic alkylaminoluciferin (CycLuc1) that can penetrate the brain more readily will be a better alternative for increased bioluminescence signal from the brain (183).

4.3 Future Directions

4.3.1 Characterizing circadian disruption in freely moving mice

Circadian disruption can occur through shift work or chronic jet lag. Interestingly, epidemiological studies showed an association of night shift workers with increased risk of disease (96, 184, 185) and a correlation of female flight attendants and breast cancer (186, 187). Research also showed that shift workers have disrupted hormone rhythms and altered lipid metabolism (92, 188). The hormone rhythms are unable to entrain to the night shift schedule thus reflecting circadian misalignment.

One of the ways researchers study circadian disruption in rodents is by dissecting the tissues to monitor their phase (52), however two studies from

Noguchi et al. (135) and Leise et al. (123) suggests that prior disruption of the light/dark cycle can influence the SCN network sensitivity, thus allowing tissues to become more susceptible to resetting by tissue dissection, compared to mice that are housed under the standard light/dark cycle. Thus, tissue monitoring *in vivo* would be better suited for studying tissue resetting after circadian disruption.

Monitoring tissue resetting, *in vivo,* bypasses the need for tissue dissection to determine phase. We showed that after a 6-h advance of the light/dark cycle, the locomotor activity rhythm resets at a faster rate than the liver. The resetting lag of the liver relative to the central oscillator resetting is considered internal desynchrony. These results are supported by studies showing that the central clock resets faster than peripheral clocks (124). This mouse model is valuable as we were able to monitor the phase resetting of a specific peripheral tissue compared to the central clock, without using invasive techniques. Crossing our conditional mice to various Cre mice, we can obtain bioluminescence signal in a variety of individual tissues. Two future questions that could be asked are 1) do other peripheral tissues also reset at a different rate compared to the central pacemaker, after circadian disruption? 2) do different peripheral organs reset at similar rates after circadian disruption?

In my thesis work, we show that liver resetting lagged 3 days behind the central pacemaker during re-entrainment to the new phase (Fig. 3.9), but what about other peripheral tissues? We can readily look at the resetting rates of other individual peripheral organs compared to the SCN by shifting the light/dark cycle

6-h in advance and monitor resetting. I hypothesize that other tissues would also reset slower than the SCN, as was shown previously (124). Typically, researchers consider locomotor activity rhythms as an output of the central clock (46, 177). With the generation of our conditional mouse model, SCN resetting can now be directly monitored in moving mice by using a Cre driver, such as NMS-Cre, that will allow *luciferase* expression in the SCN. Therefore, the resetting rates of the SCN and liver after circadian disruption can be observed in *NMS-Cre; Dbp*$^{KI/+}$ and *Alb-Cre ; Dbp*$^{KI/+}$ mice, respectively, or a transgenic mouse that expresses *luciferase* in both the SCN and liver (i.e by having two different Cre drivers within the same mouse).

Detecting bioluminescence from the SCN, *in vivo*, can be challenging as the SCN is located in the ventral portion of the brain. Thus, a cranial window will be essential for allowing better signal output. A cranial window is a method used for *in vivo* brain imaging (189, 190). Researchers like Erik Herzog and colleagues utilized a cranial window to monitor PER2::LUC rhythms from the olfactory bulb (OB). Similar to Herzog's protocol, a dental drill can be used to create a craniotomy over where the SCN is located and a glass coverslip can be placed over the region where the brain is exposed (190), thus allowing for better signal output.

The advantage of our conditional mouse line is that *in vivo* experiments can now be more feasible by crossing our reporter line to different Cre lines. As described below, different peripheral organs appear to have variable resetting

kinetics, depending on the type of circadian disruption. It would be interesting to see if the liver resets faster than other tissues such as the kidney, after a disruption in the light/dark cycle, *in vivo*.

After circadian disruption due to restricted feeding, peripheral tissues have different resetting kinetics, as shown by *Dbp* gene expression (126). Interestingly, the heart *Dbp* rhythms seem to reset slower than organs that are involved with metabolism and digestion, such as the liver and kidney. It would be interesting to see if this is the case *in vivo*. To investigate if this is true *in vivo*, conditional reporter mice expressing *luciferase* in a specific tissue can be administered luciferin in their drinking water and bioluminescence rhythms can be monitored from the freely moving mice in a Lumicycle *in vivo*. I would use Cre lines that will promote *luciferase* expression in a tissue involved in metabolism such as the liver and compare its resetting rate to a tissue that is not involved in metabolism such as skeletal muscle tissue. For observing peripheral organ phase resetting, I would place these reporter mice on restricted food and allow them to consume food only during their resting phase. There would also be a control group that has access to food ad libitum, and a third control that has access to food only at night. I would compare the phase resetting rates of the individual tissues over time during the food restriction. If I see differences in resetting rates between individual organs, this would suggest that, at least during restricted feeding, organs such as the liver which have a critical role in food metabolism must adapt to the new environment faster.

A shortcoming of experiments monitoring signal from freely moving mice is that monitoring internal desynchrony between peripheral organs in the same mouse can be quite difficult. For example, if a mouse is emitting bioluminescence signal from two different organs, one would not be able to discern where the signal is coming from. Generating a population of mice with each organ reporting (i.e using different Cre-lines) and comparing the populations would prove to be a better approach for observing individual organ resetting. It is important to note that for experiments which involve freely moving mice, I would use albino mice as consistent shaving would not be necessary. This experiment could provide insight into how individual organs respond to an alteration to the circadian cycle. In addition, the information gained from these types of experiments can potentially aid in identify therapies that can reset components of the circadian system at similar rates, while avoiding internal desynchrony.

4.3.2 Characterizing phase resetting in specific SCN neurons, in vivo

The SCN has robust rhythms *in vitro* that can persist for weeks at a time. This is thought to be due to the SCN's neuronal circuitry (52). Liu et al. showed that in molecular clock mutant knockouts (*Per1*$^{-/-}$, *Per3*$^{-/-}$, *Cry1*$^{-/-}$, and *Cry2*$^{-/-}$) PER2::LUC SCN bioluminescence rhythms had robust and persistent rhythms *in vitro*, unlike PER2::LUC lung explants where bioluminescence rhythms were disrupted in *Per1*$^{-/-}$ and *Cry1*$^{-/-}$ mutant mice (52). This suggests that the SCN isn't as vulnerable to the effects of molecular clock perturbations as the SCN was able

to still produce bioluminescence rhythms. Interestingly, dispersed PER2::LUC SCN neurons from *Cry2*$^{-/-}$ mutant mice were unable to produce robust bioluminescence rhythms as compared to the SCN tissue slice culture, suggesting that it is indeed neuronal coupling within the SCN tissue slice that is contributing to robust rhythm output (52). Additionally, dispersed *Cry2*$^{-/-}$ SCN neurons displayed variable peak phases of PER2::LUC bioluminescence, and in contrast *Cry2*$^{-/-}$ neurons within the SCN tissue slice had similar phases, suggesting that the SCN's cell coupling is what aids in synchronization of rhythms (52). Welsh et al. showed that there was uncoupling within rat SCN neuronal cell culture in which different phases in firing rate occurred within the same culture (51). By monitoring firing rates over time, Welsh and colleagues revealed that these neurons are not synchronized (51). These studies suggest that cell-coupling in the SCN aids in sustaining the synchronization.

One of the directions the field is moving into is the characterization of individual SCN neurons during resetting. Early studies investigating neuronal phase was limited to *in vitro* experiments as there was not a mouse model widely available that researchers could use to detect specific neuronal populations, *in vivo*. Studying phase differences *in vitro* after circadian disruption is not ideal as the SCN has to undergo the dissection procedure which can reset the clock. Instead, determining phase differences between SCN neuronal types after circadian disruption, *in vivo*, will be required. I showed that our conditional reporter mouse can report bioluminescence rhythms from specific cell-types by

crossing the *Dbp*$^{KI/+}$ conditional reporter mouse to an AVP-Cre or NMS-Cre mouse driver (Fig. 3.10). We can utilize the *Dbp*$^{KI/+}$ conditional reporter mouse to monitor phase resetting in specific SCN neurons, *in vivo*, after circadian disruption. I would breed *Dbp*$^{KI/+}$ reporter mice with either VIP-Cre or AVP-Cre mouse lines so that *luciferase* is expressed in VIP- and AVP-expressing neurons, respectively. VIP neurons populate the core of the SCN and receive photic input from the RHT, which in turn synchronizes their own rhythm (191). The SCN core communicates with neurons in the shell, including AVP-expressing neurons (192); this synchronizes shell neurons. Additionally, there is research showing that both VIP and AVP neurons contribute to SCN rhythm synchrony (193), thus it would be interesting to investigate the phase resetting rates of these neurons, *in vivo*, using our conditional mouse model. Herzog's group observed VIP neuronal activity rhythms, *in vivo*, using photometry (194). They used a viral delivery approach to express GCaMP6s in VIP neurons (194). This approach was sufficient to monitor rhythms, however it was invasive. Additionally, off target injections is a technical concern when performing viral-mediated experiments. The circadian rhythm field can now bypass surgeries and monitor SCN neuronal rhythms and phase resetting, *in vivo*, using the *Dbp*$^{KI/+}$ conditional mouse model.

To investigate phase resetting between VIP and AVP neurons, I would set up this experiment similar to the phase-resetting experiment described in chapter 2. Briefly, *VIP-Cre ; Dbp*$^{KI/+}$ and *AVP-Cre ; Dbp*$^{KI/+}$ mice will entrain to the 4-h skeleton photoperiod for a few weeks while consuming Cycluc1 amide in their

drinking water; Cycluc1 amide is a better luciferase substrate for penetration into the brain (183). Then I will advance the light/dark cycle 6-h and monitor the resetting rate of both the VIP and AVP neurons, in separate animals. I hypothesize that the VIP neurons will reset faster than the AVP neurons, as VIP neurons receive direct photic input (192). An advantage with monitoring rhythms in freely moving mice is that their locomotor rhythms can also be observed, unlike if the mice were anesthetized for IVIS imaging. This future experiment could provide information on how specific SCN neurons respond to shifting stimuli, which can potentially impact organismal behavior. A caveat of this approach is that bioluminescence signal maybe coming out from other brain regions that may have VIP or AVP neurons (195, 196), thus this would have to be taken into consideration when trying to assess SCN VIP or AVP phase resetting. Also, because bioluminescence signal will be originating from specific neurons, signal intensity may not be as robust. To circumvent this, a cranial window can be used to help increase bioluminescence signal output.

4.3.3 Disease Model

Circadian disruption increases the risk of cancer. Human studies investigating the impact of shift work on human health suggest a role of circadian disruption underlying the increased risk of disease (96, 184). Multiple shift work studies, specifically including healthcare professionals, showed that nurses who spend a significant amount of time working the night shift or worked a rotating

shift have increased risk of breast cancer relative to nurses who never worked on a shift schedule (95, 184). Hormones, like melatonin, are dysregulated in night shift workers which could contribute to the increased risk of cancers (178). Indeed, reduced melatonin can result in altered estrogen receptor function and increased estrogen production (178).

Human studies showed that SNPs in clock genes are associated with various types of cancers (80, 197-199), and many cancers have disrupted clock gene expression (200, 201), which may provide an underlying mechanism of how the SNP could be functioning. Specifically, *Per1*, *Per2*, *Per3*, and *Cry2* genes have decreased expression in hepatocellular carcinoma (202).

In vitro studies have shown that deletion of core clock genes can promote cell proliferation by altering the expression of downstream oncogenic genes and cell cycle genes (106, 203). Additionally, whole animal loss of *Per2* or *Bmal1* had increased lung tumor growth and progression, as well as survival (106). These data suggests clock genes may play a role in tumor suppression (204). Interestingly, in the same study, simulated jetlag also led to similar adverse health outcomes (106). The data described above shows how important it is to understand the connection between circadian disruption and cancer. This is especially critical because we live in a society that sometimes demands unusual work schedules.

Bioluminescence rhythms from healthy liver and liver tumors were monitored by Alec Davidson et al. (23). Hepatocellular carcinoma was induced in

Per1-luciferase rats by administrating diethylnitrosamine, a carcinogen, in their drinking water (205). *In vitro* measurements showed similar rhythm pattern of *Per1-luciferase* bioluminescence rhythms within the liver tumors compared to healthy liver, however tumors had a shorter period and lower amplitude (205). Davidson et al. showed that after advancing or delaying the light/dark cycle 6-h in *Per1-luciferase* rats, both liver tumor and healthy liver shift at similar rates (205). It seems to be that the host circadian system can still influence the rhythms of the tumor, at least in the context of shifting the light/dark cycle. However, during a restricted feeding paradigm where *Per1-luciferase* rats were fed during the daytime, liver tumors from rats fed during the day peaked 3 hours later than healthy livers (205). The phase difference of liver tumors and healthy liver tissue from *Per1-luciferase* rats fed during the day versus nighttime feeding was 6.3 hours and 11.5 hours, respectively. This suggest that liver tumors are less sensitive to restricted feeding (205). This is actually quite puzzling because restricted feeding seems to be a stronger Zeitgeber for peripheral tissue entrainment compared to light (126). It would be interesting to further investigate why tumors are differentially sensitive to certain Zeitgebers, and whether this varies by tumor type. Evidence from Lakatua et al. supported the idea that tumors are differentially sensitive to different Zeitgebers; transplanted Harding-Passey melanoma from mice were sensitive to photic shifting, but not restricted food (206).

The above study describes monitoring resetting in liver tumors vs. healthy liver tissue, in real time using the *Per1-luciferase* bioluminescence reporter rat. These resetting experiments were done using liver tissue explants. As described previously, dissection can alter the resetting of the tissue, thus a future direction would be to study tumor resetting *in vivo* to get a more accurate assessment of tumor resetting rates. Cancer can be induced in *Alb-Cre ; Dbp*$^{Ki/+}$ mice by administering a carcinogen in their drinking water as described in Davidson et al. (205). Once we see apparent tumors, we can either place these liver reporter mice in a resetting paradigm similar to the one described in the results section (Fig 3.9), with the light/dark cycle as the Zeitgeber, or place the mice in a restricted feeding paradigm. Difference in rhythm resetting can be monitored specifically from the liver of healthy liver reporter mice and liver reporter mice that have liver tumors. I hypothesize that both healthy and unhealthy liver tissue will produce bioluminescence rhythms, similar to what was seen in liver tissue explants (205). I predict that the cancerous and healthy liver tissue will shift at similar rates after shifting the light/dark cycle, but the liver tumor would be less sensitive to restricted feeding. The advantage of our conditional mouse model is that circadian rhythms and resetting of specific tissues that have tumors can be monitored in freely moving mice. Furthermore, we can investigate how cancerous tissues influence circadian rhythms of other tissues, *in vivo*. For example, we can promote cancer in a specific tissue such as the liver, and monitor how it affects the resetting of the kidney, using a kidney driver. There is evidence that lung

adenocarcinoma distally rewires hepatic circadian homeostatis, so investigating how liver tumors can affect the rhythms of other organs would be interesting (207).

Fascinatingly, the conclusions provided by Davidson et al. suggested that there may be a method for dissociating the rhythms of the tumor from the host by restricting the animal's feeding, as restrcted feeding caused an alteration in phase-relationship between tumor and non-tumor liver tissues (205). Further investigating this concept, *in vivo*, may provide a way to dissociate phase between tumor and healthy tissue. This may further enhance the ability to select an optimal time at which a cancer drug should be administered to have anti-tumor efficacy, while avoiding toxicity of healthy tissue.

For my thesis work, I have successfully validated a conditional reporter mouse that can be used to monitor circadian rhythms in specific tissue- and cell-types, *in vivo* and *in vitr*o, respectively. The utility of the reporter mouse was clearly demonstrated by phase-resetting studies in ambulatory mouse and bioluminescence rhythms studies in SCN tissue slice culture. I proposed future directions in which we can utilize the reporter mouse; specifically investigating phase resetting between central and peripheral oscillators, between neuronal types in the SCN, as well as investigating phase resetting in a disease model. The future directions I describe is only but a subset of avenues the field can pursue. This novel conditional reporter mouse will advance the circadian rhythm

field’s knowledge on how circadian disruption can affect specific tissue or cell rhythms, *in vivo*.

APPENDIX V

Do Interpeduncular α3-containing Nicotinic Acetylcholine Receptors Modulate Anxiety, Novelty-seeking, and/or Nicotine Aversion?

Ciearra B. Smith[1], Susanna Molas[2], Andrew R. Tapper[2], Paul D. Gardner[2]

[1]Program in Neuroscience and Department of Neurobiology
[2]Brudnick Neuropsychiatric Research Institute, University of Massachusetts Medical School, Worcester, MA

Author Contributions

C.B.S and P.D.G were involved in the conception of the project. C.B.S, P.D.G, and A.T designed the experiments. C.B.S performed and analyzed all experiments and data, respectively, except the open field test (OFT). S.M analyzed the OFT data. C.B.S wrote the appendix section with edits from P.D.G and D.R.W.

Introduction

Tobacco use causes many adverse health effects, making it the most preventable cause of death worldwide, killing more than 6 million people each year (208). Because tobacco use can result in cardiovascular disease, lung disease, and lung cancer, the generation of better smoking cessation therapies is essential. Pharmaceutical smoking cessation therapies are currently available, however these drugs, particularly varenicline and bupropion, have limited efficacy. For example, in randomized control trials, patients taking these drugs showed a decreased percentage of smoking abstinence as time progressed (209). Furthermore, these drugs produce severe side effects among users, calling for better options for smoking cessation therapeutics. The high incidence of tobacco use is due to nicotine, the addictive component of tobacco (210). Nicotine binds to and activates nicotinic acetylcholine receptors (nAChRs) and as a consequence, modulates neurotransmission within the addiction pathway.

Koob's model of addiction describes the cycle as being three stages: 1) binge/intoxication, 2) withdrawal/negative affect, 3) preoccupation/anticipation (211). Humans who have a novelty-seeking trait or neuropsychiatric disorders such as anxiety tend to be especially vulnerable to drug addiction (212-214). Novelty-seeking in humans is highly correlated with an increased risk of using addictive drugs, as well as drug relapse (214). In addition, people who have a mental illness are twice as likely to smoke tobacco as compared to people

without a mental illness (215). Multiple studies have shown that people who suffer from increased anxiety are more likely to smoke (212).

Nicotinic Acetylcholine Receptors

nAChRs are ligand-gated cation channels that are endogenously activated by acetylcholine (ACh) (216, 217). Mammalian neuronal nAChRs are pentameric receptors that contain α2-α7, α9, α10, and β2-β4 subunits, encoded by the genes *Chrna2-Chrna7*, *Chrna9*, *Chrna10*, and *Chrnb2-Chrnb4*, respectively (216). These subunits make up homomeric and heteromeric receptor subtypes that have different affinities for nicotine. Upon ligand binding, the receptor undergoes a conformational change (216), which makes the receptor's central pore permeable to cations (218). On a molecular level, after chronic exposure to ACh or nicotine, the receptor becomes desensitized, resulting in decreased ion flow, nAChR upregulation, and long-term changes in receptor properties (216, 218). Desensitization of nAChRs is believed to play a role in nicotine tolerance and dependence (219). nAChRs are highly expressed in two major brain pathways involved in nicotine reward (220) and withdrawal and aversion (220-222), the mesocorticolimbic pathway and the medial habenula-interpeduncular tract (mHb-IPN) (221, 223), respectively. The mHb-IPN is also important for phenotypes associated with the susceptibility to nicotine addiction including anxiety (224) and novelty preference (225).

CHRNA5/A3/B4 cluster

In the past, research primarily focused on α4β2* (asterisk indicates that other nAChR subunits may be present) nAChRs and their roles in nicotine addiction (226-228). This is due to the high expression of α4β2* nAChRs in the mesocorticolimbic pathway and their high affinity for nicotine (220). However, various twin studies demonstrated heritability to liability for nicotine dependence (229-233), which led to further investigation of nAChR genetic factors that may play a role in nicotine dependence. Numerous candidate-based gene studies and genome-wide association studies (GWAS) in diverse populations identified an association between genetic factors in nAChR genes and nicotine dependence (234-242). These studies led to the identification of variants in the *CHRNA5/A3/B4* gene cluster that are associated with nicotine dependence (234-236, 241, 242). These three genes form a tight cluster on chromosome 15q.25.1 and studies have shown that the genes within the cluster play a role in nicotine addiction (217, 220, 221, 243). Fowler et al. showed that knockout of the α5 nAChR subunit increases nicotine self-administration (244), suggesting that α5* nAChRs are involved in nicotine aversion. Frahm et al. showed that transgenic mice with targeted over-expression of β4 nAChRs subunit in the mHb increases aversion to nicotine (245). In addition, both knockouts of α5 or β4 subunit expression resulted in decreased somatic nicotine withdrawal symptoms (221, 243). Various knockout studies also showed that α5 and β4 nAChR subunits are

important for anxiety-like behaviors (246, 247), and that β4 nAChR subunits are important for social behavior (248).

In contrast, little is known about the role of the α3 nAChR subunit as α3 nAChR subunit knockout mice die shortly after birth (249). However, high expression of α3 nAChR subunits in the habenulo-interpeduncular pathway (250) suggests a role for α3* nAChRs in anxiety, novelty-seeking behaviors, and nicotine aversion. Therefore, I hypothesize that α3* nAChRs within the IPN are necessary for these behaviors. To test this hypothesis, I performed experiments to identify short hairpin RNAs (shRNA) that disrupt *Chrna3* mRNA expression *in vitro*, administered the 'lead sequence' to target *Chrna3* mRNA in the IPN, and performed behavioral studies to assess their impact on behaviors associated with the susceptibility to nicotine addiction and nicotine-related behaviors.

Materials and Methods

Animals

All animal experiments were conducted in accordance with the guidelines for care and use of laboratory animals by the National Research Council and with an animal protocol approved by the Institutional Animal Care and Use Committee of the University of Massachusetts Medical School. Wild-type C57BL/6J mice (Jackson Labs) were grouped-housed in a colony room with a 12-hour light: 12-hour dark lighting cycle; lights on at 7:00 A.M. and lights off at 7:00 P.M. Food and water were provided *ad libitum*.

In vitro knockdown of *Chrna3* mRNA expression with pGIPZ-shRNA lentivirus

The mouse neuroblastoma cell line Neuro2A (N2A) was used to test for *Chrna3* knockdown efficiency by shRNA. N2A cells were grown in 1X Minimum Essential Medium (MEM) (Corning), supplemented with 10% fetal bovine serum (FBS) and 1 mM sodium pyruvate. N2A cells were plated in duplicate at a density of $2.5x10^4$ cells per well, in a 24-well plate. The next day, N2A cells were infected with three different commercially available pGIPZ-shRNAs (Dharmacon), one of which is a scramble control and two that target *Chrna3*. The following pGIPZ-shRNAs were used: V2LMM_9543 and V2LMM_8843, which target the sequences 5′-AATCTTCAAACAGGTACTG-3′ and 5′-TTGCTTCAGCCACAGGTTG-3′, respectively. Cells were transduced with the concentrated shRNA lentiviruses (multiplicity of infection: 0.5 for V2LMM_9543 and 0.4 for V2LMM_8843) using 8 μg/ml of polybrene in a total of 250 μl in each well. After 5 hours, 1 ml of fresh growth medium (1X MEM + 10% FBS + 1 mM sodium pyruvate) was added to each well. Growth medium was aspirated and cells were given 500 μl of fresh growth medium containing 4 μg/ml of puromycin 48 hours post-transduction to select for cells infected with the lentivirus. The pGIPZ lentivirus plasmid contains a puromycin selection gene. Virus-expressing cells were selected for 5 days, then cells were harvested and total RNA was isolated using the RNAqueous Total RNA Isolation Kit (ThermoFisher AM1912). RNA (1 μg) was reverse transcribed using M-MLV Reverse Transcriptase

(ThermoFisher Cat. No. 28025013), following the manufacturer's protocol. Relative *Chrna3*, *Chrna5*, and *Chrnb4* mRNA expression were measured by reverse transcription quantitative polymerase chain reaction (RT-qPCR) using Taqman assays *Chrna3* Mm00520145_m1, *Chrna5* Mm00616329_m1, *Chrnb4* Mm00804952_m1, and *B2M* Mm00437762_m1 (ThermoFisher). Data were analyzed using the $2^{-\Delta\Delta Ct}$ method described previously (251).

Overexpression of pGIPZ-scramble control or pGIPZ-shRNA 8843 lentiviruses in the IPN

To knockdown *Chrna3* expression, *in vivo*, pGIPZ-scramble control or pGIPZ-shRNA 8843 was injected into the IPN of male 8 week-old WT mice using the following coordinates, relative to Bregma: anterior/posterior (A/P: -3.30 mm), medial/lateral (M/L: ±0 mm), and dorsal/ventral (D/V: -4.80 mm). Unilateral stereotaxic injections were performed under aseptic conditions, using a 26 s gauge 10 μl syringe (701RN, Hamilton) to deliver 0.3 μl or 1 μl of lentivirus into the IPN. To minimize spread from the target location, virus was delivered at a rate of 60 nl/min and the needle was withdrawn 5 minutes after completion of injection. The lentivirus was expressed for 2.5 weeks and a battery of behavioral assays was performed.

The pGIPZ lentivirus plasmid encodes GFP. To confirm virus expression in the IPN, fluorescence microscopy was performed. Brains were dissected and frozen in dry ice post behavioral assays. Frozen brains were sectioned (12 μm)

using a cryostat and mounted on glass slides. A blind experimenter confirmed virus expression. To confirm knockdown of *Chrna3* mRNA expression, brain slices were fixed and dehydrated as described previously (252). Laser-capture microdissection (LCM; Arcturus) was performed to isolate GFP-positive neurons. Total RNA was isolated and RT-qPCR was performed to measure *Chrna3*, *Chrna5*, and *Chrnb4* mRNA expression as described above.

Behavioral Assays

After surgeries, mice were placed in the colony room overnight to recover, and then were placed in a reverse light/dark cycle room for 2.5 weeks prior to behavioral experiments. All behavioral assays, except the elevated plus maze (EPM), were done solely in red light.

EPM: The EPM was performed in dim white light, as described in Zhao-Shea et al. (253). Briefly, mice were habituated to the test room for at least 30 minutes. Individual mice were placed in the center of the EPM and were allowed to explore for 5 minutes. Time spent in the open arms, number of entries into the open arms, and total arm entries were measured using the MED-PC IV software (MED Associates, Inc.). The EPM apparatus was cleaned thoroughly with Micro90 cleaning solution between each trial.

Open Field Test (OFT): Mice were habituated to the test room for 1 hour prior to the test. Individual mice were placed in an open field arena (42 × 38 × 30 cm) with its face towards one of the walls of the arena. Mice were allowed to explore the arena for 10 minutes. The movement of the mouse was video recorded and

time spent in the center of the arena and latency to center was determined using EthoVision XT 11.5 (Noldus Apparatus). The open field arena was cleaned thoroughly with Micro90 cleaning solution between each trial.

Marble Burying Test (MBT): The MBT was performed as previously described in Zhao-Shea et al. (253). Briefly, mice were habituated to a standard mouse cage filled with bedding for 2 days (1 hour/day). On test day, 15 glass marbles were placed on top of the bedding, in 5 rows of 3 marbles. The marbles were evenly spaced approximately 4 cm apart. After the 30-minute test, the number of buried marbles was counted.

Social Preference: Mice were habituated to the test room for 1 hour prior to the test. Mice were habituated to a three-chamber box containing dividers for 5 minutes. The two side chambers have the dimensions 42 × 24 × 30 cm and the middle chamber has the dimensions 42 × 15 × 30 cm. A C57BL/6J male juvenile mouse (approximately 6 weeks of age) was placed in a plastic cylinder and positioned in the corner of the arena. The experimental mouse was allowed to explore for 5 minutes. A C57BL/6J male novel juvenile mouse was then placed in another cylinder in the opposite side of the arena. The experimental mouse was allowed to explore for 5 minutes. The experiment was video recorded (HDR-CX4440 camera, Sony) and time of investigation was manually scored by an individual blind to the treatment groups. The arena and cylinders were cleaned thoroughly with Micro90 cleaning solution between each trial and the cylinders were counter-balanced to prevent biases to one side of the arena. Novelty

preference was measured by calculating the difference in time of interaction with the novel mouse and time of interaction with the familiar mouse, divided by the total time.

Conditioned Place Aversion (CPA): The CPA assay consists of a 6-day protocol that includes habituation, pre-test, conditioning, and post-test. On day 1, mice were habituated to the syringe needle by injecting (i.p) them with a volume of saline equal to their body weight divided by the overall average mouse body weight, multiplied by 100 microliters. On day 2, the pre-test day, individual mice were placed in the CPA arena and allowed to freely explore for 20 minutes to determine any bias to one side. The CPA arena consists of three chambers, two side chambers (13 × 15 × 12 cm) and a middle chamber (13 × 10 × 12 cm). The two side chambers differ in their characteristics: one chamber has white walls with a grid metal floor, while the other chamber has black walls with a striped metal floor. These differences allow the mice to differentiate between the two chambers. The mice were then habituated to the syringe needle again by injecting (i.p) saline as described above. Days 3-5 are the conditioning days in which mice were injected (i.p) with saline in the morning and placed in the saline-paired chamber for 20 minutes. Four hours later mice were injected (i.p) with a high dose of nicotine (1.5 mg/kg) and placed in the drug-paired chamber for 20 minutes. The preferred side, as determined on the pre-test day, was paired with the drug. On day 6, the post test, individual mice were placed in the middle chamber and were allowed to freely explore for 20 minutes. The time spent in

each chamber was recorded using the MED-PC IV software. The difference score was calculated as the time spent in an individual chamber during the post-test subtracted by the time spent in an individual chamber during the pre-test.

Results

Chrna3 knockdown in N2A cells by pGIPZ-shRNA 8843 lentivirus

To investigate whether α3* nAChRs are necessary for behaviors that tend to precede addiction, as well as nicotine aversion, I used an shRNA approach to knockdown *Chrna3* mRNA expression. I first tested two different shRNAs that were designed to target *Chrna3*, pGIPZ-shRNA 9543 and pGIPZ-shRNA 8843. After expression of pGIPZ-shRNA 8843 in the mouse neuronal-like cell line N2A, *Chrna3* mRNA expression was significantly downregulated compared to the pGIPZ-scramble control (Fig. 5.1). Expression of pGIPZ-shRNA 9543 did not significantly downregulate *Chrna3* mRNA expression compared to the scramble control. Thus, for future experiments I used pGIPZ-shRNA 8843.

I also measured *Chrna5* and *Chrnb4* mRNA after expression of the shRNAs. It is well known that *Chrna5*, *Chrna3*, and *Chrnb4* are tightly clustered together on chromosome 15 in humans and chromosome 9 in mice, and thus susceptible to similar regulatory proteins (254). Therefore, I wanted to determine if *Chrna5* and *Chrnb4* expression changes when *Chrna3* expression is reduced. Knocking down *Chrna3* mRNA expression did not significantly alter the mRNA levels of *Chrna5* and *Chrnb4*.

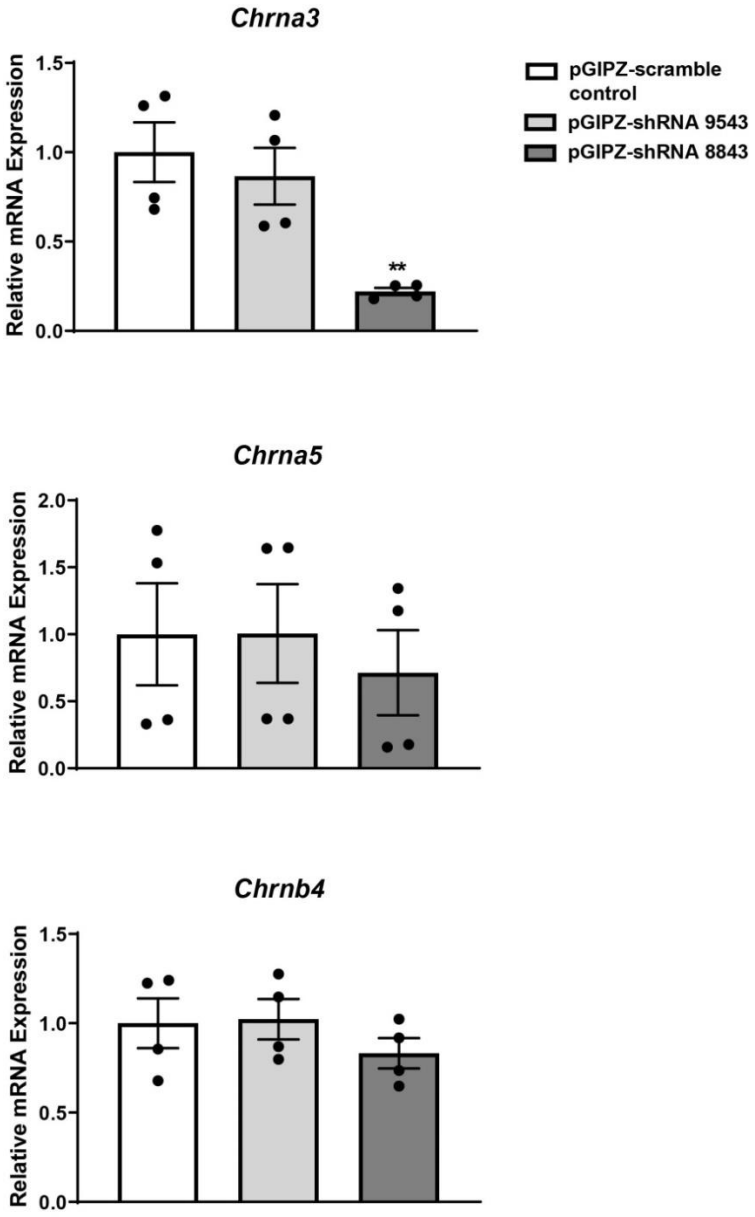

Figure 5.1 Knockdown of *Chrna3* mRNA expression in N2A cells

Quantification of *Chrna3* (top), *Chrna5* (middle), and *Chrnb4* (bottom) mRNA expression after overexpression of pGIPZ-scramble control, pGIPZ-shRNA 9543, or pGIPZ-shRNA 8843 lentiviruses in N2A cells. Data are displayed as mean ± SEM. n=2 Each dot represents a cell plate well. There were 2 wells/experiment. One-way ANOVA with Tukey's multiple comparisons was used for statistical analysis. **p<0.01.

Infection of pGIPZ-shRNA 8843 lentivirus in the mouse IPN did not alter anxiety, novelty preference, or nicotine aversion

The IPN is involved in various behaviors including anxiety (255), novelty preference (225), and nicotine-associated behaviors (244, 253), and it is known that nAChRs play a role in modulating these behaviors, but little is known about the role of α3* nAChRs in these behaviors. Thus, I investigated whether IPN α3* nAChRs can modulate these behaviors as well. Due to whole animal α3 nAChR subunit knock out mice dying shortly after birth (249), knocking down *Chrna3* mRNA expression via viral delivery seemed to be a good approach. I injected 0.3 μl of pGIPZ-shRNA 8843 into the IPN of 8 week-old male mice using a stereotaxic injector. The virus was expressed for 2.5 weeks prior to the behavioral assays.

Anxiety

Rodents undergo somatic and affective anxiety-like behaviors similar to humans; these anxiety-like behaviors can be measured by multiple tests. Some of the most common anxiety assays are the EPM and OFT. The Gardner/Tapper lab also uses the MBT as a measurement of anxiety, which is typically used in combination with other anxiety assays. Mice usually favor hiding versus being exposed to open spaces. Both the EPM and OFT are assays that test this kind of anxiety. Additionally, the EPM is elevated off of the ground, which can present an additional layer of anxiety for the rodent. For the EPM assay, the mouse is placed at the center of the EPM and the time spent inside each arm is measured,

as well as the number of entries. Motion sensors in the maze can detect where the mouse is located. The more time the mouse spends in the open arm is indicative of decreased anxiety. In contrast, the more time the mouse spends in the closed arms means that there is increased anxiety. Due to studies showing that knockout of nAChR subunits alleviate anxiety-like behaviors (246, 247, 256, 257), I hypothesized that knockdown of *Chrna3* mRNA expression in the IPN would also alleviate anxiety-like behaviors. However, we did not observe any change in time spent in open arms and open arm entries between pGIPZ-scramble control- and pGIPZ-shRNA 8843-infected mice (Fig. 5.2a). Total arm entries were measured to be sure that the result we see in the EPM is not attributed to altered locomotor activity; there was no difference in total arm entries.

The OFT was used to measure anxiety. In this test, mice were placed in the center of a box and the time in the center and latency to the center were measured. The more time the mouse spends in the center and a low latency to center means they have low anxiety. There was no difference in time spent in the center or latency to center between pGIPZ-scramble control- and pGIPZ-shRNA 8843-infected mice in the OFT (Fig. 5.2b). Total distance travelled was also measured to assess locomotor activity; it did not differ between the treatment groups.

Lastly, I used the MBT as a complementary anxiety assay. In the MBT, the number of buried marbles reflects to the level of anxiety, higher the number,

higher the anxiety. The MBT revealed that there was no change in marbles buried between pGIPZ-scramble control- and pGIPZ-shRNA 8843-infected mice (Fig. 5.2c). These data suggest that IPN α3* nAChRs are not necessary for anxiety-like behaviors.

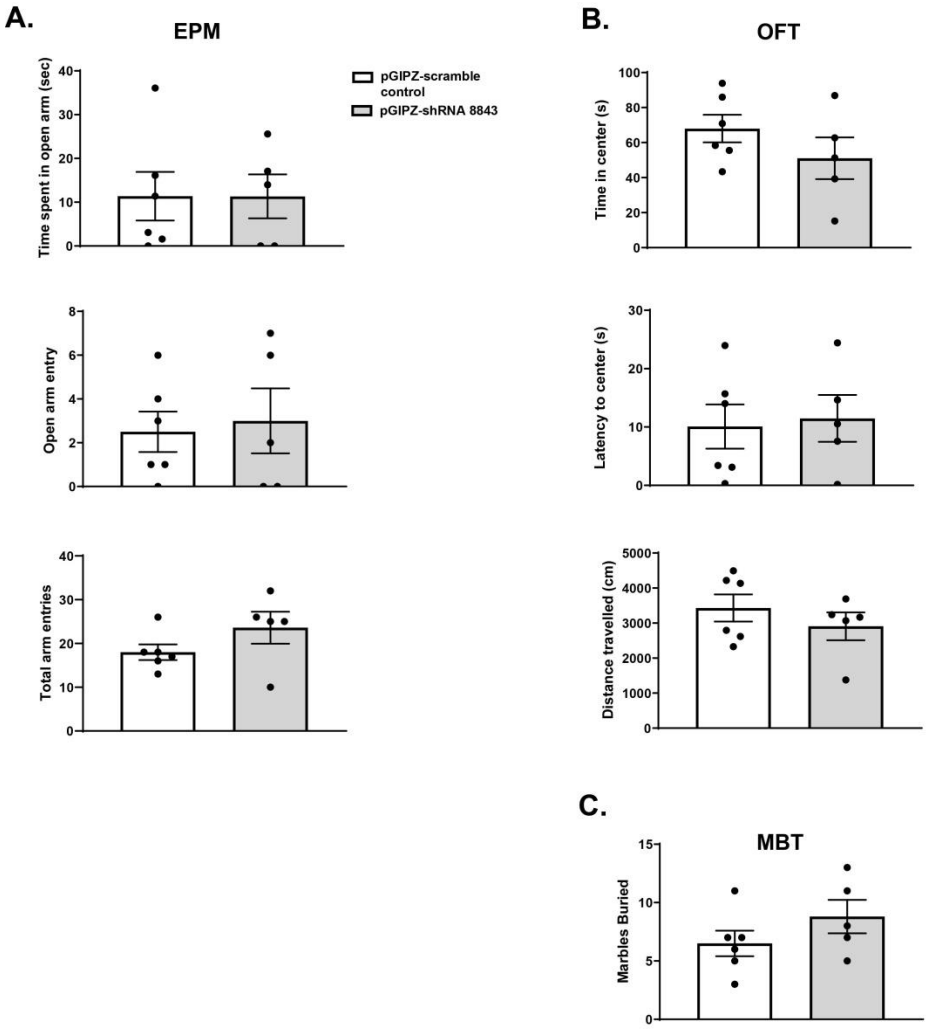

Figure 5.2 Infection of pGIPZ-shRNA 8443 in the IPN did not alleviate anxiety-like behavior

A. Average time spent in open arms, average open arm entries, and total arm entries in the EPM of mice injected with pGIPZ-scramble control or pGIPZ-shRNA 8843 in the IPN. **B.** Average time spent in the center, average latency to center, and average distance travelled in the OFT of mice injected with pGIPZ-scramble control or pGIPZ-shRNA 8843. **C.** Average number of marbles buried in the MBT of mice injected with pGIPZ-scramble control or pGIPZ-shRNA 8843. Data are displayed as mean ± SEM. Individual values are also shown as dots. n=5-6 Unpaired t-test was used for statistical analysis. $P > 0.05$ for all comparisons between the treatment groups.

Social Preference

Like many psychiatric disorders such as anxiety, novelty-seeking behavior can be a prerequisite to drug abuse (214). One of the ways investigators can test for novelty preference is via a novelty preference assay (225). The Tapper lab has utilized the novelty preference assay described in Molas et al. to uncover a novel neurocircuitry underlying familiarity signaling (225); this novel circuitry included the IPN. Inhibiting the IPN using optogenetic techniques resulted in the experimental mouse identifying the familiar mouse as novel. These data suggest a role for the IPN in familiarity signaling (225). Furthermore, β4* nAChRs are necessary for normal social behavior (248). In this study, wild-type mice spent more time investigating the novel mouse compared to the familiar mouse. Conversely, the β4 nAChR subunit knockout mice spent similar amounts of time investigating both the novel and familiar mice (247). The studies described above suggest a role for both the IPN and nAChRs in novelty preference and social behavior. I investigated if IPN α3* nAChRs are necessary for novelty preference. I hypothesized that decreased *Chrna3* mRNA expression in the IPN would increase investigation of the familiar stimulus, mimicking what was seen after shutting off the IPN via optogenetics (225). Scramble control mice spent significantly more time investigating the novel mouse relative to the familiar mouse, which was expected as mice tend to favor novel stimuli (225). Although there was a trend for mice infected with pGIPZ-shRNA 8843 to spend more time

investigating the novel mouse, this did not reach significance (Fig. 5.3, top), likely due to variability in this group. The preference ratio was calculated and showed that there was no significant difference in the preference ratio between pGIPZ-scramble control- and pGIPZ-shRNA 8843-infected mice (Fig. 5.3, center). The total time of investigation was measured to control for locomotor behavior; there was no difference in total time of investigation between pGIPZ-scramble control- and pGIPZ-shRNA 8843-infected mice (Fig. 5.3, bottom). If IPN α3* nAChRs were necessary to modulate novelty preference, I would expect the knockdown mice to spend significantly less time investigating the novel mouse compared to the pGIPZ-scramble control mouse. However, these data suggest that α3* nAChRs may not be modulating novelty preference.

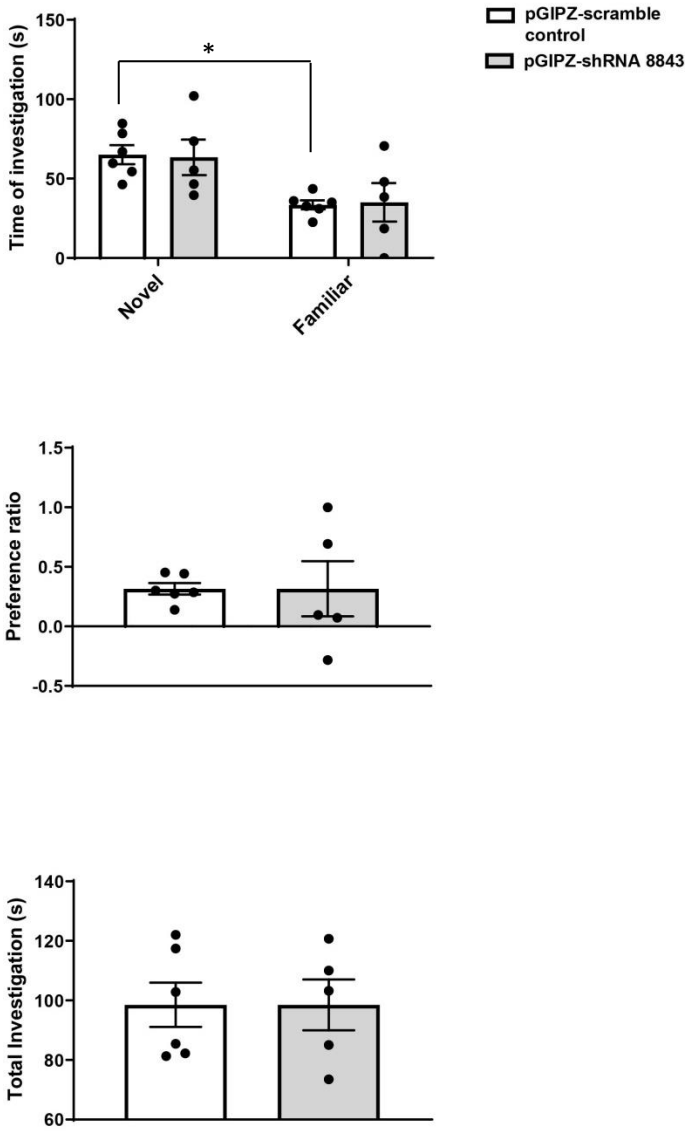

Figure 5.3 Infection of pGIPZ-shRNA 8843 in the IPN did not alter novelty preference

Average time of investigation between the familiar and novel mice (top), preference ratio (middle), and total time of investigation (bottom) of mice infected with pGIPZ-scramble control or pGIPZ-shRNA 8843 lentiviruses. Data are displayed as mean ± SEM. Individual data points are shown as dots. n=5-6 Two-way ANOVA, Tukey's multiple comparisons was used for statistical analysis for time of investigation. Un-paired t-test was used for statistical analysis for the preference ratio and total investigation time. *p<0.05

Conditioned Place Aversion

Nicotine is rewarding at a dose of 0.5 mg/kg, but this drug is aversive if high doses are given (1.5 mg/kg) (258, 259). Interestingly, α5* nAChRs in the habenulo-interpeduncular pathway modulate nicotine intake. Fowler et al. showed that α5 subunit knockout mice had increased nicotine self-administration when given a high nicotine dose; after re-expressing the α5 nAChR subunits in the mHb of α5-null mice, this rescued the effect (244). Furthermore, high doses of nicotine activate the IPN in wild-type mice, but this activation was abolished in α5 knockout mice. These data suggest that α5* nAChRs in the habenulo-interpeduncular pathway modulate nicotine intake. Indeed, habenulo-interpeduncular α5* nAChRs, as well as β4* nAChRs, are necessary for modulating nicotine aversion (244). To determine if α3* nAChRs in the habenulo-interpeduncular tract play a similar role in modulating nicotine aversion, we determined whether knockdown of *Chrna3* mRNA expression in the IPN decreased aversion to high doses of nicotine. I performed the conditioned place aversion paradigm to measure the aversive effect of nicotine. The test consists of a 3-chamber apparatus, with one compartment designed to have different features from the other compartment (white vs. black walls and horizontal grid vs. cross-grid flooring), and a 'neutral' center chamber (260). Mice injected with the pGIPZ-shRNA 8843 showed a trend toward aversion to the high dose of nicotine, relative to saline, although this result did not reach significance. Mice injected with the pGIPZ-scramble control did not show aversion to the high dose of

nicotine, compared to saline (Fig. 5.4). This result is quite puzzling as I would expect that the high dose of nicotine would be aversive to the pGIPZ-scramble control mice. Thus, it is difficult to interpret these data as the controls did not show aversion to the high nicotine dose which makes the comparison between the pGIPZ-scramble control and pGIPZ-shRNA 8843, in regards to nicotine aversion, confounded.

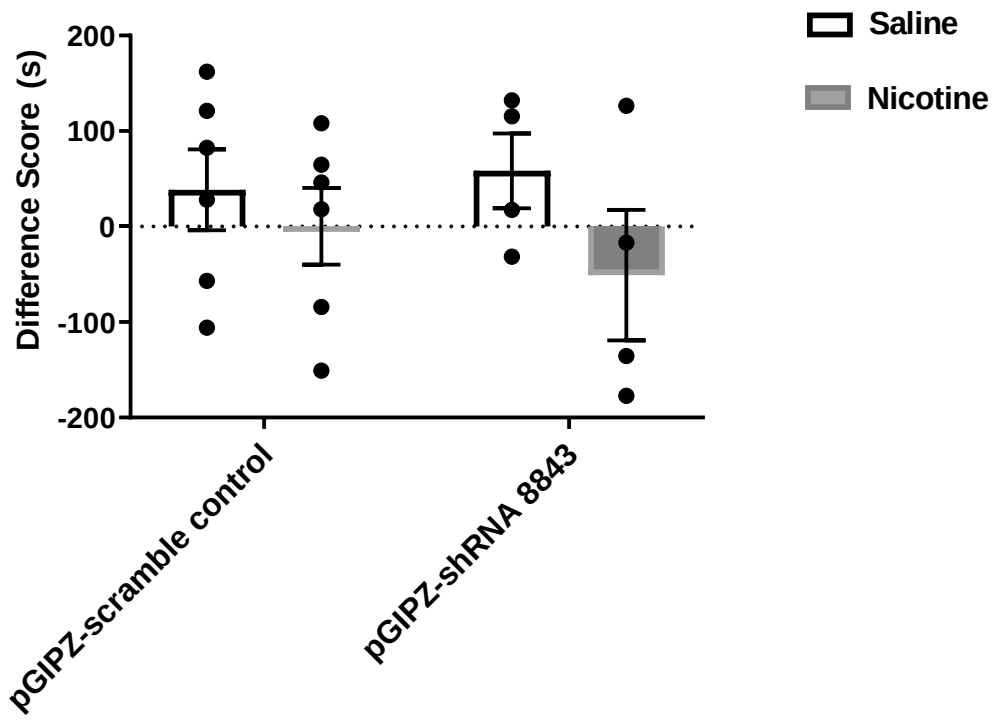

Figure 5.4 Infection of pGIPZ-shRNA 8843 in the IPN did not alter nicotine aversion

The average difference score between mice injected with pGIPZ-scramble or pGIPZ-shRNA 8843 in the IPN. White bars represent mice that were injected (i.p) with saline control and gray bars represent mice injected (i.p) with 1.5mg/kg nicotine. Data are displayed as mean ± SEM. n=4-6 Two-way ANOVA, with Tukey's multiple comparisons were used for statistical analysis. $P > 0.05$ for all comparisons.

Confirming knockdown of *Chrna3* mRNA expression in the IPN

The behavioral assays suggest that α3* nAChRs may not be playing a role in anxiety, novelty preference, or nicotine aversion. To make these conclusions, however, *Chrna3* mRNA knockdown in the IPN must be confirmed. I confirmed lentivirus expression in the IPN (Fig. 5.5a), and performed LCM and RT-qPCR to measure *Chrna3*, *Chrna5*, and *Chrnb4* mRNA expression. Although there was a trend toward decreased *Chrna3* mRNA expression, this did not reach significance (Fig 5.5b), which could be attributed to variability and low sample size. Interestingly, I also saw non-significant reduction of *Chrna5* mRNA expression in mouse brains infected with pGIPZ-shRNA 8843 lentivirus (Fig. 5.5b), suggesting that manipulating *Chrna3* mRNA expression may secondarily disrupt *Chrna5* mRNA expression. Because I did not see significant knockdown of *Chrna3* mRNA expression when mice were injected with 0.3 μl of the shRNA lentivirus (0.3 μl was used for the behavioral assays), I increased the volume of virus to 1 μl and tested for *Chrna3* knockdown. After infecting the pGIPZ-shRNA 8843 into the mouse IPN, I saw an approximately 50% decrease of *Chrna3* mRNA expression (Fig. 5.6), which proved to be statistically significant. Similar to what I saw previously, *Chrna5* mRNA had a trend of decreased expression after knockdown of *Chrna3* mRNA expression, and there was no change in *Chrnb4* expression (Fig. 5.6).

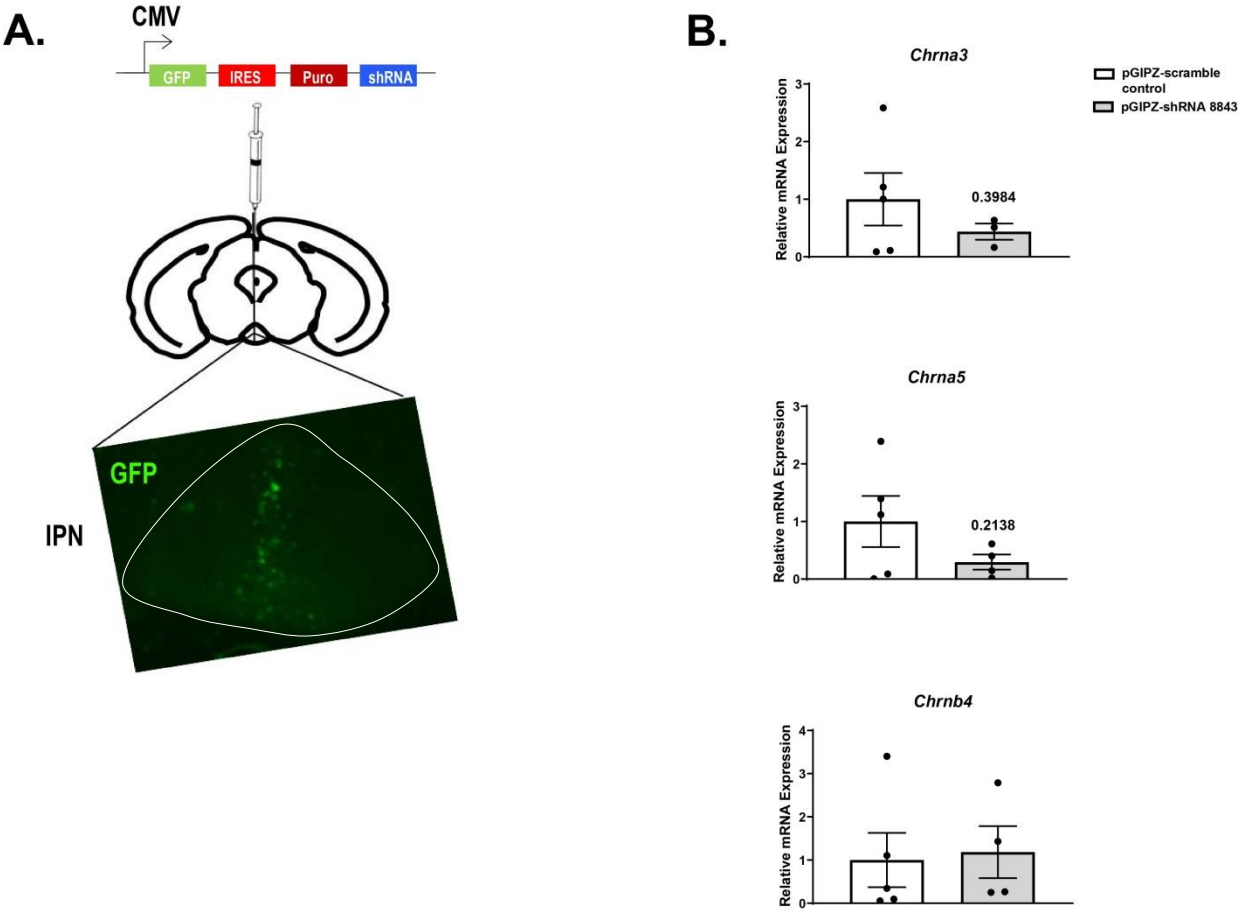

Figure 5.5 Infection of pGIPZ-shRNA 8843 (0.3μl) in the IPN did not knockdown *Chrna3* mRNA expression

A. Virus and coronal brain slice schematic, and representative fluorescence microscopy image of the IPN in a mouse infected with pGIPZ-shRNA 8843. GFP indicates that the neurons are infected with virus. **B.** *Chrna3* (top), *Chrna5* (middle), and *Chrnb4* (bottom) mRNA expression levels measured by RT-qPCR after IPN injection of pGIPZ-scramble control or pGIPZ-shRNA 8843 lentivirus. Data are displayed as mean ± SEM. Individual values are shown as dots. n=3-5 Unpaired t-test was used for statistical analysis. $P > 0.05$ for all comparisons.

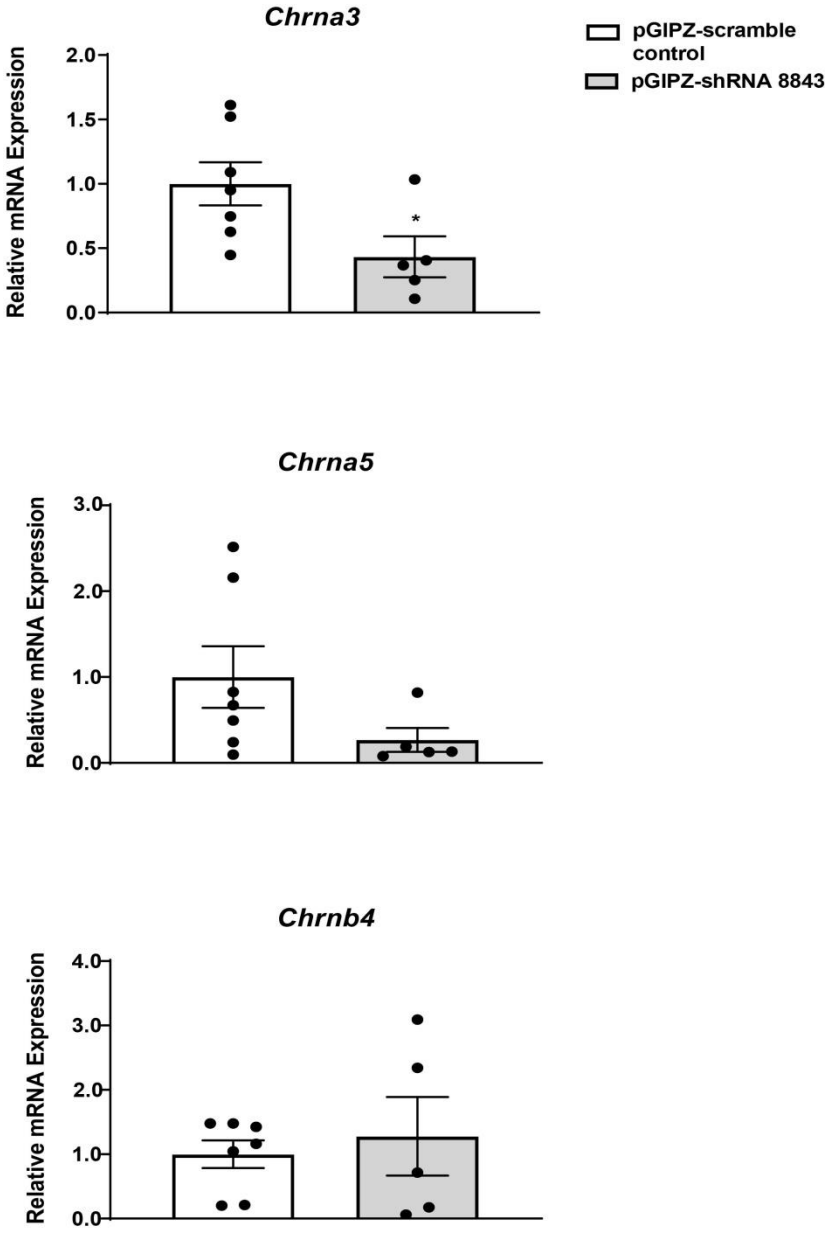

Figure 5.6 Knockdown of *Chrna3* mRNA expression after infection of pGIPZ-shRNA 8843 (1μl) in the IPN

Quantification of *Chrna3* (top), *Chrna5* (middle), and *Chrnb4* (bottom) mRNA expression by RT-qPCR after overexpression of pGIPZ-scramble control or pGIPZ-shRNA 8843 lentiviruses in the IPN. Data are displayed as mean ± SEM. n=5-7 Unpaired t-test was used for statistical analysis. *p<0.05

Discussion

The IPN and nAChRs are involved in behavioral phenotypes involved in the susceptibility to drug addiction, such as anxiety and novelty-seeking behaviors, as well as drug addiction itself (221, 225, 243, 244, 246-248, 255), however the role of α3* nAChRs in these behaviors has not previously been undertaken in part because α3 whole body knockout mice die shortly after birth (249). The goal of this project was to determine if α3* nAChRs contribute to anxiety, novelty-seeking, and nicotine aversion. To investigate this, I took an shRNA lentiviral-mediated approach to knock down *Chrna3* mRNA expression in the IPN. I first tested two pGIPZ-shRNAs to determine their knockdown efficiency. pGIPZ-shRNA 8843 significantly knocked down *Chrna3* mRNA expression, *in vitro*. I also determined that reduced *Chrna3* mRNA expression does not alter the mRNA expression of tightly clustered nAChR subunits *Chrna5* and *Chrnb4*. To investigate if knockdown of *Chrna3* mRNA expression alters behavior, I injected pGIPZ-shRNA 8843 lentivirus into the IPN and expressed the virus for 2.5 weeks prior to the behavioral assays. I first tested anxiety-like behaviors by performing the EPM, OFT, and MBT. The results from these assays suggest that α3* nAChRs are not important for anxiety. Next I assessed social novelty-seeking behavior. There was no difference in novelty preference between pGIPZ-scramble control- and pGIPZ-shRNA 8843-injected mice, suggesting that α3* nAChRs are not involved in social novelty-seeking behaviors. Lastly, I

investigated if α3* nAChRs modulate nicotine aversion, similar to α5 and β4 nAChR subunits. I did not see a significant difference in nicotine aversion between pGIPZ-scramble control- and pGIPZ-shRNA 8843-injected mice, suggesting that α3* nAChRs are not important for nicotine aversion.

After the behavioral assays, lentivirus expression in the IPN was confirmed and *Chrna3* mRNA expression knockdown was measured. *Chrna3* mRNA expression in the IPN was not significantly knocked down, however there was a clear trend for decreased *Chrna3*, as well as *Chrna5* mRNA expression. I wouldn't have expected this as I did not see *Chrna5* mRNA expression change after knocking down *Chrna3* in N2A cells. The lack of significant knockdown of *Chrna3* mRNA expression could be attributed to the low number of samples. Thus, before repeating any behavioral experiments, I wanted to confirm that pGIPZ-shRNA 8843 could significantly knockdown *Chrna3* mRNA expression in the IPN. After increasing the lentivirus volume to 1 μl and increasing the sample size, *Chrna3* mRNA expression was significantly knocked down. Again, *Chrna5* mRNA expression also showed a trend toward decreased expression.

Caveats and Drawbacks

The conclusions from the behavioral assays should be taken with a grain of salt. When analyzing the anxiety behaviors, particularly the EPM data (Fig. 5.2), I noticed that half of the pGIPZ-scramble control mice were very anxious as they barely explored the open arm of the maze. This is unusual as C57BL/6J mice usually spend at least 50 seconds in the open arm of the EPM (253). This is

concerning as comparing anxiety-like behaviors between the two groups can be difficult if the controls already have high levels of anxiety. Additionally, some of the behavioral assays performed were quite variable, including the novelty-seeking and CPA assays; this could be the reason I did not see any significant differences between treatment groups. Specifically, in the novelty-seeking behavior, pGIPZ-scramble control mice spent significantly more time investigating the novel mouse, but this was not seen for pGIPZ-shRNA 8843 mice (Fig. 5.3). Notably, the scatter dots on the bar graphs show that the pGIPZ-shRNA 8843 time of investigating the novel mouse was more variable than pGIPZ-scramble control, which could contribute to the lack of significance. Additionally, the CPA assay showed that the high dose of nicotine was not aversive for either group of animals, which is quite puzzling as high doses of nicotine is known to be aversive (244). However, there was a trend toward nicotine aversion in pGIPZ-shRNA 8843-injected mice, but this did not reach significance due to variability. Regardless, because the high dose of nicotine seemed to not be aversive to the pGIPZ-scramble control mice, this makes the results difficult to interpret. Another caveat of the project is that the pGIPZ-shRNA lentivirus had poor cell infection. As shown in the representative image of the virus expression (Fig. 5.5a), many of the IPN cells were not infected; this was surprising as lentiviruses are known to have wide-spread expression. The lack of pGIPZ-shRNA 8843-infected IPN cells could have contributed to the negative behavioral results. Lastly, because *Chrna5* mRNA expression seems to be

altered after knocking down *Chrna3* mRNA expression, determining the role of α3* nAChRs in phenotypes associated with the susceptibility to nicotine addiction and nicotine addiction itself will be difficult. Any positive behavioral result I would see could be attributed to altered *Chrna5* mRNA expression, and not necessarily due to disrupted *Chrna3* mRNA expression.

Bibliography

1. Patke A, Young MW, Axelrod S. Molecular mechanisms and physiological importance of circadian rhythms. Nat Rev Mol Cell Biol. 2020;21(2):67-84. doi: 10.1038/s41580-019-0179-2. PubMed PMID: 31768006.
2. Xie Y, Tang Q, Chen G, Xie M, Yu S, Zhao J, Chen L. New Insights Into the Circadian Rhythm and Its Related Diseases. Front Physiol. 2019;10:682. doi: 10.3389/fphys.2019.00682. PubMed PMID: 31293431; PMCID: PMC6603140.
3. McClung CR. Plant circadian rhythms. Plant Cell. 2006;18(4):792-803. doi: 10.1105/tpc.106.040980. PubMed PMID: 16595397; PMCID: PMC1425852.
4. Sharma VK. Adaptive significance of circadian clocks. Chronobiol Int. 2003;20(6):901-19. doi: 10.1081/cbi-120026099. PubMed PMID: 14680135.
5. Physiologie Vegetale. Med Chir Rev. 1834;21(42):353-9. PubMed PMID: 29917987; PMCID: PMC5086893.
6. Webb HM. The Physiological Clock: Endogenous Diurnal Rhythms and Biological Chronometry. Erwin Bünning The Physiology of Diurnal Rhythms. Janet Harker. Physiological Zoology. 1965;38(3):322-3. doi: 10.1086/physzool.38.3.30152841.
7. Pittendrigh CS, Bruce VG, Rosensweig NS, Rubin ML. Growth Patterns in Neurospora: A Biological Clock in Neurospora. Nature. 1959;184(4681):169-70. doi: 10.1038/184169a0.
8. Konopka RJ, Benzer S. Clock mutants of Drosophila melanogaster. Proceedings of the National Academy of Sciences of the United States of America. 1971;68(9):2112-6. doi: 10.1073/pnas.68.9.2112. PubMed PMID: 5002428; PMCID: PMC389363.
9. Reddy P, Zehring WA, Wheeler DA, Pirrotta V, Hadfield C, Hall JC, Rosbash M. Molecular analysis of the period locus in Drosophila melanogaster and identification of a transcript involved in biological rhythms. Cell. 1984;38(3):701-10. doi: 10.1016/0092-8674(84)90265-4. PubMed PMID: 6435882.
10. Bargiello TA, Young MW. Molecular genetics of a biological clock in Drosophila. Proceedings of the National Academy of Sciences of the United States of America. 1984;81(7):2142-6. doi: 10.1073/pnas.81.7.2142. PubMed PMID: 16593450; PMCID: PMC345453.
11. Dunlap JC. Molecular bases for circadian clocks. Cell. 1999;96(2):271-90. doi: 10.1016/s0092-8674(00)80566-8. PubMed PMID: 9988221.
12. Young MW, Kay SA. Time zones: a comparative genetics of circadian clocks. Nat Rev Genet. 2001;2(9):702-15. doi: 10.1038/35088576. PubMed PMID: 11533719.
13. Reppert SM, Weaver DR. Coordination of circadian timing in mammals. Nature. 2002;418(6901):935-41. doi: 10.1038/nature00965. PubMed PMID: 12198538.
14. Richter HG, Torres-Farfan C, Rojas-Garcia PP, Campino C, Torrealba F, Seron-Ferre M. The circadian timing system: making sense of day/night gene expression. Biol Res. 2004;37(1):11-28. doi: 10.4067/s0716-97602004000100003. PubMed PMID: 15174302.
15. Stephan FK, Zucker I. Circadian rhythms in drinking behavior and locomotor activity of rats are eliminated by hypothalamic lesions. Proceedings of the National Academy of Sciences of the United States of America. 1972;69(6):1583-6. doi: 10.1073/pnas.69.6.1583. PubMed PMID: 4556464; PMCID: PMC426753.

16. Moore RY, Eichler VB. Loss of a circadian adrenal corticosterone rhythm following suprachiasmatic lesions in the rat. Brain Res. 1972;42(1):201-6. doi: 10.1016/0006-8993(72)90054-6. PubMed PMID: 5047187.
17. Bunger MK, Wilsbacher LD, Moran SM, Clendenin C, Radcliffe LA, Hogenesch JB, Simon MC, Takahashi JS, Bradfield CA. Mop3 is an essential component of the master circadian pacemaker in mammals. Cell. 2000;103(7):1009-17. doi: 10.1016/s0092-8674(00)00205-1. PubMed PMID: 11163178; PMCID: PMC3779439.
18. Ralph MR, Menaker M. A mutation of the circadian system in golden hamsters. Science (New York, NY). 1988;241(4870):1225-7. doi: 10.1126/science.3413487. PubMed PMID: 3413487.
19. Debruyne JP, Noton E, Lambert CM, Maywood ES, Weaver DR, Reppert SM. A clock shock: mouse CLOCK is not required for circadian oscillator function. Neuron. 2006;50(3):465-77. doi: 10.1016/j.neuron.2006.03.041. PubMed PMID: 16675400.
20. Dudley CA, Erbel-Sieler C, Estill SJ, Reick M, Franken P, Pitts S, McKnight SL. Altered patterns of sleep and behavioral adaptability in NPAS2-deficient mice. Science (New York, NY). 2003;301(5631):379-83. doi: 10.1126/science.1082795. PubMed PMID: 12843397.
21. van der Horst GT, Muijtjens M, Kobayashi K, Takano R, Kanno S, Takao M, de Wit J, Verkerk A, Eker AP, van Leenen D, Buijs R, Bootsma D, Hoeijmakers JH, Yasui A. Mammalian Cry1 and Cry2 are essential for maintenance of circadian rhythms. Nature. 1999;398(6728):627-30. doi: 10.1038/19323. PubMed PMID: 10217146.
22. Bae K, Jin X, Maywood ES, Hastings MH, Reppert SM, Weaver DR. Differential functions of mPer1, mPer2, and mPer3 in the SCN circadian clock. Neuron. 2001;30(2):525-36. doi: 10.1016/s0896-6273(01)00302-6. PubMed PMID: 11395012.
23. Ralph MR, Foster RG, Davis FC, Menaker M. Transplanted suprachiasmatic nucleus determines circadian period. Science (New York, NY). 1990;247(4945):975-8. doi: 10.1126/science.2305266. PubMed PMID: 2305266.
24. Loudon AS, Semikhodskii AG, Crosthwaite SK. A brief history of circadian time. Trends Genet. 2000;16(11):477-81. doi: 10.1016/s0168-9525(00)02122-3. PubMed PMID: 11074285.
25. Yang G, Chen L, Grant GR, Paschos G, Song WL, Musiek ES, Lee V, McLoughlin SC, Grosser T, Cotsarelis G, FitzGerald GA. Timing of expression of the core clock gene Bmal1 influences its effects on aging and survival. Sci Transl Med. 2016;8(324):324ra16. doi: 10.1126/scitranslmed.aad3305. PubMed PMID: 26843191; PMCID: PMC4870001.
26. Gekakis N, Staknis D, Nguyen HB, Davis FC, Wilsbacher LD, King DP, Takahashi JS, Weitz CJ. Role of the CLOCK protein in the mammalian circadian mechanism. Science (New York, NY). 1998;280(5369):1564-9. doi: 10.1126/science.280.5369.1564. PubMed PMID: 9616112.
27. Hogenesch JB, Gu YZ, Jain S, Bradfield CA. The basic-helix-loop-helix-PAS orphan MOP3 forms transcriptionally active complexes with circadian and hypoxia factors. Proceedings of the National Academy of Sciences of the United States of America. 1998;95(10):5474-9. doi: 10.1073/pnas.95.10.5474. PubMed PMID: 9576906; PMCID: PMC20401.
28. Preitner N, Damiola F, Lopez-Molina L, Zakany J, Duboule D, Albrecht U, Schibler U. The orphan nuclear receptor REV-ERBalpha controls circadian transcription within the positive limb of the mammalian circadian oscillator. Cell. 2002;110(2):251-60. doi: 10.1016/s0092-8674(02)00825-5. PubMed PMID: 12150932.
29. Sato TK, Panda S, Miraglia LJ, Reyes TM, Rudic RD, McNamara P, Naik KA, FitzGerald GA, Kay SA, Hogenesch JB. A functional genomics strategy reveals Rora as a component of the

mammalian circadian clock. Neuron. 2004;43(4):527-37. doi: 10.1016/j.neuron.2004.07.018. PubMed PMID: 15312651.

30. Shearman LP, Jin X, Lee C, Reppert SM, Weaver DR. Targeted disruption of the mPer3 gene: subtle effects on circadian clock function. Mol Cell Biol. 2000;20(17):6269-75. doi: 10.1128/mcb.20.17.6269-6275.2000. PubMed PMID: 10938103; PMCID: PMC86101.

31. DeBruyne JP, Weaver DR, Reppert SM. CLOCK and NPAS2 have overlapping roles in the suprachiasmatic circadian clock. Nat Neurosci. 2007;10(5):543-5. doi: 10.1038/nn1884. PubMed PMID: 17417633; PMCID: PMC2782643.

32. Etchegaray JP, Machida KK, Noton E, Constance CM, Dallmann R, Di Napoli MN, DeBruyne JP, Lambert CM, Yu EA, Reppert SM, Weaver DR. Casein kinase 1 delta regulates the pace of the mammalian circadian clock. Mol Cell Biol. 2009;29(14):3853-66. doi: 10.1128/MCB.00338-09. PubMed PMID: 19414593; PMCID: PMC2704743.

33. Meng QJ, Logunova L, Maywood ES, Gallego M, Lebiecki J, Brown TM, Sladek M, Semikhodskii AS, Glossop NRJ, Piggins HD, Chesham JE, Bechtold DA, Yoo SH, Takahashi JS, Virshup DM, Boot-Handford RP, Hastings MH, Loudon ASI. Setting clock speed in mammals: the CK1 epsilon tau mutation in mice accelerates circadian pacemakers by selectively destabilizing PERIOD proteins. Neuron. 2008;58(1):78-88. doi: 10.1016/j.neuron.2008.01.019. PubMed PMID: 18400165; PMCID: PMC3756141.

34. Lee H, Chen R, Lee Y, Yoo S, Lee C. Essential roles of CKIdelta and CKIepsilon in the mammalian circadian clock. Proceedings of the National Academy of Sciences of the United States of America. 2009;106(50):21359-64. doi: 10.1073/pnas.0906651106. PubMed PMID: 19948962; PMCID: PMC2795500.

35. Akashi M, Tsuchiya Y, Yoshino T, Nishida E. Control of intracellular dynamics of mammalian period proteins by casein kinase I epsilon (CKIepsilon) and CKIdelta in cultured cells. Mol Cell Biol. 2002;22(6):1693-703. doi: 10.1128/mcb.22.6.1693-1703.2002. PubMed PMID: 11865049; PMCID: PMC135601.

36. Eide EJ, Vielhaber EL, Hinz WA, Virshup DM. The circadian regulatory proteins BMAL1 and cryptochromes are substrates of casein kinase Iepsilon. The Journal of biological chemistry. 2002;277(19):17248-54. doi: 10.1074/jbc.M111466200. PubMed PMID: 11875063; PMCID: PMC1513548.

37. Lee C, Etchegaray JP, Cagampang FR, Loudon AS, Reppert SM. Posttranslational mechanisms regulate the mammalian circadian clock. Cell. 2001;107(7):855-67. doi: 10.1016/s0092-8674(01)00610-9. PubMed PMID: 11779462.

38. van der Vinne V, Swoap SJ, Vajtay TJ, Weaver DR. Desynchrony between brain and peripheral clocks caused by CK1delta/epsilon disruption in GABA neurons does not lead to adverse metabolic outcomes. Proceedings of the National Academy of Sciences of the United States of America. 2018;115(10):E2437-E46. doi: 10.1073/pnas.1712324115. PubMed PMID: 29463694; PMCID: PMC5877989.

39. Mehra A, Baker CL, Loros JJ, Dunlap JC. Post-translational modifications in circadian rhythms. Trends Biochem Sci. 2009;34(10):483-90. doi: 10.1016/j.tibs.2009.06.006. PubMed PMID: 19740663; PMCID: PMC2765057.

40. Weaver DR, van der Vinne V, Giannaris EL, Vajtay TJ, Holloway KL, Anaclet C. Functionally Complete Excision of Conditional Alleles in the Mouse Suprachiasmatic Nucleus by Vgat-ires-Cre. J Biol Rhythms. 2018;33(2):179-91. doi: 10.1177/0748730418757006. PubMed PMID: 29671710; PMCID: PMC6497156.

41. Abrahamson EE, Moore RY. Suprachiasmatic nucleus in the mouse: retinal innervation, intrinsic organization and efferent projections. Brain Res. 2001;916(1-2):172-91. doi: 10.1016/s0006-8993(01)02890-6. PubMed PMID: 11597605.
42. Cassone VM, Speh JC, Card JP, Moore RY. Comparative anatomy of the mammalian hypothalamic suprachiasmatic nucleus. J Biol Rhythms. 1988;3(1):71-91. doi: 10.1177/074873048800300106. PubMed PMID: 2979633.
43. Leak RK, Moore RY. Topographic organization of suprachiasmatic nucleus projection neurons. J Comp Neurol. 2001;433(3):312-34. doi: 10.1002/cne.1142. PubMed PMID: 11298358.
44. Harmar AJ, Marston HM, Shen S, Spratt C, West KM, Sheward WJ, Morrison CF, Dorin JR, Piggins HD, Reubi JC, Kelly JS, Maywood ES, Hastings MH. The VPAC(2) receptor is essential for circadian function in the mouse suprachiasmatic nuclei. Cell. 2002;109(4):497-508. doi: 10.1016/s0092-8674(02)00736-5. PubMed PMID: 12086606.
45. Aton SJ, Colwell CS, Harmar AJ, Waschek J, Herzog ED. Vasoactive intestinal polypeptide mediates circadian rhythmicity and synchrony in mammalian clock neurons. Nat Neurosci. 2005;8(4):476-83. doi: 10.1038/nn1419. PubMed PMID: 15750589; PMCID: PMC1628303.
46. Welsh DK, Takahashi JS, Kay SA. Suprachiasmatic nucleus: cell autonomy and network properties. Annu Rev Physiol. 2010;72:551-77. doi: 10.1146/annurev-physiol-021909-135919. PubMed PMID: 20148688; PMCID: PMC3758475.
47. Smyllie NJ, Chesham JE, Hamnett R, Maywood ES, Hastings MH. Temporally chimeric mice reveal flexibility of circadian period-setting in the suprachiasmatic nucleus. Proceedings of the National Academy of Sciences of the United States of America. 2016;113(13):3657-62. doi: 10.1073/pnas.1511351113. PubMed PMID: 26966234; PMCID: PMC4822582.
48. Mieda M, Okamoto H, Sakurai T. Manipulating the Cellular Circadian Period of Arginine Vasopressin Neurons Alters the Behavioral Circadian Period. Curr Biol. 2016;26(18):2535-42. doi: 10.1016/j.cub.2016.07.022. PubMed PMID: 27568590.
49. Moore RY, Lenn NJ. A retinohypothalamic projection in the rat. J Comp Neurol. 1972;146(1):1-14. doi: 10.1002/cne.901460102. PubMed PMID: 4116104.
50. Hendrickson AE, Wagoner N, Cowan WM. An autoradiographic and electron microscopic study of retino-hypothalamic connections. Z Zellforsch Mikrosk Anat. 1972;135(1):1-26. doi: 10.1007/bf00307084. PubMed PMID: 4629413.
51. Welsh DK, Logothetis DE, Meister M, Reppert SM. Individual neurons dissociated from rat suprachiasmatic nucleus express independently phased circadian firing rhythms. Neuron. 1995;14(4):697-706. doi: 10.1016/0896-6273(95)90214-7. PubMed PMID: 7718233.
52. Liu AC, Welsh DK, Ko CH, Tran HG, Zhang EE, Priest AA, Buhr ED, Singer O, Meeker K, Verma IM, Doyle FJ, 3rd, Takahashi JS, Kay SA. Intercellular coupling confers robustness against mutations in the SCN circadian clock network. Cell. 2007;129(3):605-16. doi: 10.1016/j.cell.2007.02.047. PubMed PMID: 17482552; PMCID: PMC3749832.
53. Yoo SH, Yamazaki S, Lowrey PL, Shimomura K, Ko CH, Buhr ED, Siepka SM, Hong HK, Oh WJ, Yoo OJ, Menaker M, Takahashi JS. PERIOD2::LUCIFERASE real-time reporting of circadian dynamics reveals persistent circadian oscillations in mouse peripheral tissues. Proceedings of the National Academy of Sciences of the United States of America. 2004;101(15):5339-46. doi: 10.1073/pnas.0308709101. PubMed PMID: 14963227; PMCID: PMC397382.
54. Panda S, Antoch MP, Miller BH, Su AI, Schook AB, Straume M, Schultz PG, Kay SA, Takahashi JS, Hogenesch JB. Coordinated transcription of key pathways in the mouse by the

circadian clock. Cell. 2002;109(3):307-20. doi: 10.1016/s0092-8674(02)00722-5. PubMed PMID: 12015981.

55. Allen G, Rappe J, Earnest DJ, Cassone VM. Oscillating on borrowed time: diffusible signals from immortalized suprachiasmatic nucleus cells regulate circadian rhythmicity in cultured fibroblasts. The Journal of neuroscience : the official journal of the Society for Neuroscience. 2001;21(20):7937-43. PubMed PMID: 11588167; PMCID: PMC6763840.

56. King DP, Zhao Y, Sangoram AM, Wilsbacher LD, Tanaka M, Antoch MP, Steeves TD, Vitaterna MH, Kornhauser JM, Lowrey PL, Turek FW, Takahashi JS. Positional cloning of the mouse circadian clock gene. Cell. 1997;89(4):641-53. doi: 10.1016/s0092-8674(00)80245-7. PubMed PMID: 9160755; PMCID: PMC3815553.

57. Tei H, Okamura H, Shigeyoshi Y, Fukuhara C, Ozawa R, Hirose M, Sakaki Y. Circadian oscillation of a mammalian homologue of the Drosophila period gene. Nature. 1997;389(6650):512-6. doi: 10.1038/39086. PubMed PMID: 9333243.

58. Yagita K, Tamanini F, van Der Horst GT, Okamura H. Molecular mechanisms of the biological clock in cultured fibroblasts. Science (New York, NY). 2001;292(5515):278-81. doi: 10.1126/science.1059542. PubMed PMID: 11303101.

59. Nagoshi E, Saini C, Bauer C, Laroche T, Naef F, Schibler U. Circadian gene expression in individual fibroblasts: cell-autonomous and self-sustained oscillators pass time to daughter cells. Cell. 2004;119(5):693-705. doi: 10.1016/j.cell.2004.11.015. PubMed PMID: 15550250.

60. Welsh DK, Yoo SH, Liu AC, Takahashi JS, Kay SA. Bioluminescence imaging of individual fibroblasts reveals persistent, independently phased circadian rhythms of clock gene expression. Curr Biol. 2004;14(24):2289-95. doi: 10.1016/j.cub.2004.11.057. PubMed PMID: 15620658; PMCID: PMC3777438.

61. Balsalobre A, Damiola F, Schibler U. A serum shock induces circadian gene expression in mammalian tissue culture cells. Cell. 1998;93(6):929-37. doi: 10.1016/s0092-8674(00)81199-x. PubMed PMID: 9635423.

62. Yamazaki S, Numano R, Abe M, Hida A, Takahashi R, Ueda M, Block GD, Sakaki Y, Menaker M, Tei H. Resetting central and peripheral circadian oscillators in transgenic rats. Science (New York, NY). 2000;288(5466):682-5. doi: 10.1126/science.288.5466.682. PubMed PMID: 10784453.

63. Guo H, Brewer JM, Lehman MN, Bittman EL. Suprachiasmatic regulation of circadian rhythms of gene expression in hamster peripheral organs: effects of transplanting the pacemaker. The Journal of neuroscience : the official journal of the Society for Neuroscience. 2006;26(24):6406-12. doi: 10.1523/JNEUROSCI.4676-05.2006. PubMed PMID: 16775127; PMCID: PMC6674028.

64. Silver R, LeSauter J, Tresco PA, Lehman MN. A diffusible coupling signal from the transplanted suprachiasmatic nucleus controlling circadian locomotor rhythms. Nature. 1996;382(6594):810-3. doi: 10.1038/382810a0. PubMed PMID: 8752274.

65. Ueyama T, Krout KE, Nguyen XV, Karpitskiy V, Kollert A, Mettenleiter TC, Loewy AD. Suprachiasmatic nucleus: a central autonomic clock. Nat Neurosci. 1999;2(12):1051-3. doi: 10.1038/15973. PubMed PMID: 10570479.

66. Balsalobre A, Brown SA, Marcacci L, Tronche F, Kellendonk C, Reichardt HM, Schutz G, Schibler U. Resetting of circadian time in peripheral tissues by glucocorticoid signaling. Science (New York, NY). 2000;289(5488):2344-7. doi: 10.1126/science.289.5488.2344. PubMed PMID: 11009419.

67. Balsalobre A, Marcacci L, Schibler U. Multiple signaling pathways elicit circadian gene expression in cultured Rat-1 fibroblasts. Curr Biol. 2000;10(20):1291-4. doi: 10.1016/s0960-9822(00)00758-2. PubMed PMID: 11069111.
68. McNamara P, Seo SB, Rudic RD, Sehgal A, Chakravarti D, FitzGerald GA. Regulation of CLOCK and MOP4 by nuclear hormone receptors in the vasculature: a humoral mechanism to reset a peripheral clock. Cell. 2001;105(7):877-89. doi: 10.1016/s0092-8674(01)00401-9. PubMed PMID: 11439184.
69. Oishi K, Sakamoto K, Okada T, Nagase T, Ishida N. Humoral signals mediate the circadian expression of rat period homologue (rPer2) mRNA in peripheral tissues. Neurosci Lett. 1998;256(2):117-9. doi: 10.1016/s0304-3940(98)00765-4. PubMed PMID: 9853717.
70. Guo H, Brewer JM, Champhekar A, Harris RB, Bittman EL. Differential control of peripheral circadian rhythms by suprachiasmatic-dependent neural signals. Proceedings of the National Academy of Sciences of the United States of America. 2005;102(8):3111-6. doi: 10.1073/pnas.0409734102. PubMed PMID: 15710878; PMCID: PMC548796.
71. Stehle JH, von Gall C, Korf HW. Melatonin: a clock-output, a clock-input. J Neuroendocrinol. 2003;15(4):383-9. doi: 10.1046/j.1365-2826.2003.01001.x. PubMed PMID: 12622838.
72. Pando MP, Morse D, Cermakian N, Sassone-Corsi P. Phenotypic rescue of a peripheral clock genetic defect via SCN hierarchical dominance. Cell. 2002;110(1):107-17. doi: 10.1016/s0092-8674(02)00803-6. PubMed PMID: 12151001.
73. Brown SA, Zumbrunn G, Fleury-Olela F, Preitner N, Schibler U. Rhythms of mammalian body temperature can sustain peripheral circadian clocks. Curr Biol. 2002;12(18):1574-83. doi: 10.1016/s0960-9822(02)01145-4. PubMed PMID: 12372249.
74. Ohnishi N, Tahara Y, Kuriki D, Haraguchi A, Shibata S. Warm water bath stimulates phase-shifts of the peripheral circadian clocks in PER2::LUCIFERASE mouse. PloS one. 2014;9(6):e100272. doi: 10.1371/journal.pone.0100272. PubMed PMID: 24933288; PMCID: PMC4059754.
75. Buhr ED, Yoo SH, Takahashi JS. Temperature as a universal resetting cue for mammalian circadian oscillators. Science (New York, NY). 2010;330(6002):379-85. doi: 10.1126/science.1195262. PubMed PMID: 20947768; PMCID: PMC3625727.
76. Stratmann M, Schibler U. Properties, entrainment, and physiological functions of mammalian peripheral oscillators. J Biol Rhythms. 2006;21(6):494-506. doi: 10.1177/0748730406293889. PubMed PMID: 17107939.
77. Hara R, Wan K, Wakamatsu H, Aida R, Moriya T, Akiyama M, Shibata S. Restricted feeding entrains liver clock without participation of the suprachiasmatic nucleus. Genes Cells. 2001;6(3):269-78. doi: 10.1046/j.1365-2443.2001.00419.x. PubMed PMID: 11260270.
78. Vetter C. Circadian disruption: What do we actually mean? Eur J Neurosci. 2020;51(1):531-50. doi: 10.1111/ejn.14255. PubMed PMID: 30402904; PMCID: PMC6504624.
79. Qian J, Scheer F. Circadian System and Glucose Metabolism: Implications for Physiology and Disease. Trends Endocrinol Metab. 2016;27(5):282-93. doi: 10.1016/j.tem.2016.03.005. PubMed PMID: 27079518; PMCID: PMC4842150.
80. Lesicka M, Jablonska E, Wieczorek E, Peplonska B, Gromadzinska J, Seroczynska B, Kalinowski L, Skokowski J, Reszka E. Circadian Gene Polymorphisms Associated with Breast Cancer Susceptibility. Int J Mol Sci. 2019;20(22). doi: 10.3390/ijms20225704. PubMed PMID: 31739444; PMCID: PMC6888181.

81. Scott EM, Carter AM, Grant PJ. Association between polymorphisms in the Clock gene, obesity and the metabolic syndrome in man. Int J Obes (Lond). 2008;32(4):658-62. doi: 10.1038/sj.ijo.0803778. PubMed PMID: 18071340.
82. Sookoian S, Castano G, Gemma C, Gianotti TF, Pirola CJ. Common genetic variations in CLOCK transcription factor are associated with nonalcoholic fatty liver disease. World J Gastroenterol. 2007;13(31):4242-8. doi: 10.3748/wjg.v13.i31.4242. PubMed PMID: 17696255; PMCID: PMC4250625.
83. Sookoian S, Gemma C, Gianotti TF, Burgueno A, Castano G, Pirola CJ. Genetic variants of Clock transcription factor are associated with individual susceptibility to obesity. Am J Clin Nutr. 2008;87(6):1606-15. doi: 10.1093/ajcn/87.6.1606. PubMed PMID: 18541547.
84. Englund A, Kovanen L, Saarikoski ST, Haukka J, Reunanen A, Aromaa A, Lonnqvist J, Partonen T. NPAS2 and PER2 are linked to risk factors of the metabolic syndrome. J Circadian Rhythms. 2009;7:5. doi: 10.1186/1740-3391-7-5. PubMed PMID: 19470168; PMCID: PMC2697141.
85. Maury E, Ramsey KM, Bass J. Circadian rhythms and metabolic syndrome: from experimental genetics to human disease. Circ Res. 2010;106(3):447-62. doi: 10.1161/CIRCRESAHA.109.208355. PubMed PMID: 20167942; PMCID: PMC2837358.
86. Kim MJ, Son KH, Park HY, Choi DJ, Yoon CH, Lee HY, Cho EY, Cho MC. Association between shift work and obesity among female nurses: Korean Nurses' Survey. BMC Public Health. 2013;13:1204. doi: 10.1186/1471-2458-13-1204. PubMed PMID: 24354395; PMCID: PMC3878177.
87. Canuto R, Pattussi MP, Macagnan JB, Henn RL, Olinto MT. Sleep deprivation and obesity in shift workers in southern Brazil. Public Health Nutr. 2014;17(11):2619-23. doi: 10.1017/S1368980013002838. PubMed PMID: 24168892.
88. Esquirol Y, Bongard V, Ferrieres J, Verdier H, Perret B. Shiftwork and higher pancreatic secretion: early detection of an intermediate state of insulin resistance? Chronobiol Int. 2012;29(9):1258-66. doi: 10.3109/07420528.2012.719959. PubMed PMID: 23005602.
89. Pan A, Schernhammer ES, Sun Q, Hu FB. Rotating night shift work and risk of type 2 diabetes: two prospective cohort studies in women. PLoS Med. 2011;8(12):e1001141. doi: 10.1371/journal.pmed.1001141. PubMed PMID: 22162955; PMCID: PMC3232220.
90. Shan Z, Li Y, Zong G, Guo Y, Li J, Manson JE, Hu FB, Willett WC, Schernhammer ES, Bhupathiraju SN. Rotating night shift work and adherence to unhealthy lifestyle in predicting risk of type 2 diabetes: results from two large US cohorts of female nurses. BMJ. 2018;363:k4641. doi: 10.1136/bmj.k4641. PubMed PMID: 30464025; PMCID: PMC6247172 at www.icmje.org/coi_disclosure.pdf (available on request from the corresponding author) and declare: no support from any organization for the submitted work other than those detailed above; no financial relationships with any organizations that might have an interest in the submitted work in the previous three years; no other relationships or activities that could appear to have influenced the submitted work.
91. Ika K, Suzuki E, Mitsuhashi T, Takao S, Doi H. Shift work and diabetes mellitus among male workers in Japan: does the intensity of shift work matter? Acta Med Okayama. 2013;67(1):25-33. doi: 10.18926/AMO/49254. PubMed PMID: 23439506.
92. Romon M, Nuttens MC, Fievet C, Pot P, Bard JM, Furon D, Fruchart JC. Increased triglyceride levels in shift workers. Am J Med. 1992;93(3):259-62. doi: 10.1016/0002-9343(92)90230-9. PubMed PMID: 1524076.

93. Nakamura K, Shimai S, Kikuchi S, Tominaga K, Takahashi H, Tanaka M, Nakano S, Motohashi Y, Nakadaira H, Yamamoto M. Shift work and risk factors for coronary heart disease in Japanese blue-collar workers: serum lipids and anthropometric characteristics. Occup Med (Lond). 1997;47(3):142-6. doi: 10.1093/occmed/47.3.142. PubMed PMID: 9156468.
94. Dochi M, Suwazono Y, Sakata K, Okubo Y, Oishi M, Tanaka K, Kobayashi E, Nogawa K. Shift work is a risk factor for increased total cholesterol level: a 14-year prospective cohort study in 6886 male workers. Occup Environ Med. 2009;66(9):592-7. doi: 10.1136/oem.2008.042176. PubMed PMID: 19690156.
95. Schernhammer ES, Laden F, Speizer FE, Willett WC, Hunter DJ, Kawachi I, Colditz GA. Rotating night shifts and risk of breast cancer in women participating in the nurses' health study. J Natl Cancer Inst. 2001;93(20):1563-8. doi: 10.1093/jnci/93.20.1563. PubMed PMID: 11604480.
96. Megdal SP, Kroenke CH, Laden F, Pukkala E, Schernhammer ES. Night work and breast cancer risk: a systematic review and meta-analysis. Eur J Cancer. 2005;41(13):2023-32. doi: 10.1016/j.ejca.2005.05.010. PubMed PMID: 16084719.
97. Weibel L, Brandenberger G. Disturbances in hormonal profiles of night workers during their usual sleep and work times. J Biol Rhythms. 1998;13(3):202-8. doi: 10.1177/074873098129000048. PubMed PMID: 9615284.
98. Midwinter MJ, Arendt J. Adaptation of the melatonin rhythm in human subjects following night-shift work in Antarctica. Neurosci Lett. 1991;122(2):195-8. doi: 10.1016/0304-3940(91)90856-o. PubMed PMID: 2027519.
99. Ross JK, Arendt J, Horne J, Haston W. Night-shift work in Antarctica: sleep characteristics and bright light treatment. Physiol Behav. 1995;57(6):1169-74. doi: 10.1016/0031-9384(95)00018-e. PubMed PMID: 7652039.
100. Waterhouse J, Edwards B, Nevill A, Carvalho S, Atkinson G, Buckley P, Reilly T, Godfrey R, Ramsay R. Identifying some determinants of "jet lag" and its symptoms: a study of athletes and other travellers. Br J Sports Med. 2002;36(1):54-60. doi: 10.1136/bjsm.36.1.54. PubMed PMID: 11867494; PMCID: PMC1724441.
101. Cho K, Ennaceur A, Cole JC, Suh CK. Chronic jet lag produces cognitive deficits. The Journal of neuroscience : the official journal of the Society for Neuroscience. 2000;20(6):RC66. PubMed PMID: 10704520; PMCID: PMC6772481.
102. Cho K. Chronic 'jet lag' produces temporal lobe atrophy and spatial cognitive deficits. Nat Neurosci. 2001;4(6):567-8. doi: 10.1038/88384. PubMed PMID: 11369936.
103. Eastman CI, Burgess HJ. How To Travel the World Without Jet lag. Sleep Med Clin. 2009;4(2):241-55. doi: 10.1016/j.jsmc.2009.02.006. PubMed PMID: 20204161; PMCID: PMC2829880.
104. Scheer FA, Hilton MF, Mantzoros CS, Shea SA. Adverse metabolic and cardiovascular consequences of circadian misalignment. Proceedings of the National Academy of Sciences of the United States of America. 2009;106(11):4453-8. doi: 10.1073/pnas.0808180106. PubMed PMID: 19255424; PMCID: PMC2657421.
105. Morris CJ, Purvis TE, Hu K, Scheer FA. Circadian misalignment increases cardiovascular disease risk factors in humans. Proceedings of the National Academy of Sciences of the United States of America. 2016;113(10):E1402-11. doi: 10.1073/pnas.1516953113. PubMed PMID: 26858430; PMCID: PMC4790999.
106. Papagiannakopoulos T, Bauer MR, Davidson SM, Heimann M, Subbaraj L, Bhutkar A, Bartlebaugh J, Vander Heiden MG, Jacks T. Circadian Rhythm Disruption Promotes Lung

Tumorigenesis. Cell Metab. 2016;24(2):324-31. doi: 10.1016/j.cmet.2016.07.001. PubMed PMID: 27476975; PMCID: PMC5367626.
107. Tsai LL, Tsai YC, Hwang K, Huang YW, Tzeng JE. Repeated light-dark shifts speed up body weight gain in male F344 rats. Am J Physiol Endocrinol Metab. 2005;289(2):E212-7. doi: 10.1152/ajpendo.00603.2004. PubMed PMID: 15741238.
108. Filipski E, Subramanian P, Carriere J, Guettier C, Barbason H, Levi F. Circadian disruption accelerates liver carcinogenesis in mice. Mutat Res. 2009;680(1-2):95-105. doi: 10.1016/j.mrgentox.2009.10.002. PubMed PMID: 19833225.
109. Lamia KA, Storch KF, Weitz CJ. Physiological significance of a peripheral tissue circadian clock. Proceedings of the National Academy of Sciences of the United States of America. 2008;105(39):15172-7. doi: 10.1073/pnas.0806717105. PubMed PMID: 18779586; PMCID: PMC2532700.
110. Rudic RD, McNamara P, Curtis AM, Boston RC, Panda S, Hogenesch JB, Fitzgerald GA. BMAL1 and CLOCK, two essential components of the circadian clock, are involved in glucose homeostasis. PLoS Biol. 2004;2(11):e377. doi: 10.1371/journal.pbio.0020377. PubMed PMID: 15523558; PMCID: PMC524471.
111. Vitaterna MH, King DP, Chang AM, Kornhauser JM, Lowrey PL, McDonald JD, Dove WF, Pinto LH, Turek FW, Takahashi JS. Mutagenesis and mapping of a mouse gene, Clock, essential for circadian behavior. Science (New York, NY). 1994;264(5159):719-25. doi: 10.1126/science.8171325. PubMed PMID: 8171325; PMCID: PMC3839659.
112. Turek FW, Joshu C, Kohsaka A, Lin E, Ivanova G, McDearmon E, Laposky A, Losee-Olson S, Easton A, Jensen DR, Eckel RH, Takahashi JS, Bass J. Obesity and metabolic syndrome in circadian Clock mutant mice. Science (New York, NY). 2005;308(5724):1043-5. doi: 10.1126/science.1108750. PubMed PMID: 15845877; PMCID: PMC3764501.
113. Antoch MP, Song EJ, Chang AM, Vitaterna MH, Zhao Y, Wilsbacher LD, Sangoram AM, King DP, Pinto LH, Takahashi JS. Functional identification of the mouse circadian Clock gene by transgenic BAC rescue. Cell. 1997;89(4):655-67. doi: 10.1016/s0092-8674(00)80246-9. PubMed PMID: 9160756; PMCID: PMC3764491.
114. Tsang AH, Astiz M, Leinweber B, Oster H. Rodent Models for the Analysis of Tissue Clock Function in Metabolic Rhythms Research. Front Endocrinol (Lausanne). 2017;8:27. doi: 10.3389/fendo.2017.00027. PubMed PMID: 28243224; PMCID: PMC5304405.
115. Shostak A, Meyer-Kovac J, Oster H. Circadian regulation of lipid mobilization in white adipose tissues. Diabetes. 2013;62(7):2195-203. doi: 10.2337/db12-1449. PubMed PMID: 23434933; PMCID: PMC3712056.
116. Zheng B, Larkin DW, Albrecht U, Sun ZS, Sage M, Eichele G, Lee CC, Bradley A. The mPer2 gene encodes a functional component of the mammalian circadian clock. Nature. 1999;400(6740):169-73. doi: 10.1038/22118. PubMed PMID: 10408444.
117. Dallmann R, Weaver DR. Altered body mass regulation in male mPeriod mutant mice on high-fat diet. Chronobiol Int. 2010;27(6):1317-28. doi: 10.3109/07420528.2010.489166. PubMed PMID: 20653457; PMCID: PMC2911971.
118. Cho H, Zhao X, Hatori M, Yu RT, Barish GD, Lam MT, Chong LW, DiTacchio L, Atkins AR, Glass CK, Liddle C, Auwerx J, Downes M, Panda S, Evans RM. Regulation of circadian behaviour and metabolism by REV-ERB-alpha and REV-ERB-beta. Nature. 2012;485(7396):123-7. doi: 10.1038/nature11048. PubMed PMID: 22460952; PMCID: PMC3367514.

119. Yang X, Wood PA, Oh EY, Du-Quiton J, Ansell CM, Hrushesky WJ. Down regulation of circadian clock gene Period 2 accelerates breast cancer growth by altering its daily growth rhythm. Breast Cancer Res Treat. 2009;117(2):423-31. doi: 10.1007/s10549-008-0133-z. PubMed PMID: 18651214.
120. West AC, Smith L, Ray DW, Loudon ASI, Brown TM, Bechtold DA. Misalignment with the external light environment drives metabolic and cardiac dysfunction. Nat Commun. 2017;8(1):417. doi: 10.1038/s41467-017-00462-2. PubMed PMID: 28900189; PMCID: PMC5595905.
121. Nagano M, Adachi A, Nakahama K, Nakamura T, Tamada M, Meyer-Bernstein E, Sehgal A, Shigeyoshi Y. An abrupt shift in the day/night cycle causes desynchrony in the mammalian circadian center. The Journal of neuroscience : the official journal of the Society for Neuroscience. 2003;23(14):6141-51. PubMed PMID: 12853433; PMCID: PMC6740348.
122. Yamaguchi Y, Suzuki T, Mizoro Y, Kori H, Okada K, Chen Y, Fustin JM, Yamazaki F, Mizuguchi N, Zhang J, Dong X, Tsujimoto G, Okuno Y, Doi M, Okamura H. Mice genetically deficient in vasopressin V1a and V1b receptors are resistant to jet lag. Science (New York, NY). 2013;342(6154):85-90. doi: 10.1126/science.1238599. PubMed PMID: 24092737.
123. Leise TL, Goldberg A, Michael J, Montoya G, Solow S, Molyneux P, Vetrivelan R, Harrington ME. Recurring circadian disruption alters circadian clock sensitivity to resetting. Eur J Neurosci. 2018. doi: 10.1111/ejn.14179. PubMed PMID: 30269396; PMCID: PMC6441381.
124. Nicholls SK, Casiraghi LP, Wang W, Weber ET, Harrington ME. Evidence for Internal Desynchrony Caused by Circadian Clock Resetting. Yale J Biol Med. 2019;92(2):259-70. PubMed PMID: 31249487; PMCID: PMC6585527.
125. Reddy AB, Field MD, Maywood ES, Hastings MH. Differential resynchronisation of circadian clock gene expression within the suprachiasmatic nuclei of mice subjected to experimental jet lag. The Journal of neuroscience : the official journal of the Society for Neuroscience. 2002;22(17):7326-30. PubMed PMID: 12196553; PMCID: PMC6757999.
126. Damiola F, Le Minh N, Preitner N, Kornmann B, Fleury-Olela F, Schibler U. Restricted feeding uncouples circadian oscillators in peripheral tissues from the central pacemaker in the suprachiasmatic nucleus. Genes Dev. 2000;14(23):2950-61. doi: 10.1101/gad.183500. PubMed PMID: 11114885; PMCID: PMC317100.
127. Nakamura W, Yamazaki S, Takasu NN, Mishima K, Block GD. Differential response of Period 1 expression within the suprachiasmatic nucleus. The Journal of neuroscience : the official journal of the Society for Neuroscience. 2005;25(23):5481-7. doi: 10.1523/JNEUROSCI.0889-05.2005. PubMed PMID: 15944376; PMCID: PMC6724974.
128. Hamada T, Sutherland K, Ishikawa M, Miyamoto N, Honma S, Shirato H, Honma K. In vivo imaging of clock gene expression in multiple tissues of freely moving mice. Nat Commun. 2016;7:11705. doi: 10.1038/ncomms11705. PubMed PMID: 27285820; PMCID: PMC5446038.
129. Mei L, Fan Y, Lv X, Welsh DK, Zhan C, Zhang EE. Long-term in vivo recording of circadian rhythms in brains of freely moving mice. Proceedings of the National Academy of Sciences of the United States of America. 2018;115(16):4276-81. doi: 10.1073/pnas.1717735115. PubMed PMID: 29610316; PMCID: PMC5910830.
130. Saini C, Liani A, Curie T, Gos P, Kreppel F, Emmenegger Y, Bonacina L, Wolf JP, Poget YA, Franken P, Schibler U. Real-time recording of circadian liver gene expression in freely moving mice reveals the phase-setting behavior of hepatocyte clocks. Genes Dev. 2013;27(13):1526-36. doi: 10.1101/gad.221374.113. PubMed PMID: 23824542; PMCID: PMC3713432.

131. Tahara Y, Yamazaki M, Sukigara H, Motohashi H, Sasaki H, Miyakawa H, Haraguchi A, Ikeda Y, Fukuda S, Shibata S. Gut Microbiota-Derived Short Chain Fatty Acids Induce Circadian Clock Entrainment in Mouse Peripheral Tissue. Sci Rep. 2018;8(1):1395. doi: 10.1038/s41598-018-19836-7. PubMed PMID: 29362450; PMCID: PMC5780501.
132. Takamure M, Murakami N, Takahashi K, Kuroda H, Etoh T. Rapid reentrainment of the circadian clock itself, but not the measurable activity rhythms to a new light-dark cycle in the rat. Physiol Behav. 1991;50(2):443-9. doi: 10.1016/0031-9384(91)90092-3. PubMed PMID: 1745692.
133. van der Vinne V, Burgos BM, Harrington ME, Weaver DR. Deconstructing circadian disruption: Assessing the contribution of reduced peripheral oscillator amplitude on obesity and glucose intolerance in mice. J Pineal Res. 2020. doi: 10.1111/jpi.12654. PubMed PMID: 32243642.
134. Davidson AJ, Sellix MT, Daniel J, Yamazaki S, Menaker M, Block GD. Chronic jet-lag increases mortality in aged mice. Curr Biol. 2006;16(21):R914-6. doi: 10.1016/j.cub.2006.09.058. PubMed PMID: 17084685; PMCID: PMC1635966.
135. Noguchi T, Harrison EM, Sun J, May D, Ng A, Welsh DK, Gorman MR. Circadian rhythm bifurcation induces flexible phase resetting by reducing circadian amplitude. Eur J Neurosci. 2018. doi: 10.1111/ejn.14086. PubMed PMID: 30044021.
136. Ramanathan C, Khan SK, Kathale ND, Xu H, Liu AC. Monitoring cell-autonomous circadian clock rhythms of gene expression using luciferase bioluminescence reporters. J Vis Exp. 2012(67). doi: 10.3791/4234. PubMed PMID: 23052244; PMCID: PMC3490247.
137. Millar AJ, Short SR, Chua NH, Kay SA. A novel circadian phenotype based on firefly luciferase expression in transgenic plants. Plant Cell. 1992;4(9):1075-87. doi: 10.1105/tpc.4.9.1075. PubMed PMID: 1392609; PMCID: PMC160198.
138. Kondo T, Strayer CA, Kulkarni RD, Taylor W, Ishiura M, Golden SS, Johnson CH. Circadian rhythms in prokaryotes: luciferase as a reporter of circadian gene expression in cyanobacteria. Proceedings of the National Academy of Sciences of the United States of America. 1993;90(12):5672-6. doi: 10.1073/pnas.90.12.5672. PubMed PMID: 8516317; PMCID: PMC46783.
139. Brandes C, Plautz JD, Stanewsky R, Jamison CF, Straume M, Wood KV, Kay SA, Hall JC. Novel features of drosophila period Transcription revealed by real-time luciferase reporting. Neuron. 1996;16(4):687-92. doi: 10.1016/s0896-6273(00)80088-4. PubMed PMID: 8607986.
140. Plautz JD, Kaneko M, Hall JC, Kay SA. Independent photoreceptive circadian clocks throughout Drosophila. Science (New York, NY). 1997;278(5343):1632-5. doi: 10.1126/science.278.5343.1632. PubMed PMID: 9374465.
141. Wilsbacher LD, Yamazaki S, Herzog ED, Song EJ, Radcliffe LA, Abe M, Block G, Spitznagel E, Menaker M, Takahashi JS. Photic and circadian expression of luciferase in mPeriod1-luc transgenic mice invivo. Proceedings of the National Academy of Sciences of the United States of America. 2002;99(1):489-94. doi: 10.1073/pnas.012248599. PubMed PMID: 11752392; PMCID: PMC117587.
142. Yamaguchi S, Kobayashi M, Mitsui S, Ishida Y, van der Horst GT, Suzuki M, Shibata S, Okamura H. View of a mouse clock gene ticking. Nature. 2001;409(6821):684. doi: 10.1038/35055628. PubMed PMID: 11217850.
143. Tahara Y, Kuroda H, Saito K, Nakajima Y, Kubo Y, Ohnishi N, Seo Y, Otsuka M, Fuse Y, Ohura Y, Komatsu T, Moriya Y, Okada S, Furutani N, Hirao A, Horikawa K, Kudo T, Shibata S. In

vivo monitoring of peripheral circadian clocks in the mouse. Curr Biol. 2012;22(11):1029-34. doi: 10.1016/j.cub.2012.04.009. PubMed PMID: 22578421.
144. Yasuda S, Iwami S, Tamura K, Ikeda Y, Kamagata M, Sasaki H, Haraguchi A, Miyamatsu M, Hanashi S, Takato Y, Shibata S. Phase resetting of circadian peripheral clocks using human and rodent diets in mouse models of type 2 diabetes and chronic kidney disease. Chronobiol Int. 2019;36(6):851-69. doi: 10.1080/07420528.2019.1594245. PubMed PMID: 30990101.
145. Kuhlman SJ, Quintero JE, McMahon DG. GFP fluorescence reports Period 1 circadian gene regulation in the mammalian biological clock. Neuroreport. 2000;11(7):1479-82. PubMed PMID: 10841361.
146. Smyllie NJ, Pilorz V, Boyd J, Meng QJ, Saer B, Chesham JE, Maywood ES, Krogager TP, Spiller DG, Boot-Handford R, White MR, Hastings MH, Loudon AS. Visualizing and Quantifying Intracellular Behavior and Abundance of the Core Circadian Clock Protein PERIOD2. Curr Biol. 2016;26(14):1880-6. doi: 10.1016/j.cub.2016.05.018. PubMed PMID: 27374340; PMCID: PMC4963210.
147. Kuhlman SJ, Silver R, Le Sauter J, Bult-Ito A, McMahon DG. Phase resetting light pulses induce Per1 and persistent spike activity in a subpopulation of biological clock neurons. The Journal of neuroscience : the official journal of the Society for Neuroscience. 2003;23(4):1441-50. PubMed PMID: 12598633; PMCID: PMC3281758.
148. Cheng HY, Alvarez-Saavedra M, Dziema H, Choi YS, Li A, Obrietan K. Segregation of expression of mPeriod gene homologs in neurons and glia: possible divergent roles of mPeriod1 and mPeriod2 in the brain. Human molecular genetics. 2009;18(16):3110-24. doi: 10.1093/hmg/ddp252. PubMed PMID: 19477955; PMCID: PMC2714730.
149. Mei L, Zhan C, Zhang EE. In Vivo Monitoring of Circadian Clock Gene Expression in the Mouse Suprachiasmatic Nucleus Using Fluorescence Reporters. J Vis Exp. 2018(137). doi: 10.3791/56765. PubMed PMID: 30035762; PMCID: PMC6102045.
150. Shaner NC, Steinbach PA, Tsien RY. A guide to choosing fluorescent proteins. Nat Methods. 2005;2(12):905-9. doi: 10.1038/nmeth819. PubMed PMID: 16299475.
151. Kitsera N, Khobta A, Epe B. Destabilized green fluorescent protein detects rapid removal of transcription blocks after genotoxic exposure. Biotechniques. 2007;43(2):222-7. doi: 10.2144/000112479. PubMed PMID: 17824390.
152. Niswender KD, Blackman SM, Rohde L, Magnuson MA, Piston DW. Quantitative imaging of green fluorescent protein in cultured cells: comparison of microscopic techniques, use in fusion proteins and detection limits. J Microsc. 1995;180(Pt 2):109-16. doi: 10.1111/j.1365-2818.1995.tb03665.x. PubMed PMID: 8537958.
153. Kalfalah F, Janke L, Schiavi A, Tigges J, Ix A, Ventura N, Boege F, Reinke H. Crosstalk of clock gene expression and autophagy in aging. Aging (Albany NY). 2016;8(9):1876-95. doi: 10.18632/aging.101018. PubMed PMID: 27574892; PMCID: PMC5076443.
154. Lavery DJ, Lopez-Molina L, Margueron R, Fleury-Olela F, Conquet F, Schibler U, Bonfils C. Circadian expression of the steroid 15 alpha-hydroxylase (Cyp2a4) and coumarin 7-hydroxylase (Cyp2a5) genes in mouse liver is regulated by the PAR leucine zipper transcription factor DBP. Mol Cell Biol. 1999;19(10):6488-99. doi: 10.1128/mcb.19.10.6488. PubMed PMID: 10490589; PMCID: PMC84619.
155. Moman RN, Varacallo M. Physiology, Albumin. StatPearls. Treasure Island (FL)2020.
156. Yamajuku D, Shibata Y, Kitazawa M, Katakura T, Urata H, Kojima T, Takayasu S, Nakata O, Hashimoto S. Cellular DBP and E4BP4 proteins are critical for determining the period length

of the circadian oscillator. FEBS Lett. 2011;585(14):2217-22. doi: 10.1016/j.febslet.2011.05.038. PubMed PMID: 21635892.
157. Lopez-Molina L, Conquet F, Dubois-Dauphin M, Schibler U. The DBP gene is expressed according to a circadian rhythm in the suprachiasmatic nucleus and influences circadian behavior. EMBO J. 1997;16(22):6762-71. doi: 10.1093/emboj/16.22.6762. PubMed PMID: 9362490; PMCID: PMC1170280.
158. Zhang R, Lahens NF, Ballance HI, Hughes ME, Hogenesch JB. A circadian gene expression atlas in mammals: implications for biology and medicine. Proceedings of the National Academy of Sciences of the United States of America. 2014;111(45):16219-24. doi: 10.1073/pnas.1408886111. PubMed PMID: 25349387; PMCID: PMC4234565.
159. Fonjallaz P, Ossipow V, Wanner G, Schibler U. The two PAR leucine zipper proteins, TEF and DBP, display similar circadian and tissue-specific expression, but have different target promoter preferences. EMBO J. 1996;15(2):351-62. PubMed PMID: 8617210; PMCID: PMC449950.
160. Yoo SH, Kojima S, Shimomura K, Koike N, Buhr ED, Furukawa T, Ko CH, Gloston G, Ayoub C, Nohara K, Reyes BA, Tsuchiya Y, Yoo OJ, Yagita K, Lee C, Chen Z, Yamazaki S, Green CB, Takahashi JS. Period2 3'-UTR and microRNA-24 regulate circadian rhythms by repressing PERIOD2 protein accumulation. Proceedings of the National Academy of Sciences of the United States of America. 2017;114(42):E8855-E64. doi: 10.1073/pnas.1706611114. PubMed PMID: 28973913; PMCID: PMC5651750.
161. Yamazaki S, Takahashi JS. Real-time luminescence reporting of circadian gene expression in mammals. Methods Enzymol. 2005;393:288-301. doi: 10.1016/S0076-6879(05)93012-7. PubMed PMID: 15817295; PMCID: PMC3793321.
162. Leise TL, Harrington ME. Wavelet-based time series analysis of circadian rhythms. J Biol Rhythms. 2011;26(5):454-63. doi: 10.1177/0748730411416330. PubMed PMID: 21921299.
163. Leise TL. Analysis of Nonstationary Time Series for Biological Rhythms Research. J Biol Rhythms. 2017;32(3):187-94. doi: 10.1177/0748730417709105. PubMed PMID: 28569118.
164. Evans JA, Leise TL, Castanon-Cervantes O, Davidson AJ. Intrinsic regulation of spatiotemporal organization within the suprachiasmatic nucleus. PloS one. 2011;6(1):e15869. doi: 10.1371/journal.pone.0015869. PubMed PMID: 21249213; PMCID: PMC3017566.
165. Evans JA, Leise TL, Castanon-Cervantes O, Davidson AJ. Dynamic interactions mediated by nonredundant signaling mechanisms couple circadian clock neurons. Neuron. 2013;80(4):973-83. doi: 10.1016/j.neuron.2013.08.022. PubMed PMID: 24267653; PMCID: PMC3841113.
166. Leise TL, Harrington ME, Molyneux PC, Song I, Queenan H, Zimmerman E, Lall GS, Biello SM. Voluntary exercise can strengthen the circadian system in aged mice. Age (Dordr). 2013;35(6):2137-52. doi: 10.1007/s11357-012-9502-y. PubMed PMID: 23340916; PMCID: PMC3825002.
167. Mali P, Aach J, Stranges PB, Esvelt KM, Moosburner M, Kosuri S, Yang L, Church GM. CAS9 transcriptional activators for target specificity screening and paired nickases for cooperative genome engineering. Nat Biotech. 2013;31(9):833-8. doi: 10.1038/nbt.2675

http://www.nature.com/nbt/journal/v31/n9/abs/nbt.2675.html#supplementary-information.
168. Liu Z, Chen O, Wall JBJ, Zheng M, Zhou Y, Wang L, Ruth Vaseghi H, Qian L, Liu J. Systematic comparison of 2A peptides for cloning multi-genes in a polycistronic vector. Sci Rep.

2017;7(1):2193. doi: 10.1038/s41598-017-02460-2. PubMed PMID: 28526819; PMCID: PMC5438344.
169. Menet JS, Rodriguez J, Abruzzi KC, Rosbash M. Nascent-Seq reveals novel features of mouse circadian transcriptional regulation. Elife. 2012;1:e00011. doi: 10.7554/eLife.00011. PubMed PMID: 23150795; PMCID: PMC3492862.
170. Punia S, Rumery KK, Yu EA, Lambert CM, Notkins AL, Weaver DR. Disruption of gene expression rhythms in mice lacking secretory vesicle proteins IA-2 and IA-2beta. Am J Physiol Endocrinol Metab. 2012;303(6):E762-76. doi: 10.1152/ajpendo.00513.2011. PubMed PMID: 22785238; PMCID: PMC3468428.
171. Sasaki H, Hattori Y, Ikeda Y, Kamagata M, Iwami S, Yasuda S, Tahara Y, Shibata S. Forced rather than voluntary exercise entrains peripheral clocks via a corticosterone/noradrenaline increase in PER2::LUC mice. Sci Rep. 2016;6:27607. doi: 10.1038/srep27607. PubMed PMID: 27271267; PMCID: PMC4897787.
172. Tahara Y, Aoyama S, Shibata S. The mammalian circadian clock and its entrainment by stress and exercise. J Physiol Sci. 2017;67(1):1-10. doi: 10.1007/s12576-016-0450-7. PubMed PMID: 27084533; PMCID: PMC5138246.
173. Tahara Y, Shiraishi T, Kikuchi Y, Haraguchi A, Kuriki D, Sasaki H, Motohashi H, Sakai T, Shibata S. Entrainment of the mouse circadian clock by sub-acute physical and psychological stress. Sci Rep. 2015;5:11417. doi: 10.1038/srep11417. PubMed PMID: 26073568; PMCID: PMC4466793.
174. Lee IT, Chang AS, Manandhar M, Shan Y, Fan J, Izumo M, Ikeda Y, Motoike T, Dixon S, Seinfeld JE, Takahashi JS, Yanagisawa M. Neuromedin s-producing neurons act as essential pacemakers in the suprachiasmatic nucleus to couple clock neurons and dictate circadian rhythms. Neuron. 2015;85(5):1086-102. doi: 10.1016/j.neuron.2015.02.006. PubMed PMID: 25741729; PMCID: PMC5811223.
175. Mieda M, Ono D, Hasegawa E, Okamoto H, Honma K, Honma S, Sakurai T. Cellular clocks in AVP neurons of the SCN are critical for interneuronal coupling regulating circadian behavior rhythm. Neuron. 2015;85(5):1103-16. doi: 10.1016/j.neuron.2015.02.005. PubMed PMID: 25741730.
176. Dibner C, Schibler U, Albrecht U. The mammalian circadian timing system: organization and coordination of central and peripheral clocks. Annu Rev Physiol. 2010;72:517-49. doi: 10.1146/annurev-physiol-021909-135821. PubMed PMID: 20148687.
177. Mohawk JA, Green CB, Takahashi JS. Central and peripheral circadian clocks in mammals. Annu Rev Neurosci. 2012;35:445-62. doi: 10.1146/annurev-neuro-060909-153128. PubMed PMID: 22483041; PMCID: PMC3710582.
178. Stevens RG. Circadian disruption and breast cancer: from melatonin to clock genes. Epidemiology. 2005;16(2):254-8. doi: 10.1097/01.ede.0000152525.21924.54. PubMed PMID: 15703542.
179. Lamont EW, Legault-Coutu D, Cermakian N, Boivin DB. The role of circadian clock genes in mental disorders. Dialogues Clin Neurosci. 2007;9(3):333-42. PubMed PMID: 17969870; PMCID: PMC3202489.
180. Walker WH, 2nd, Walton JC, DeVries AC, Nelson RJ. Circadian rhythm disruption and mental health. Transl Psychiatry. 2020;10(1):28. doi: 10.1038/s41398-020-0694-0. PubMed PMID: 32066704; PMCID: PMC7026420.

181. Poulsen RC, Warman GR, Sleigh J, Ludin NM, Cheeseman JF. How does general anaesthesia affect the circadian clock? Sleep Med Rev. 2018;37:35-44. doi: 10.1016/j.smrv.2016.12.002. PubMed PMID: 28162920.
182. Berger F, Paulmurugan R, Bhaumik S, Gambhir SS. Uptake kinetics and biodistribution of 14C-D-luciferin--a radiolabeled substrate for the firefly luciferase catalyzed bioluminescence reaction: impact on bioluminescence based reporter gene imaging. Eur J Nucl Med Mol Imaging. 2008;35(12):2275-85. doi: 10.1007/s00259-008-0870-6. PubMed PMID: 18661130; PMCID: PMC4157642.
183. Simonyan H, Hurr C, Young CN. A synthetic luciferin improves in vivo bioluminescence imaging of gene expression in cardiovascular brain regions. Physiol Genomics. 2016;48(10):762-70. doi: 10.1152/physiolgenomics.00055.2016. PubMed PMID: 27614203; PMCID: PMC5243229.
184. Lie JA, Kjuus H, Zienolddiny S, Haugen A, Stevens RG, Kjaerheim K. Night work and breast cancer risk among Norwegian nurses: assessment by different exposure metrics. Am J Epidemiol. 2011;173(11):1272-9. doi: 10.1093/aje/kwr014. PubMed PMID: 21454824.
185. Brum MC, Filho FF, Schnorr CC, Bottega GB, Rodrigues TC. Shift work and its association with metabolic disorders. Diabetol Metab Syndr. 2015;7:45. doi: 10.1186/s13098-015-0041-4. PubMed PMID: 25991926; PMCID: PMC4436793.
186. Rafnsson V, Tulinius H, Jonasson JG, Hrafnkelsson J. Risk of breast cancer in female flight attendants: a population-based study (Iceland). Cancer Causes Control. 2001;12(2):95-101. doi: 10.1023/a:1008983416836. PubMed PMID: 11246849.
187. McNeely E, Mordukhovich I, Staffa S, Tideman S, Gale S, Coull B. Cancer prevalence among flight attendants compared to the general population. Environ Health. 2018;17(1):49. doi: 10.1186/s12940-018-0396-8. PubMed PMID: 29940975; PMCID: PMC6019786.
188. Ulhoa MA, Marqueze EC, Burgos LG, Moreno CR. Shift work and endocrine disorders. Int J Endocrinol. 2015;2015:826249. doi: 10.1155/2015/826249. PubMed PMID: 25892993; PMCID: PMC4393906.
189. Park K, You J, Du C, Pan Y. Cranial window implantation on mouse cortex to study microvascular change induced by cocaine. Quant Imaging Med Surg. 2015;5(1):97-107. doi: 10.3978/j.issn.2223-4292.2014.11.31. PubMed PMID: 25694959; PMCID: PMC4312290.
190. Miller JE, Granados-Fuentes D, Wang T, Marpegan L, Holy TE, Herzog ED. Vasoactive intestinal polypeptide mediates circadian rhythms in mammalian olfactory bulb and olfaction. The Journal of neuroscience : the official journal of the Society for Neuroscience. 2014;34(17):6040-6. doi: 10.1523/JNEUROSCI.4713-13.2014. PubMed PMID: 24760863; PMCID: PMC3996221.
191. Welsh DK. Gate cells see the light. J Biol Rhythms. 2007;22(1):26-8. doi: 10.1177/0748730406297067. PubMed PMID: 17229922.
192. Moore RY. Entrainment pathways and the functional organization of the circadian system. Prog Brain Res. 1996;111:103-19. doi: 10.1016/s0079-6123(08)60403-3. PubMed PMID: 8990910.
193. Mieda M. The Network Mechanism of the Central Circadian Pacemaker of the SCN: Do AVP Neurons Play a More Critical Role Than Expected? Front Neurosci. 2019;13:139. doi: 10.3389/fnins.2019.00139. PubMed PMID: 30858797; PMCID: PMC6397828.
194. Jones JR, Simon T, Lones L, Herzog ED. SCN VIP Neurons Are Essential for Normal Light-Mediated Resetting of the Circadian System. The Journal of neuroscience : the official journal of

the Society for Neuroscience. 2018;38(37):7986-95. doi: 10.1523/JNEUROSCI.1322-18.2018. PubMed PMID: 30082421; PMCID: PMC6596148.
195. Pei H, Sutton AK, Burnett KH, Fuller PM, Olson DP. AVP neurons in the paraventricular nucleus of the hypothalamus regulate feeding. Mol Metab. 2014;3(2):209-15. doi: 10.1016/j.molmet.2013.12.006. PubMed PMID: 24634830; PMCID: PMC3953699.
196. Staiger JF, Zilles K, Freund TF. Innervation of VIP-immunoreactive neurons by the ventroposteromedial thalamic nucleus in the barrel cortex of the rat. J Comp Neurol. 1996;367(2):194-204. doi: 10.1002/(SICI)1096-9861(19960401)367:2<194::AID-CNE3>3.0.CO;2-0. PubMed PMID: 8708004.
197. Zhu Y, Stevens RG, Hoffman AE, Fitzgerald LM, Kwon EM, Ostrander EA, Davis S, Zheng T, Stanford JL. Testing the circadian gene hypothesis in prostate cancer: a population-based case-control study. Cancer Res. 2009;69(24):9315-22. doi: 10.1158/0008-5472.CAN-09-0648. PubMed PMID: 19934327; PMCID: PMC2955869.
198. Benna C, Helfrich-Forster C, Rajendran S, Monticelli H, Pilati P, Nitti D, Mocellin S. Genetic variation of clock genes and cancer risk: a field synopsis and meta-analysis. Oncotarget. 2017;8(14):23978-95. doi: 10.18632/oncotarget.15074. PubMed PMID: 28177907; PMCID: PMC5410358.
199. Morales-Santana S, Morell S, Leon J, Carazo-Gallego A, Jimenez-Lopez JC, Morell M. An Overview of the Polymorphisms of Circadian Genes Associated With Endocrine Cancer. Front Endocrinol (Lausanne). 2019;10:104. doi: 10.3389/fendo.2019.00104. PubMed PMID: 30873119; PMCID: PMC6401647.
200. Salavaty A. Carcinogenic effects of circadian disruption: an epigenetic viewpoint. Chin J Cancer. 2015;34(9):375-83. doi: 10.1186/s40880-015-0043-5. PubMed PMID: 26253128; PMCID: PMC4593354.
201. Angelousi A, Kassi E, Ansari-Nasiri N, Randeva H, Kaltsas G, Chrousos G. Clock genes and cancer development in particular in endocrine tissues. Endocr Relat Cancer. 2019;26(6):R305-R17. doi: 10.1530/ERC-19-0094. PubMed PMID: 30959483.
202. Lin YM, Chang JH, Yeh KT, Yang MY, Liu TC, Lin SF, Su WW, Chang JG. Disturbance of circadian gene expression in hepatocellular carcinoma. Mol Carcinog. 2008;47(12):925-33. doi: 10.1002/mc.20446. PubMed PMID: 18444243.
203. Matsuo T, Yamaguchi S, Mitsui S, Emi A, Shimoda F, Okamura H. Control mechanism of the circadian clock for timing of cell division in vivo. Science (New York, NY). 2003;302(5643):255-9. doi: 10.1126/science.1086271. PubMed PMID: 12934012.
204. Fu L, Lee CC. The circadian clock: pacemaker and tumour suppressor. Nat Rev Cancer. 2003;3(5):350-61. doi: 10.1038/nrc1072. PubMed PMID: 12724733.
205. Davidson AJ, Straume M, Block GD, Menaker M. Daily timed meals dissociate circadian rhythms in hepatoma and healthy host liver. Int J Cancer. 2006;118(7):1623-7. doi: 10.1002/ijc.21591. PubMed PMID: 16231323; PMCID: PMC1464797.
206. Lakatua DJ, White M, Sackett-Lundeen LL, Haus E. Change in phase relations of circadian rhythms in cell proliferation induced by time-limited feeding in BALB/c X DBA/2F1 mice bearing a transplantable Harding-Passey tumor. Cancer Res. 1983;43(9):4068-72. PubMed PMID: 6871848.
207. Masri S, Papagiannakopoulos T, Kinouchi K, Liu Y, Cervantes M, Baldi P, Jacks T, Sassone-Corsi P. Lung Adenocarcinoma Distally Rewires Hepatic Circadian Homeostasis. Cell.

2016;165(4):896-909. doi: 10.1016/j.cell.2016.04.039. PubMed PMID: 27153497; PMCID: PMC5373476.
208. Gowing LR, Ali RL, Allsop S, Marsden J, Turf EE, West R, Witton J. Global statistics on addictive behaviours: 2014 status report. Addiction. 2015;110(6):904-19. doi: 10.1111/add.12899.
209. Jorenby DE, Hays JT, Rigotti NA, Azoulay S, Watsky EJ, Williams KE, Billing CB, Gong J, Reeves KR, Varenicline Phase 3 Study G. Efficacy of varenicline, an alpha4beta2 nicotinic acetylcholine receptor partial agonist, vs placebo or sustained-release bupropion for smoking cessation: a randomized controlled trial. JAMA. 2006;296(1):56-63. doi: 10.1001/jama.296.1.56. PubMed PMID: 16820547.
210. De Biasi M, Dani JA. Reward, addiction, withdrawal to nicotine. Annu Rev Neurosci. 2011;34:105-30. doi: 10.1146/annurev-neuro-061010-113734. PubMed PMID: 21438686; PMCID: PMC3137256.
211. Koob GF, Volkow ND. Neurocircuitry of addiction. Neuropsychopharmacology : official publication of the American College of Neuropsychopharmacology. 2010;35(1):217-38. doi: 10.1038/npp.2009.110. PubMed PMID: 19710631; PMCID: PMC2805560.
212. Patton GC, Carlin JB, Coffey C, Wolfe R, Hibbert M, Bowes G. Depression, anxiety, and smoking initiation: a prospective study over 3 years. Am J Public Health. 1998;88(10):1518-22. doi: 10.2105/ajph.88.10.1518. PubMed PMID: 9772855; PMCID: PMC1508459.
213. Morissette SB, Tull MT, Gulliver SB, Kamholz BW, Zimering RT. Anxiety, anxiety disorders, tobacco use, and nicotine: a critical review of interrelationships. Psychol Bull. 2007;133(2):245-72. doi: 10.1037/0033-2909.133.2.245. PubMed PMID: 17338599.
214. Wingo T, Nesil T, Choi JS, Li MD. Novelty Seeking and Drug Addiction in Humans and Animals: From Behavior to Molecules. J Neuroimmune Pharmacol. 2016;11(3):456-70. doi: 10.1007/s11481-015-9636-7. PubMed PMID: 26481371; PMCID: PMC4837094.
215. Lasser K, Boyd JW, Woolhandler S, Himmelstein DU, McCormick D, Bor DH. Smoking and mental illness: A population-based prevalence study. JAMA. 2000;284(20):2606-10. doi: 10.1001/jama.284.20.2606. PubMed PMID: 11086367.
216. Albuquerque EX, Pereira EFR, Alkondon M, Rogers SW. Mammalian Nicotinic Acetylcholine Receptors: From Structure to Function. Physiological Reviews. 2009;89(1):73-120. doi: 10.1152/physrev.00015.2008.
217. Improgo MRD, Scofield MD, Tapper AR, Gardner PD. The nicotinic acetylcholine receptor CHRNA5/A3/B4 gene cluster: Dual role in nicotine addiction and lung cancer. Progress in Neurobiology. 2010;92(2):212-26. doi: http://dx.doi.org/10.1016/j.pneurobio.2010.05.003.
218. Changeux JP. Nicotine addiction and nicotinic receptors: lessons from genetically modified mice. Nat Rev Neurosci. 2010;11(6):389-401. doi: 10.1038/nrn2849. PubMed PMID: 20485364.
219. Benowitz NL. Pharmacologic Aspects of Cigarette Smoking and Nicotine Addiction. New England Journal of Medicine. 1988;319(20):1318-30. doi: doi:10.1056/NEJM198811173192005. PubMed PMID: 3054551.
220. Fowler CD, Arends MA, Kenny PJ. Subtypes of nicotinic acetylcholine receptors in nicotine reward, dependence, and withdrawal: evidence from genetically modified mice. Behavioural pharmacology. 2008;19(5-6):461-84. Epub 2008/08/12. doi: 10.1097/FBP.0b013e32830c360e. PubMed PMID: 18690103; PMCID: PMC2669417.

221. Salas R, Sturm R, Boulter J, De Biasi M. Nicotinic receptors in the habenulo-interpeduncular system are necessary for nicotine withdrawal in mice. The Journal of neuroscience : the official journal of the Society for Neuroscience. 2009;29(10):3014-8. Epub 2009/03/13. doi: 10.1523/jneurosci.4934-08.2009. PubMed PMID: 19279237; PMCID: PMC3862238.
222. Wolfman SL, Gill DF, Bogdanic F, Long K, Al-Hasani R, McCall JG, Bruchas MR, McGehee DS. Nicotine aversion is mediated by GABAergic interpeduncular nucleus inputs to laterodorsal tegmentum. Nat Commun. 2018;9(1):2710. doi: 10.1038/s41467-018-04654-2. PubMed PMID: 30006624; PMCID: PMC6045623.
223. Antolin-Fontes B, Ables JL, Gorlich A, Ibanez-Tallon I. The habenulo-interpeduncular pathway in nicotine aversion and withdrawal. Neuropharmacology. 2015;96(Pt B):213-22. Epub 2014/12/06. doi: 10.1016/j.neuropharm.2014.11.019. PubMed PMID: 25476971; PMCID: PMC4452453.
224. McLaughlin I, Dani JA, De Biasi M. The medial habenula and interpeduncular nucleus circuitry is critical in addiction, anxiety, and mood regulation. J Neurochem. 2017;142 Suppl 2:130-43. doi: 10.1111/jnc.14008. PubMed PMID: 28791703; PMCID: PMC6740332.
225. Molas S, Zhao-Shea R, Liu L, DeGroot SR, Gardner PD, Tapper AR. A circuit-based mechanism underlying familiarity signaling and the preference for novelty. Nat Neurosci. 2017;20(9):1260-8. doi: 10.1038/nn.4607. PubMed PMID: 28714952.
226. Picciotto MR, Zoli M, Rimondini R, Lena C, Marubio LM, Pich EM, Fuxe K, Changeux JP. Acetylcholine receptors containing the beta2 subunit are involved in the reinforcing properties of nicotine. Nature. 1998;391(6663):173-7. Epub 1998/01/15. doi: 10.1038/34413. PubMed PMID: 9428762.
227. Pons S, Fattore L, Cossu G, Tolu S, Porcu E, McIntosh JM, Changeux JP, Maskos U, Fratta W. Crucial role of alpha4 and alpha6 nicotinic acetylcholine receptor subunits from ventral tegmental area in systemic nicotine self-administration. The Journal of neuroscience : the official journal of the Society for Neuroscience. 2008;28(47):12318-27. Epub 2008/11/21. doi: 10.1523/jneurosci.3918-08.2008. PubMed PMID: 19020025; PMCID: PMC2819191.
228. Tapper AR, McKinney SL, Nashmi R, Schwarz J, Deshpande P, Labarca C, Whiteaker P, Marks MJ, Collins AC, Lester HA. Nicotine activation of alpha4* receptors: sufficient for reward, tolerance, and sensitization. Science (New York, NY). 2004;306(5698):1029-32. Epub 2004/11/06. doi: 10.1126/science.1099420. PubMed PMID: 15528443.
229. Lessov CN, Martin NG, Statham DJ, Todorov AA, Slutske WS, Bucholz KK, Heath AC, Madden PA. Defining nicotine dependence for genetic research: evidence from Australian twins. Psychological medicine. 2004;34(5):865-79. Epub 2004/10/27. PubMed PMID: 15500307.
230. Lessov-Schlaggar CN, Pang Z, Swan GE, Guo Q, Wang S, Cao W, Unger JB, Johnson CA, Lee L. Heritability of cigarette smoking and alcohol use in Chinese male twins: the Qingdao twin registry. International journal of epidemiology. 2006;35(5):1278-85. Epub 2006/07/19. doi: 10.1093/ije/dyl148. PubMed PMID: 16847025.
231. Maes HH, Sullivan PF, Bulik CM, Neale MC, Prescott CA, Eaves LJ, Kendler KS. A twin study of genetic and environmental influences on tobacco initiation, regular tobacco use and nicotine dependence. Psychological medicine. 2004;34(7):1251-61. Epub 2005/02/09. PubMed PMID: 15697051.

232. Li MD, Cheng R, Ma JZ, Swan GE. A meta-analysis of estimated genetic and environmental effects on smoking behavior in male and female adult twins. Addiction. 2003;98(1):23-31. Epub 2002/12/21. PubMed PMID: 12492752.
233. Li MD. The genetics of nicotine dependence. Current psychiatry reports. 2006;8(2):158-64. Epub 2006/03/17. PubMed PMID: 16539894.
234. Saccone SF, Hinrichs AL, Saccone NL, Chase GA, Konvicka K, Madden PA, Breslau N, Johnson EO, Hatsukami D, Pomerleau O, Swan GE, Goate AM, Rutter J, Bertelsen S, Fox L, Fugman D, Martin NG, Montgomery GW, Wang JC, Ballinger DG, Rice JP, Bierut LJ. Cholinergic nicotinic receptor genes implicated in a nicotine dependence association study targeting 348 candidate genes with 3713 SNPs. Human molecular genetics. 2007;16(1):36-49. Epub 2006/12/01. doi: 10.1093/hmg/ddl438. PubMed PMID: 17135278; PMCID: PMC2270437.
235. Wen L, Jiang K, Yuan W, Cui W, Li MD. Contribution of Variants in CHRNA5/A3/B4 Gene Cluster on Chromosome 15 to Tobacco Smoking: From Genetic Association to Mechanism. Molecular neurobiology. 2016;53(1):472-84. Epub 2014/12/05. doi: 10.1007/s12035-014-8997-x. PubMed PMID: 25471942.
236. Bierut LJ, Madden PAF, Breslau N, Johnson EO, Hatsukami D, Pomerleau OF, Swan GE, Rutter J, Bertelsen S, Fox L, Fugman D, Goate AM, Hinrichs AL, Konvicka K, Martin NG, Montgomery GW, Saccone NL, Saccone SF, Wang JC, Chase GA, Rice JP, Ballinger DG. Novel Genes Identified in a High Density Genome Wide Association Study for Nicotine Dependence. Human molecular genetics. 2007;16(1):24-35. doi: 10.1093/hmg/ddl441. PubMed PMID: PMC2278047.
237. Weiss RB, Baker TB, Cannon DS, von Niederhausern A, Dunn DM, Matsunami N, Singh NA, Baird L, Coon H, McMahon WM, Piper ME, Fiore MC, Scholand MB, Connett JE, Kanner RE, Gahring LC, Rogers SW, Hoidal JR, Leppert MF. A candidate gene approach identifies the CHRNA5-A3-B4 region as a risk factor for age-dependent nicotine addiction. PLoS genetics. 2008;4(7):e1000125. Epub 2008/07/12. doi: 10.1371/journal.pgen.1000125. PubMed PMID: 18618000; PMCID: PMC2442220.
238. Baker TB, Weiss RB, Bolt D, von Niederhausern A, Fiore MC, Dunn DM, Piper ME, Matsunami N, Smith SS, Coon H, McMahon WM, Scholand MB, Singh N, Hoidal JR, Kim S-Y, Leppert MF, Cannon DS. Human neuronal acetylcholine receptor A5-A3-B4 haplotypes are associated with multiple nicotine dependence phenotypes. Nicotine & Tobacco Research. 2009;11(7):785-96. doi: 10.1093/ntr/ntp064. PubMed PMID: PMC2699926.
239. Bierut LJ, Stitzel JA, Wang JC, Hinrichs AL, Grucza RA, Xuei X, Saccone NL, Saccone SF, Bertelsen S, Fox L, Horton WJ, Breslau N, Budde J, Cloninger CR, Dick DM, Foroud T, Hatsukami D, Hesselbrock V, Johnson EO, Kramer J, Kuperman S, Madden PA, Mayo K, Nurnberger J, Jr., Pomerleau O, Porjesz B, Reyes O, Schuckit M, Swan G, Tischfield JA, Edenberg HJ, Rice JP, Goate AM. Variants in nicotinic receptors and risk for nicotine dependence. The American journal of psychiatry. 2008;165(9):1163-71. Epub 2008/06/04. doi: 10.1176/appi.ajp.2008.07111711. PubMed PMID: 18519524; PMCID: PMC2574742.
240. Saccone NL, Saccone SF, Hinrichs AL, Stitzel JA, Duan W, Pergadia ML, Agrawal A, Breslau N, Grucza RA, Hatsukami D, Johnson EO, Madden PA, Swan GE, Wang JC, Goate AM, Rice JP, Bierut LJ. Multiple distinct risk loci for nicotine dependence identified by dense coverage of the complete family of nicotinic receptor subunit (CHRN) genes. American journal of medical genetics Part B, Neuropsychiatric genetics : the official publication of the International Society of

Psychiatric Genetics. 2009;150b(4):453-66. Epub 2009/03/05. doi: 10.1002/ajmg.b.30828. PubMed PMID: 19259974; PMCID: PMC2693307.
241. Li MD, Yoon D, Lee JY, Han BG, Niu T, Payne TJ, Ma JZ, Park T. Associations of variants in CHRNA5/A3/B4 gene cluster with smoking behaviors in a Korean population. PloS one. 2010;5(8):e12183. Epub 2010/09/03. doi: 10.1371/journal.pone.0012183. PubMed PMID: 20808433; PMCID: PMC2922326.
242. Li MD, Xu Q, Lou X-Y, Payne TJ, Niu T, Ma JZ. Association and interaction analysis of variants in CHRNA5/CHRNA3/CHRNB4 gene cluster with nicotine dependence in African and European Americans. American journal of medical genetics Part B, Neuropsychiatric genetics : the official publication of the International Society of Psychiatric Genetics. 2010;153B(3):745-56. doi: 10.1002/ajmg.b.31043. PubMed PMID: PMC2924635.
243. Salas R, Pieri F, De Biasi M. Decreased signs of nicotine withdrawal in mice null for the beta4 nicotinic acetylcholine receptor subunit. The Journal of neuroscience : the official journal of the Society for Neuroscience. 2004;24(45):10035-9. Epub 2004/11/13. doi: 10.1523/jneurosci.1939-04.2004. PubMed PMID: 15537871.
244. Fowler CD, Lu Q, Johnson PM, Marks MJ, Kenny PJ. Habenular alpha5 nicotinic receptor subunit signalling controls nicotine intake. Nature. 2011;471(7340):597-601. Epub 2011/02/01. doi: 10.1038/nature09797. PubMed PMID: 21278726; PMCID: PMC3079537.
245. Frahm S, Slimak MA, Ferrarese L, Santos-Torres J, Antolin-Fontes B, Auer S, Filkin S, Pons S, Fontaine JF, Tsetlin V, Maskos U, Ibanez-Tallon I. Aversion to nicotine is regulated by the balanced activity of beta4 and alpha5 nicotinic receptor subunits in the medial habenula. Neuron. 2011;70(3):522-35. doi: 10.1016/j.neuron.2011.04.013. PubMed PMID: 21555077.
246. Gangitano D, Salas R, Teng Y, Perez E, De Biasi M. Progesterone modulation of alpha5 nAChR subunits influences anxiety-related behavior during estrus cycle. Genes Brain Behav. 2009;8(4):398-406. doi: 10.1111/j.1601-183X.2009.00476.x. PubMed PMID: 19220484; PMCID: PMC2712346.
247. Salas R, Pieri F, Fung B, Dani JA, De Biasi M. Altered anxiety-related responses in mutant mice lacking the beta4 subunit of the nicotinic receptor. The Journal of neuroscience : the official journal of the Society for Neuroscience. 2003;23(15):6255-63. PubMed PMID: 12867510.
248. Salas R, Fung B, Sturm R, De Biasi M. Abnormal social behavior in nicotinic acetylcholine receptor beta4 subunit-null mice. Nicotine Tob Res. 2013;15(5):983-6. doi: 10.1093/ntr/nts215. PubMed PMID: 23042983; PMCID: PMC3693500.
249. Xu W, Gelber S, Orr-Urtreger A, Armstrong D, Lewis RA, Ou CN, Patrick J, Role L, De Biasi M, Beaudet AL. Megacystis, mydriasis, and ion channel defect in mice lacking the alpha3 neuronal nicotinic acetylcholine receptor. Proceedings of the National Academy of Sciences of the United States of America. 1999;96(10):5746-51. Epub 1999/05/13. PubMed PMID: 10318955; PMCID: PMC21931.
250. Shih PY, Engle SE, Oh G, Deshpande P, Puskar NL, Lester HA, Drenan RM. Differential expression and function of nicotinic acetylcholine receptors in subdivisions of medial habenula. The Journal of neuroscience : the official journal of the Society for Neuroscience. 2014;34(29):9789-802. doi: 10.1523/JNEUROSCI.0476-14.2014. PubMed PMID: 25031416; PMCID: PMC4099552.
251. Livak KJ, Schmittgen TD. Analysis of relative gene expression data using real-time quantitative PCR and the 2(-Delta Delta C(T)) Method. Methods. 2001;25(4):402-8. doi: 10.1006/meth.2001.1262. PubMed PMID: 11846609.

252. Casserly AP, Tsuji J, Zhao-Shea R, Smith CB, Molas S, Tapper AR, Weng Z, Gardner PD. Integrated miRNA-/mRNA-Seq of the Habenulo-Interpeduncular Circuit During Acute Nicotine Withdrawal. Sci Rep. 2020;10(1):813. doi: 10.1038/s41598-020-57907-w. PubMed PMID: 31965003; PMCID: PMC6972841.
253. Zhao-Shea R, Liu L, Pang X, Gardner PD, Tapper AR. Activation of GABAergic neurons in the interpeduncular nucleus triggers physical nicotine withdrawal symptoms. Current biology : CB. 2013;23(23):10.1016/j.cub.2013.09.041. doi: 10.1016/j.cub.2013.09.041. PubMed PMID: PMC3855889.
254. Improgo MR, Scofield MD, Tapper AR, Gardner PD. The nicotinic acetylcholine receptor CHRNA5/A3/B4 gene cluster: dual role in nicotine addiction and lung cancer. Prog Neurobiol. 2010;92(2):212-26. doi: 10.1016/j.pneurobio.2010.05.003. PubMed PMID: 20685379; PMCID: PMC2939268.
255. Molas S, DeGroot SR, Zhao-Shea R, Tapper AR. Anxiety and Nicotine Dependence: Emerging Role of the Habenulo-Interpeduncular Axis. Trends Pharmacol Sci. 2017;38(2):169-80. doi: 10.1016/j.tips.2016.11.001. PubMed PMID: 27890353; PMCID: PMC5258775.
256. Booker TK, Butt CM, Wehner JM, Heinemann SF, Collins AC. Decreased anxiety-like behavior in beta3 nicotinic receptor subunit knockout mice. Pharmacology, biochemistry, and behavior. 2007;87(1):146-57. doi: 10.1016/j.pbb.2007.04.011. PubMed PMID: 17509676.
257. Semenova S, Contet C, Roberts AJ, Markou A. Mice lacking the beta4 subunit of the nicotinic acetylcholine receptor show memory deficits, altered anxiety- and depression-like behavior, and diminished nicotine-induced analgesia. Nicotine Tob Res. 2012;14(11):1346-55. doi: 10.1093/ntr/nts107. PubMed PMID: 22573727; PMCID: PMC3482014.
258. Ngolab J, Liu L, Zhao-Shea R, Gao G, Gardner PD, Tapper AR. Functional Upregulation of alpha4* Nicotinic Acetylcholine Receptors in VTA GABAergic Neurons Increases Sensitivity to Nicotine Reward. The Journal of neuroscience : the official journal of the Society for Neuroscience. 2015;35(22):8570-8. Epub 2015/06/05. doi: 10.1523/jneurosci.4453-14.2015. PubMed PMID: 26041923; PMCID: PMC4588598.
259. Risinger FO, Oakes RA. Nicotine-induced conditioned place preference and conditioned place aversion in mice. Pharmacology, biochemistry, and behavior. 1995;51(2-3):457-61. Epub 1995/06/01. PubMed PMID: 7667368.
260. Prus AJ, James JR, Rosecrans JA. Conditioned Place Preference. In: Buccafusco JJ, editor. Methods of Behavior Analysis in Neuroscience. 2nd ed. Boca Raton (FL)2009.